A NEW WIDE RANGE EQUATION OF STATE FOR HELIUM-4

A Dissertation

by

DIEGO ORLANDO ORTIZ VEGA

Submitted to the Office of Graduate Studies of
Texas A&M University
in partial fulfillment of the requirements for the degree of

DOCTOR OF PHILOSOPHY

Chair of Committee,	Kenneth R. Hall
Co-Chair of Committee,	James C. Holste
Committee Members,	Perla Balbuena
	Maria Barrufet
	Mahmoud El-Halwagi
Head of Department,	M. Nazmul Karim

August 2013

Major Subject: Chemical Engineering

ABSTRACT

A multiparametric and fundamental equation of state is presented for the fluid thermodynamic properties of helium. The equation is valid for temperatures from the λ-line (~2.17 K) to 1500 K and for pressures up to 2000 MPa. The formulation can calculate all thermodynamic properties, including density, heat capacity, speed of sound, energies, entropy and saturation properties. A new equation of state is necessary to overcome difficulties associated with the current standard in the asymptotic region between the λ -line and 3 K and also difficulties related to lack of data, extrapolation performance, and accuracy at higher temperatures.

Below 50 K, the uncertainties in density are 0.20% at pressures up to 20 MPa. From 50 K to 200 K the uncertainties decrease to 0.05 % at pressures up to 80 MPa. At higher temperatures the uncertainties in density are 0.02 % up to pressures of 80 MPa. At all temperatures and at pressures higher than listed here, the uncertainties may increase to 0.3% in density. The uncertainties in the speed of sound are 0.02%. The uncertainties in vapor pressure are less than 0.02% and for the heat capacities are about 2%. Uncertainties in the critical region are higher for all properties except vapor pressure.

DEDICATION

To my parents Ubaldo Ortiz and Maria Edelia Vega, whose unique determination, unbreakable ethical standards, and everlasting love and support to their family, have inspired me to give the best of me. To you my deepest respect, gratitude and love always.

A mis padres Ubaldo Ortiz y María Edelia Vega, cuya incomparable determinación, inquebrantable calidad ética, y amor y apoyo ilimitado a sus hijos; me han inspirado a dar lo mejor de mi. A ustedes mi mas profundo respeto, gratitud y amor por siempre.

Diego

ACKNOWLEDGEMENTS

I would like to thank my graduate advisors; Dr. Kenneth Hall and Dr. James Holste, for their guidance, support and ultimately for granting me the amazing opportunity of pursuing my PhD under your supervision. It is a honor to be part of your group. Thanks also to my committee members, Dr. Perla Balbuena, Dr. Maria Barrufet and Dr. Mahmoud El-Halwagi for taking the time of refining my research with your insightful comments.

I want to extend my gratitude to Dr. Eric W. Lemmon and Dr. Vincent Arp from NIST for sharing with me your invaluable expertise on equations of state. I learnt incredible things from you and those allowed me to complete my research project successfully. Dr. Lemmon, thank you for giving me the chance to work with you on such important endeavor.

Thanks also go to my friends and colleagues and the Chemical Engineering department faculty and staff for making my time at Texas A&M University an unforgettable experience. "There is a spirit can ne'er be told," they say, and it is the spirit of all the stunning people I was lucky enough to meet during these years in Aggieland.

Finally, my deepest gratitude to my family. Their support is the backup engine that gets me back running whenever my own is failing.

TABLE OF CONTENTS

Page

LIST OF FIGURES

Page

LIST OF TABLES

Page

1. INTRODUCTION

Helium has worldwide importance in various industries, but its supply is limited and declining. Its thermodynamic properties are essential information to use it efficiently. Helium has unique properties. As a consequence, helium is a vital material for many industrial and scientific applications, and often a suitable replacement does not exist. Unlike most substances, every unit of helium produced and utilized eventually escapes the Earth's atmosphere and becomes unavailable for the future. This situation is worrisome given the uses for helium. To illustrate this point, this section also covers information on supply and extraction of helium, and the most common legislation that regulates its use and production in the United States with the intention of conserving as much as possible. Finally, the section examines the relevance of thermodynamic information for helium regarding its extraction and consumption, the current standard equation of state for helium and its problems, and how the new equation of state for helium developed herein solves those problems.

1.1 PROPERTIES OF HELIUM

Helium was essentially unknown before the twentieth century. Its first observation was in spectra collected during the solar eclipse on August 18, 1868. Spectroscopic observations had become common and well-studied since the previous solar eclipse, and at least six observers identified a new line in the atmosphere of the sun. This new line reflected a new element named helium, after the Greek word for sun. Thirty years passed before the first terrestrial observation of helium in 1895 when Sir

William Ramsay and Lord Rayleigh published the same spectroscopic observation of helium in gas evolved from uranium and thorium ores. After this publication, helium appeared in other sources, such as the atmosphere and natural gas.

Since its discovery in 1868, the unique properties became interesting both to scientists and industrial personnel. Helium is the second most abundant substance in the universe (after hydrogen) and contributes about 25% of the mass of the universe. However, the concentration of helium in our terrestrial atmosphere is only 0.0005% by volume [1]. The helium atom has the smallest volume of all elements and has the second lightest mass. It has a very stable and symmetrical structure, which makes it chemically and radiologically inert. The nucleus of the atom consists of two protons and either one or two neutrons, depending upon the isotope. Two isotopes, He-3 and He-4, form natural helium. The concentration of He-3 in natural helium is very small it varying from $2x10^{-8}$ to $1.2x10^{-5}$ % depending upon the sample. This work concentrates upon Helium-4, which is the most common form of helium.

Helium is also the element with the highest ionization potential which impedes the formation of stable compounds between helium and other elements. Interactions between helium atoms are very low as well, and the liquefaction temperature of helium is the lowest of all of the gases, and it does not freeze as the temperature approaches absolute zero. For instance, helium-4 liquefies at 4.2 K under one atmosphere pressure, whereas hydrogen does the same at 20.4 K and neon around 27.1 K. Because helium has the lowest boiling point among all elements, liquid helium provides the lowest operating temperatures of any refrigerant.

The first industrial application of helium was for lifting, specifically as a substitution for hydrogen in zeppelins, balloons and blimps. Although hydrogen provides more lifting power than helium (because is lighter), helium is preferable given the explosion hazards related to hydrogen. The properties that make helium ideal for lifting, lightness and chemical inertness, also are attractive for other applications. Other unique characteristics of helium are its thermal conductivity and diffusivity. The thermal conductivity of helium is about six times greater than that of other gases, and helium atoms can diffuse without major difficulty through solid materials. These properties are crucial for the fabrication of optical fibers in which the high thermal conductivity is advantageous during the heat treatment part of the fabrication, while the high diffusivity of helium through glass assures that no bubbles remain trapped in the fiber that might affect normal performance of the glass.

The low boiling point of helium is important for purging, pressurizing and for cryogenic applications. This latter use represents the largest single category of applications by percentage of helium consumed. These range from individuals engaged in small-scale cryogenic research to large groups using high-energy accelerators and high-field magnets. Cryogenic applications also include medical uses in equipment such as superconducting quantum interference devices (SQUIDS) and magnetic resonance imaging (MRI) devices. The ability to remain fluid at temperatures close to absolute zero is also important to cool metal alloys below their critical temperatures when creating superconductors, which are used in advanced physics research for the experimental treatment of various cancers and the measurement of properties of

materials at very low temperatures. Because helium is also used for purging and pressurizing systems, it is a crucial substance in United States space exploration and defense efforts. The National Aeronautics and Space Administration (NASA) and the Department of Defense (DOD) use huge amounts of helium, because it is the only gas that can purge and pressurize tanks and propulsion systems for rockets fueled by liquid hydrogen and oxygen. Helium is the only candidate for this role because it is the only element whose boiling point is lower than that of hydrogen Other gases would freeze into pellets that could damage the engine of the equipment.

In addition to the aforementioned properties, liquid helium is of great scientific interest because it undergoes a rare phase transition, called λ-transition, to a superfluid liquid phase (helium II) state when the temperature is lower than 2.2 K. The superfluid state is the macroscopic manifestation of a quantum fluid explained by a phenomenon known as Bose-Einstein condensation [2] [3]. When superfluid, helium is viscosity-free and experiences an extraordinarily high thermal conductivity (about one million times greater than its conductivity in the normal phase) [4]. Last but not least, helium is also a reference fluid in thermometry. The current scientific temperature scale (ITS-90) was defined utilizing helium as a standard in several ranges of temperature [5]. All these unit properties appear in Figure **1**.

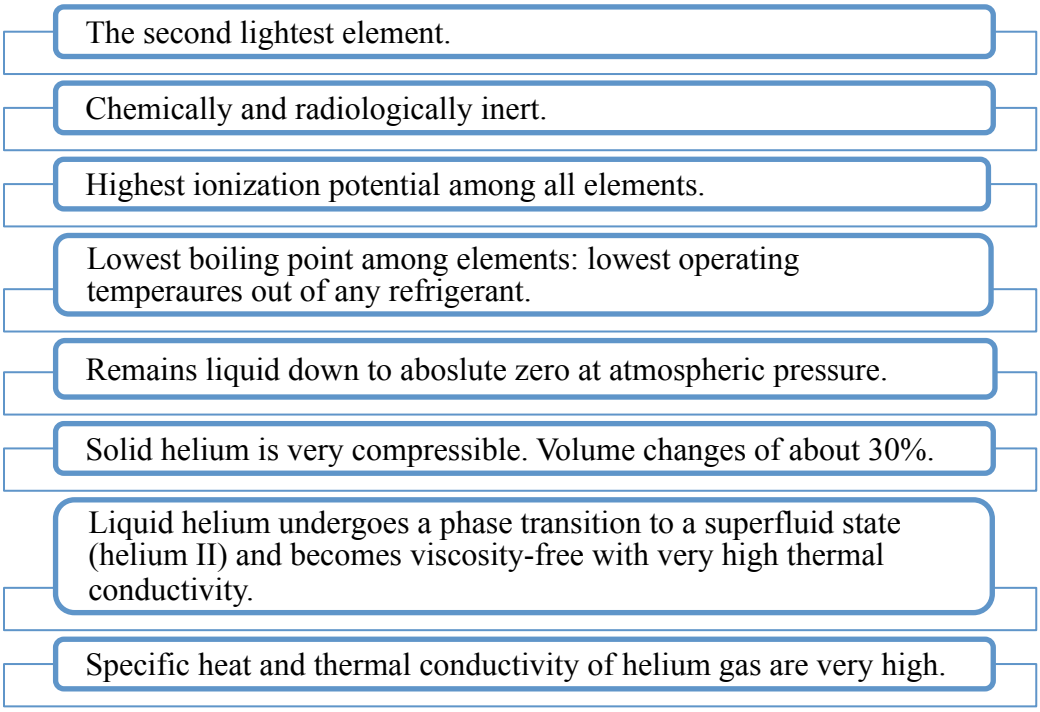

Figure 1. Unique properties of helium.

1.2 SUPPLY AND USES OF HELIUM

The remarkable properties of helium assure the use of helium for many applications. However, many still do not recognize the importance of helium in industry, military and civilian aerospace applications, medical purposes and cutting-edge research. The applications and statistical data presented herein are subject to the information provided by the Bureau of Land Management (BLM), part of the U.S. department of Interior; more specifically by the Federal Helium Program. The Federal Helium Program, established in 1925, seeks to ensure supplies of helium for the Federal Government for defense, research, and medical purposes. With time, the program has

evolved into a conservation program with a primary goal of supplying the Federal Government with high-grade helium for high-tech research and aerospace purposes.

The most recent change of the program occurred through the Helium Privatization Act of 1996, which redefined the primary functions of the program to operate and maintain a helium storage reservoir and pipeline system, provide crude helium gas to private companies, evaluate the Nation's helium-bearing gas fields, and provide responsible access to federal land for managed recovery and disposal of helium.

Helium became a matter of crucial attention the United States government during World War I. The Army recognized it as a safe, noncombustible alternative to hydrogen for use in buoyant aircraft. The Federal Program, started in 1925, was to satisfy the defense needs of the nation. The Bureau of Mines built and operated a large helium extraction and purification plant north in Amarillo, Texas, that started operating in 1929. From 1929 to 1960 the federal government was the only domestic producer of helium. During and after World War II the demand for helium increased. As a result, the Congress passed amendments to the Helium Act in 1960. The amendments provided incentives for private natural gas producers to strip helium from natural gas and sell it to the government. Some helium was also used for research, the NASA space program, and other applications, but most was injected into a storage facility known as the Federal Helium Reserve. Federal demand for helium decreased after the war, and by the 1990s private demand for helium far exceeded federal demand. The 1996 Helium Privatization Act redefined the government's role in helium production. The Bureau of Land Management was made responsible for operating the Federal Helium Reserve and

providing enriched crude helium to private companies. Figure **2** shows the major helium-bearing natural gas fields managed by the BLM today. Historically, the fields around Amarillo, TX have been the principal sources of helium. Recently, natural gas fields in Wyoming with rich helium and other non-fuel content have become a new potential source of helium.

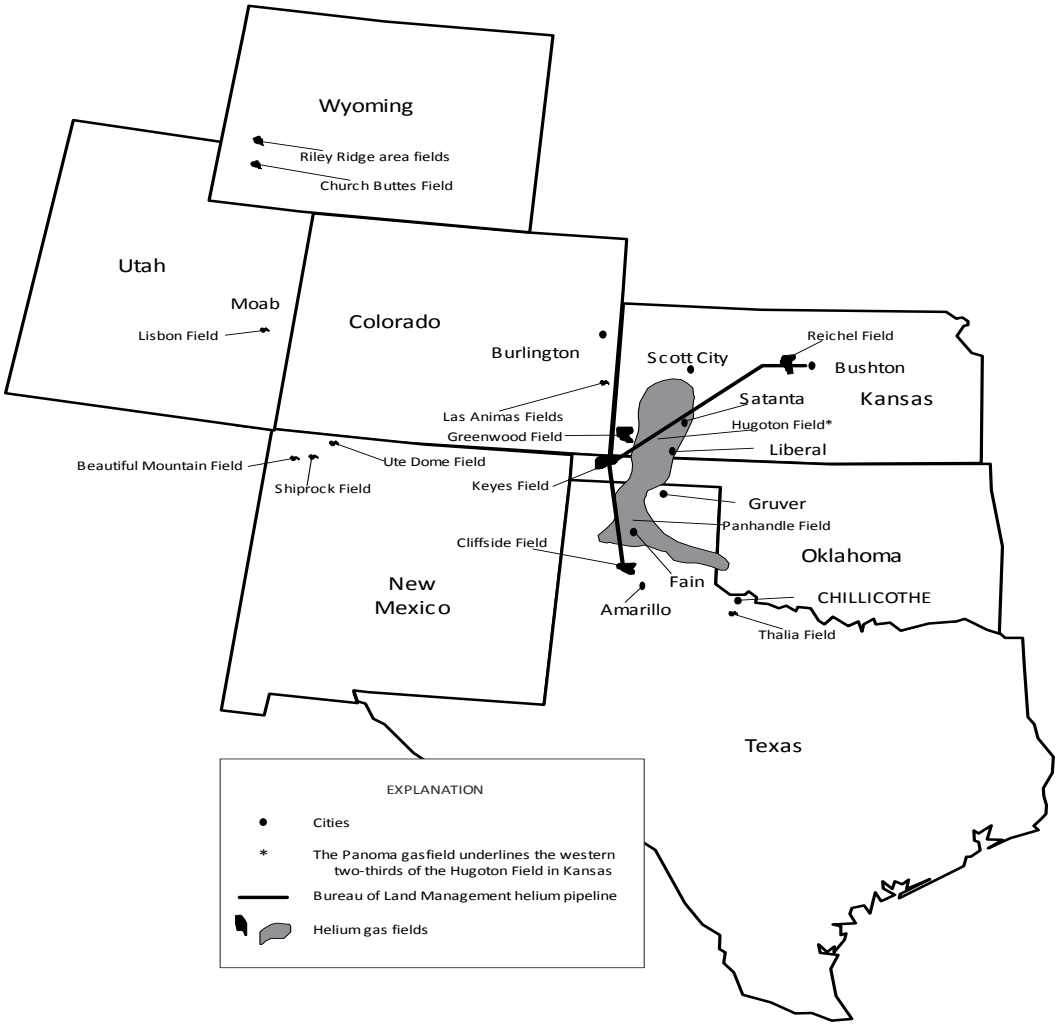

Figure 2. Major U.S. helium-bearing natural gas fields. *Acknowledgement:* U.S.G. Survey. Helium statistics-Historical statistics for mineral and material commodities in the United States [6].

Three ways exist to recover helium from natural gas in an economically feasible manner:

- As a secondary product during the production of methane or natural gas liquids (NGLs), requiring an original concentration of helium greater than 0.3 %
- Direct production of helium when the concentration of helium and other non-fuel constituents is relatively high to justify their extraction, requiring an original concentration of helium greater than 0.3 %
- During the production of liquefied natural gas (LNG), most likely liquid methane. Helium is extracted from the tail gases, the gases that remain after the methane has been liquefied. The helium concentration in those tail gases is much higher than in the original gas, allowing the economical extraction of helium even through the original natural gas might contain as little as 0.04 percent helium.

Only two reserves outside the United States are available, and they have been exploited for so many years that they are considered very mature wells by now; this is the main reason why the rest of the world has relied upon the United States as the principal source of helium. Figure 3 exhibits the amount of helium recovered and sold by the United States up to 2010 [6]. The report shows that the recovery process in the country has changed to a point that suggests the net stored helium flow is negative. This is a consequence of the maturing process of the Hugoton field in the USA, and also the effect of legislation that stopped the national production of helium: The Helium Privatization Act of 1996, Public Law 104.273 directed the Federal Helium Program to

discontinue production and sale of refined helium by April 9, 1998. The Act also directed the Government to offer for sale the helium stored in the Federal helium reserve, in excess of 600 million cubic feet, between January 1, 2005, and January 1, 2015 [6]. On the other hand, the development of large LNG plants has brought hope for new sources of helium in the world. Those plants appear mainly in Algeria, Qatar, and Russia, with smaller facilities in Australia. As a matter fact, projections for world production of helium in 2015 and 2020 favor offshore recovery rather than national production. Figure 4 illustrates this assertation.

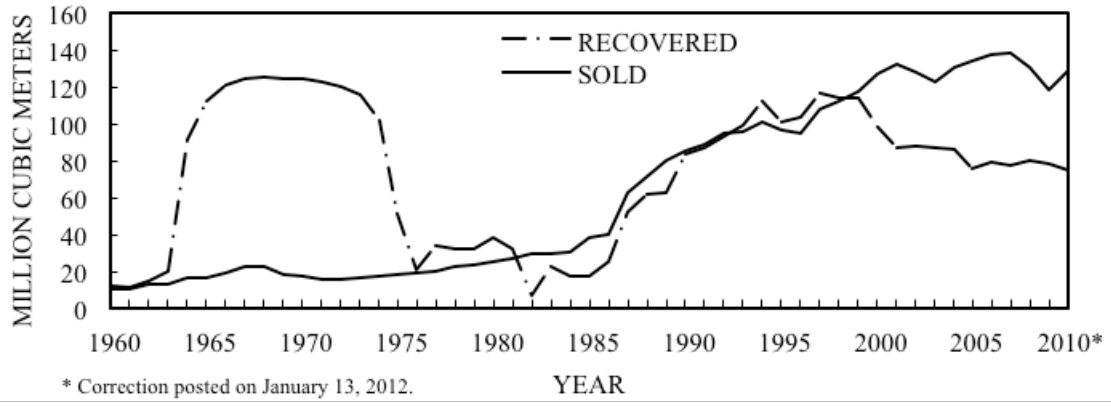

Figure 3. Helium recovery in the United States. *Acknowledgment:* U.S.G. Survey. Helium statistics-Historical statistics for mineral and material commodities in the United States [6].

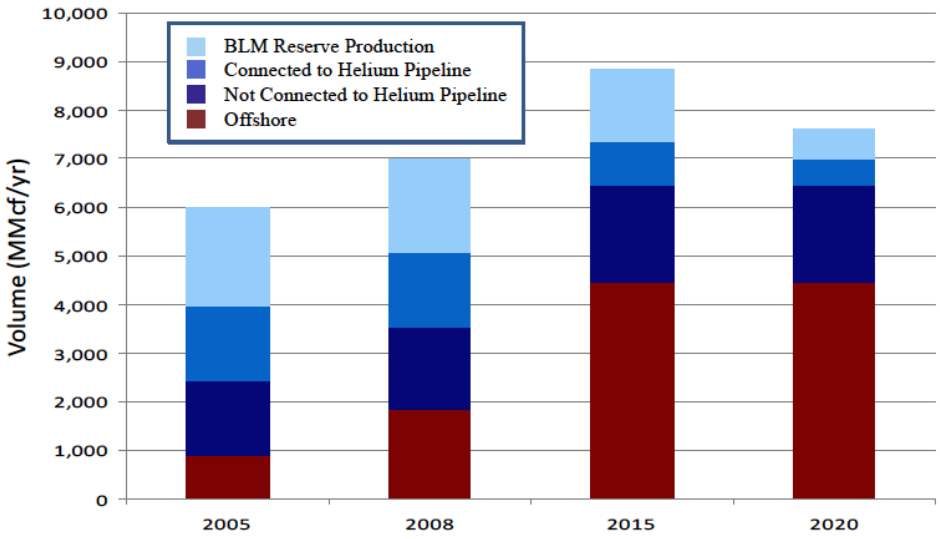

Figure 4. Actual (2005 and 2008) and estimated (2015 and 2020) crude helium capacities by crude helium source. *Acknowledgment:* U.S.G. Survey. Helium statistics-Historical statistics for mineral and material commodities in the United States [6].

In Figure 4, light blue refers to helium available from selling the federal helium reserve; medium blue represents crude helium produced from neighboring natural gas fields connected to the helium pipeline; dark blue denotes domestic helium resources, principally in Wyoming, not connected to the helium pipeline; brown denotes foreign sources of helium [6].

Regarding current production of helium, the latest data reported by the U.S. Geological Survey refers to 2010. Table **1** summarizes this information.

Table 1. Helium recovery in the United States. *Acknowledgment:* U.S.G. Survey. Helium statistics-Historical statistics for mineral and material commodities in the United States [6]. (Thousand cubic meters).

	2006	2007	2008	2009	2010
Crude helium:					
Bureau of Land Management (BLM) sold (in-kind and open market)	63,500	58,800	50,300	30,200	66,000
Private industry:					
Private helium accepted and stored by BLM	18,100	15,800	21,600	15,800	12,400
Helium withdrawn from storage	-75,800	-76,500	-71,500	-55,400	-65,200
Total net helium put into storage	-57,700	-60,700	-49,900	-39,600	-52,800
Grade-A helium:					
Private industry sold	137,100	137,700	129,500	117,600	127,900*
Total helium stored	-57,700	-60,700	-49,900	-39,600	-52,800
Helium recovery from natural gas	79,400	77,000	79,600	78,000	75,100*

[1]Negative numbers denote a net withdrawal from BLM's underground storage facility, a partially depleted natural gas reservoir at the Cliffside field near Amarillo, TX.

*Correction posted on January 13, 2012.

A common trend is the utilization of stored helium to supply most of the current demand. The BLM classifies demand for helium into seven categories: cryogenics, pressurizing and purging, welding, atmospheric control, leak detection, breathing mixtures, lifting, and other uses. Figure 5 presents the percentage of helium and the amount in million cubic meters in each application.

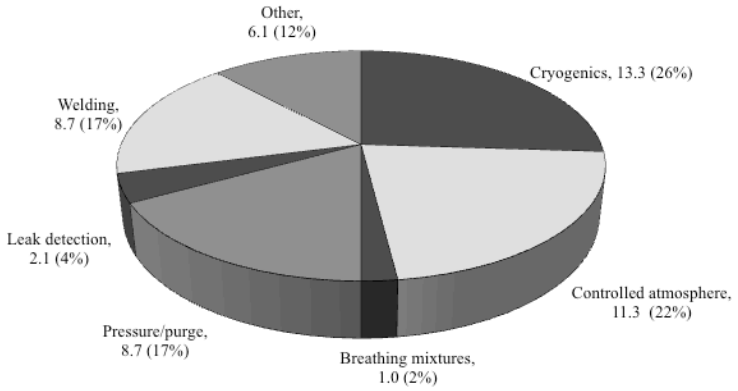

Figure 5. Estimated helium consumption, by end use, in the United States during 2010 - quantities in million cubic meters. *Acknowledgment:* U.S.G. Survey. Helium statistics-Historical statistics for mineral and material commodities in the United States [6].

The first observation in Figure 5 is that most helium consumed is used for scientific and industrial applications that require very low temperatures, such as MRI equipment. In third place lies the pressurizing and purging that involves space exploration and national defense purposes. Controlled atmospheres examples are the fabrication of optical fibers and superconductor manufacturing. Within "other" is the implementation of helium as a lifting gas, application that is most common among the public but one of the least relevant.

1.2.1 Helium in cryogenics

Cryogenics represents the largest use of helium. The main uses of helium in the cryogenics category are: magnetic resonance imaging, semiconductor processing and fundamental research at low temperatures. In respect of magnetic resonance imaging, liquid helium cools the superconductor magnets employed in many of these devices. The low temperatures available from helium and its low price make it desirable for this diagnostic tool. There are more than 4000 MRI machines in the United States, and this number is expected to grow about 15 % per year. This value makes United States one of the countries with the majority of superconducting devices in the world, and this is achieved because it is relatively simple and economic to obtain liquid helium in the country. An important point is that no substitute exists for this purpose. Perhaps using a high temperature superconducting wire might allow the implementation of other fluids at higher temperatures but the cost of doing so would be 500 times higher.

The semiconductor industry also uses helium in the fabrication of silicon wafers. Liquid helium cools superconducting magnets that are necessary to stabilize hot bubbles in semiconductor materials.

The use of helium for large-scale research focuses upon implementation of superconducting magnets and superconducting microwave and radio-frequency devices that are key parts of large, charge-particle accelerators for nuclear physics investigations. The cryogenic facilities used in accelerator plants must provide significant refrigeration (tens of kilowatts) to cool accelerator rings that may be up to 27 km in diameter [4]. These systems not only need the low liquefaction point of helium, but also its high thermal conductivity to assure constant temperature throughout the operation. Given the combination of these two properties, helium is the only refrigerant that can accomplish this particular job.

Small-scale research that requires helium mostly occurs in national laboratories and universities. The areas of science associated with liquid helium are materials science and engineering, condensed-matter physics, chemistry, astronomy and astrophysics. For example, liquid helium is necessary to cool superconducting magnets used in NMR equipment and hence supports the identification of unknown structures of substances. Liquid helium also precools mixtures of He-3 and He-4 in dilution refrigerators for obtaining ultra-low temperatures. When it comes to magnetic measurements, liquid helium is vital in superconducting quantum interference devices (SQUIDs).

Liquid helium supports astronomy and astrophysics by providing refrigeration to infrared detectors at very low temperatures allowing cancelation of noise in very weak signals.

Liquid helium by itself is of great scientific interest because of its λ-transition and superfluid state. The superfluid state is the manifestation of a quantum fluid with rare characteristics that are of interest to the scientific community. The superfluid state is a consequence of Bose-Einstein condensation [3, 7, 8], which essentially states that at very low temperatures a large fraction of atoms of a sample would occupy the lowest energy level generating a condensate. Under such conditions, the atoms look completely identical and all together adopt a single identity. When superfluid, helium is viscosity-free and its thermal conductivity is extremely high. During the lambda transition, helium undergoes singularities in heat capacities that are unique in nature. Having said that, liquid helium as a cryogenic fluid is still very important and irreplaceable and future research on this matter will bring new applications of liquid helium.

1.2.2 Helium in pressurizing and purging

Helium is the only fluid used to pressurize and purge rocket propulsion systems, and it be so as long as the propellant is a combination of liquid oxygen and liquid hydrogen. Helium gas pressurizes the propellant tanks for the engines. Pressure-fed propulsion systems also provide engine-chamber pressurization. Then, helium gas purges the propellant feed systems for liquid-hydrogen engines. Helium is unique in this

role because its normal boiling point is lower than that of hydrogen. Other gases would either freeze and damage the engine, or react with the hydrogen.

This application is common in the Army or at the National Aeronautics and Space Administration (NASA). The use of helium for these purposes should grow dramatically with the planned construction of a new International Space Station. Because helium lacks a replacement for this endeavor, recycling helium and maximizing efficiency of its use is a current concern for aerospace engineers. In addition, they hope to avoid cryogenic propellants. If that happens, the demand of helium to pressurize and purge would decrease.

1.2.3 Helium in welding

Helium has use in arc welding and laser processing. In the former case, gas metal arc welding and gas tungsten arc welding use helium. The properties of helium involved in these processes are high ionization potential, high thermal conductivity and its inertness. Helium acts as a shielding gas during the first phase preventing atmospheric contamination of the molten metal and stabilizing the arc, and in gas tungsten arc welding it shields the red-hot tungsten electrode from the environment. As a result of using helium, the penetration of the welding is greater including metals with high thermal conductivity and travel speeds are higher allowing greater productivity. Helium is not completely necessary for this application, in countries where helium is hard to obtain, argon serves as another inert shielding gas but the productivity is lower.

Helium is also used as a shielding gas in laser welding with carbon dioxide. Also it is present in the laser gas that accompanies CO_2. Carbon dioxide lasers are used for cutting, drilling, cladding, and heat treatment. However, welding is the only process that also uses helium as a shielding gas. Other inert gases can replace helium in the shielding process, but helium is the only one that prevents the formation of plasma at very high power densities. Other gases would ionize when the power is higher than 5 kW while helium remains unchanged. The presence of helium in the laser gas helps cool the excited carbon dioxide molecules. The percentage of helium in this part of the process is less than for shielding, but it is more crucial and no substitute exists.

1.2.4 Atmospheric control with helium

Helium creates inert atmospheres in many industrial processes. The areas that use helium the most for this purpose are optical fiber manufacturing, plasma-arc coating, plasma-arc melting, and heat treatment. Optical fiber technologies have accelerated the development of modern communications. This industry depends upon helium to enhance the thermal gradient and improve the uniformity of the claddings. Helium also refrigerates fresh fiber, where it is a non-reacting thermal-contact agent. An additional property of helium that is critical to this activity is its diffusivity, which prevents the formation of bubbles in the glass by expelling any traces of air trapped in the glass (they would destroy the fiber's transmission properties). Plasma-arc coating is a process used in the aerospace industry and other industries to apply wear-resistant coatings to critical components. A mixture of 10 percent helium and 90 percent argon is typical. Plasma-

arc coatings applied in 100 per cent argon atmospheres are not as adherent [4]. Plasma-arc melting makes specialty metal billets, such as titanium for jet-engine components. Helium does not have replacement for this application because although argon may provide good inertness, its specific heat is not high enough to create a deep melt in the furnace. The process provides better uniformity and control over the composition and has effectively replaced electron-beam melting, which was the traditional method. The same combination of helium's inertness and high thermal conductivity is useful in other heat treatment processes. For example, nickel-base superalloys cool rapidly in helium atmospheres. Argon can replace helium in special applications.

1.2.5 Helium for leak detection

Helium is a marvelous leak detector because of its low viscosity and large diffusion coefficient, which is a consequence of being such a small molecule. Mass spectroscopy based upon helium as a leak detector is critical for science and technology. Helium-based leak detection also is implemented in the manufacturing of rocket engines and maintenance of vacuum equipment in industry and academia. Indeed, helium leak detection is the standard in any activity requiring leak-tight systems. The usual procedure in leak testing is to spray the area outside the system being tested with helium and then try to detect its presence on the inside using a vacuum environment attached to a mass spectrometer. More sophisticated leak detectors work by filling the system with helium and then checking each single unit of the equipment where the leak may occur using a sniffer connected to a mass spectrometer. Argon could be a replacement for this

service but it would require more elaborated and expensive mass spectrometers, argon leak rates also would be about an order of magnitude smaller, making the device much less sensitive to very small leaks.

1.2.6 Helium as a lifting agent

Lifting is the most widely known application of helium among the public given its use in party balloons. Although hydrogen is the lightest gas, helium assumed the role of lifting gas because its chemical inertness makes it a safer option. Helium replaced hydrogen for blimps in the 1930s after a number of tragic accidents involving hydrogen-filled airships. Helium is used in blimps for advertising, to detect low-flying cruise missiles, and to carry radar equipment to detect drug smugglers along the nation's borders [4]. One future use of helium is as a lifting gas in devices to lift heavy loads for construction.

1.2.7 Helium in breathing mixtures

Deep-sea divers and individuals working under high atmospheric pressures for extended periods of time breathe mixtures of helium and oxygen. Helium is preferable to nitrogen because the absorption and releasing process into and out of the body is faster, thus reducing decompression times.

1.2.8 Potential uses of helium

Potential uses of helium still rely upon its availability and price in the market. Most of the potential uses have links to advances in science and technology at low temperatures. For example, superconductors offer intriguing prospective applications, and liquid helium is vital for cooling such devices. Superconducting magnets could play a role in transport technology by implementing magnetic levitation. This is very promising because if trains did not contact their tracks, they could travel much faster without frictional loses. Another use could be superconducting magnetic storage devices (SMES) that store energy in magnetic fields. SMES devices contain superconducting coils that can be fed and discharged using a switch connected to the power grid. SMES devices are one of the few ways to store energy without converting it into mechanical or chemical energy.

In addition to these previous applications, superconducting technology is an important, secondary technology for plasma confinement fusion. Helium would be appropriate to cool down the superconducting magnets that generate the magnetic containment environment. Other areas that might develop during the coming years that require helium for their operations are superfluid applications, such as in lubrication, and superconducting electronics. Superconducting systems using Rapid Single-Flux Quantum Logic are currently the leading technologies under consideration for petaflop computing. Liquid helium or cryo-coolers using helium are necessary for all the products currently commercial or under development.

1.3 IMPORTANCE OF ACCURATE THERMODYNAMIC PROPERTIES FOR HELIUM

Because helium and its unique properties are critical in several important applications in industry, science, federal agencies and national defense, it is necessary to face the problem that every unit of helium used is another unit of helium lost to the atmosphere. This situation is worrisome because no replacement for helium exists in many applications, and the sources of helium are limited. This fact motivated a new law passed by the U.S. Senate in March of 2012 known as the "Helium Stewardship Act of 2012," in which they recognize the current importance of helium and encourage research studies on its extraction, conservation, separation and possible replacement in a manner that protects the interests of private industry, the scientific, medical, and industrial communities, commercial users, and Federal agencies.

Accurate thermodynamic information for helium is absolutely essential to optimize existing processes and applications that involve helium and to assure efficient improvement of extraction, conservation, storage and final use of the fluid. Data are mandatory to design equipment for either the extraction of helium or its use in the industrial and scientific communities. In the past, many laboratories have conducted measurements on properties of helium. Thermal, volumetric and acoustic properties as wells as critical parameters and virial coefficients have been collected over a wide range of conditions (even at very low temperatures) [1]. However, tables of data are impractical to implement in computer-aided design and insufficient to cover all conditions of interest, hence, correlations have begun to replace tables. Most

correlations exist for particular properties such as virial coefficients [1, 9-13], heat capacities [1, 14-17], velocity of sound [17-19], vapor pressure [20-24], and Pressure-Volume-Temperature (PVT) data [25-27]. Even though these approaches may be accurate over a limited range, they often fail under other conditions or when predicting a derived property different from the one used to fit the data. Today, one of the most accurate sources of thermodynamic property information is an empirical multiparameter equation of state [28]. These equations have become reference sources of thermodynamic data for several pure substances [29-31], and many engineering and scientific applications that require high accuracy predictions of various thermodynamic properties (not only the explicit variables of the equation) use them over wide ranges of conditions. McCarty and Arp [32] published the current, standard equation of state for helium in 1990. It covers both superfluid and normal fluid from 0.8 to 1500 K at pressures up to 2000 MPa. Although McCarty's equation of state represents a significant contribution to helium-related research, it has some issues requiring correction:

- Although the selected data are high quality, he used only 10 sets of data, which are not a good representation of all the experimental work done on helium. Also, the equation only considers one set of data for heat capacities and two for sound speed. This does not represent a heterogeneous compilation. Another important point regarding the data is that Donnelly et al. [33] provided an important compilation of helium data at low temperatures after McCarty published his equation.

- Most of the data are not reproduced within their experimental uncertainties. This is a principal goal when developing equations of state. However, helium is a difficult fluid to fit because of its peculiar properties.
- Caloric properties yield unreasonable results and affect other properties are, such as acoustic properties.
- Unreasonable behavior in regions lacking data is a fault.
- The temperature values used for all data sets do not correspond to the current standard temperature scale (ITS-90).
- Comparisons to theoretical calculations of helium thermodynamic properties are absent.
- McCarty's equation of state appears in terms of pressure, thus it is not a "fundamental equation of state." Equations of state (like BWR-type equations) require integration to estimate caloric properties. In addition, pressure-explicit equations require supplementation by a temperature dependent correlation for the heat capacity. The integration leads to severe restrictions upon exponential terms in the equation [28].

The ultimate motivation behind this doctoral research proposal is the need of a new source of high-quality thermodynamic information for helium. This need is a consequence of the importance of helium for both industry and scientific research, and the deficiencies of the current reference equation of state for helium.

1.3.1 Objective

The goal of this work is to design a new, wide-range equation of state for helium 4. Figure 6 is a general phase diagram for helium 4 at low temperature. The new equation of state focuses upon the normal fluid part (gas and liquid He-I) and the transition to the superfluid region liquid He-II. The expected limits of the equation of state are 2.18K to 1500 K up to 2000 MPa.

In order to achieve the global objective, the development of the new equation of state focused upon several characteristics related to the following goals:

- Goal 1. Development of a multiparameter and fundamental equation of state for normal fluid behavior.

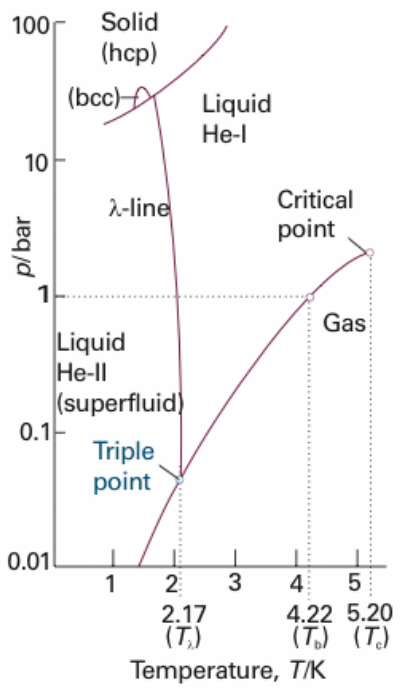

Figure 6. Phase diagram of helium 4 at low temperature. Several triple points can be observed in solid phases in equilibrium with fluid phases.

Multiparameter equations of state in terms of pressure or compressibility factor involve integration to calculate caloric properties and require supplementary equations for the heat capacity. Moreover, the integration constrains exponential terms in the equation of state [34]. A fundamental equation of state is more flexible with regard to the terms, and all thermodynamic properties are available from its derivatives. Of the thermodynamic potentials, one could use a Gibbs free energy-based or a Helmholtz free energy-based equation of state because their natural variables are considerably easier to deal with when measuring (temperature and pressure for the former case and temperature and density for the latter one). However, at the phase boundary the Gibbs energy has a discontinuity in slope between the liquid and vapor phases. Because the inputs are temperature and pressure, it is impossible to make an equation of state that does both liquid and vapor. Therefore, one of the goals is to develop a fundamental equation of state based upon the Helmholtz free energy potential.

- Goal 2. Rigorous and broad data selection process.

One relevant goal of this research project is to include a variety of experimental data covering several thermodynamic properties not included in previous equations. The new equation utilizes not only PVT, heat capacities and speed of sound data but also data on second, third and fourth virial coefficients, critical point, latent heat of vaporization, internal energy, enthalpy, derivative of pressure with respect to temperature, entropy and saturation data (vapor pressures, vapor densities, liquid densities and saturation heat capacity). The whole idea is to design an equation of state that represents all types of data. By fitting multiple properties, it is possible to improve

thermodynamic consistency among all properties. Given the current importance of quantum mechanics calculations, it is reasonable to include *ab initio* predictions of second, third and fourth virial coefficients in the new, multiparameter equation of state.

- Goal 3. Use the current temperature scale standard, ITS-90.

Data on helium are available form more than 50 years ago with values reported using different temperature scales. In the new equation of state, all data in ITS-27, IPTS-48, IPTS-68, NBS-55, IPTS-58, IPTS-68 and EPT-76 temperatures scales are converted to ITS-90. McCarty's equation of state uses the EPT-76 scale. The entity in charge of temperature scale standards is the Bureau International des Poids et Mesures (BIPM), which ensures world-wide uniformity of measurements and traceability to the International System of Units (SI).

- Goal 4. High accuracy.

The equation of state must reproduce experimental values with low deviations. Although the ultimate goal is to be within the experimental uncertainty, it is reasonable to get an equation that does better than or equal to the current standard, that is to reach uncertainties lower than 1% in densities at low temperatures (<20 K), 0.1% at temperatures between 200 and 400 K, 3% in the speed of sound in the liquid phase, 0.1% in the speed of sound between 100 and 500 K, and 5% in heat capacities.

- Goal 5. Extrapolation capabilities.

This is a key point to improve upon the current equation of state. Unreasonable behavior in regions with no data must not exist.

- Goal 6. Minimize the number of parameters used to fit the equation.

This goal relates to future application of the equation. A multiparameter equation of state with the least possible number of terms is desirable to decrease the computational time of calculations. However, decreasing the number of parameters must balance with the accuracy that more parameters might offer.

- Goal 7. Reasonable transition to the superfluid region.

Once a sufficiently good equation of state is available for the normal region, a different procedure predicts basic elements of the superfluid transition and matches the normal behavior at the lambda line (transition between normal fluid and superfluid).

Accomplishing each goal also accomplishes the global objective. As a result, the equation of state for helium-4 presented in this document represents the most suitable candidate to replace McCarty's equation of state as the new standard for helium. This doctoral project includes cooperation with the National Institute of Standards and Technology (NIST). Dr. Eric Lemmon at the Thermophysical Properties Division of NIST, provided the numerical methods used during the fitting procedures, and made his expertise available during the work.

2. EQUATIONS OF STATE – LITERATURE REVIEW

This section presents a general literature review of equations of state development through the last century. Research on and continuous about the behavior of fluids has existed for many years, however starting with the findings and results of scientists such as Boyle and Dalton in the 17th century, interest on this field increased and led to several theories and models to describe the thermodynamic behavior of fluids. "Modern" equations of state began with van der Waals in 1873 [35], not only because his predictions were closer to the real behavior of gases and liquids, but also because van der Waals introduced for the first time two important physical effects: attractive and repulsive interactions. As seen throughout this section, the reader can see how van der Waals was the inspiration for both cubic equations of state and non-cubic equations of state. The former case refers to equations with cubic dependence upon density, and the latter case mostly reflects improvements of repulsive interactions using hard-sphere models. Parallel to the progress of van der Waals- type equations of state was the derivation of virial equations of state, which added a physical meaning to their functional form because of their basis in statistical mechanics. Finally, this section contains a brief description of molecular-based equations of state. Although these equations involve several complex molecular models for interactions, generally they offer an adequate functional form for other semi-empirical equations.

2.1 VAN DER WAALS AND CUBIC EQUATIONS OF STATE

After Boyle and Marriot established the ideal gas equation of state in the 17th century [35], description of properties of real fluids became a priority in the scientific community. However, a practical and reasonably accurate form did not evolve until 1873 when van del Waals proposed a cubic equation in molar volume that could represent both gas and liquid phases, supercritical states, and vapor-liquid equilibrium qualitatively correctly [36]. The van der Waals equation also contains a "hard sphere term + attractive term:" van der Waals assumed molecules have a finite diameter, which decreases the available volume for molecular motion and increases the number of collisions with walls thus increasing the pressure. He defined the actual volume available for molecule motion as v-b, where b is the volume of the molecules (a constant) for each fluid. Besides this effect, van der Waals considered that intermolecular attractions decrease the pressure, and that this event is directly proportional to the number of molecules in a vessel, and inversely proportional to the volume v of the vessel. He postulated this term as $(-a/v^2)$, where a corresponds to a fluid specific parameter. Then, it is logical to think that both effects would lead to the ideal gas law at the zero density limit; so the resulting van de Waals equation is,

$$\left(p+\frac{a}{v^2}\right)(v-b)=RT \tag{1}$$

or in terms of pressure,

$$p = \frac{RT}{v-b} - \frac{a}{v^2} \tag{2}$$

in which the two terms correspond to repulsive and attractive contributions to pressure respectively. Interestingly, the attractive term corresponds qualitatively to the quantum mechanical prediction for molecules at large separations. Information of the critical point of the fluid is necessary to determine *a* and *b* for the substance. For that purpose, the following critical constraint applies,

$$\left(\frac{\partial p}{\partial v}\right)_T = \left(\frac{\partial^2 p}{\partial v^2}\right)_T = 0 \tag{3}$$

knowing T_c, p_c, and v_c and solving Eq. (3) results in

$$a = \frac{27R^2T_c^2}{64\,p_c} \tag{4}$$

$$b = \frac{RT_c}{8\,p_c} \tag{5}$$

although van der Waals equation was a relevant contribution to explain qualitatively and from a theoretical point of view the behavior of fluids, the accuracy was not very good. For example, the critical compressibility factor for mixtures and pure components predicted by van der Waals is around 0.375, but the actual value for most hydrocarbons is around 0.27 [37]. This fact combined with lack of accuracy in other regions was the driving force that led to new cubic equations of state resulting from modifications of the van der Waals expression.

In 1949 Redlich and Kwong [38] modified empirically the attractive term of van der Waals equation making it temperature dependent; resulting in

$$p = \frac{RT}{v-b} - \frac{a}{v(v+b)T^{0.5}} \tag{6}$$

$$a = 0.4278\frac{R^2T_c^{2.5}}{p_c} \tag{7}$$

$$b = 0.0867\frac{RT_c}{p_c} \tag{8}$$

the Redlich-Kwong equation of state (RK) has been used successfully in several cases for the prediction of properties of gas mixtures [39-43], the calculation of fugacities, and high-pressure phase equilibrium of mixtures [44, 45]. However, the Redlich-Kwong equation still could not estimate properties of both gas and liquid phases. The temperature dependence of the attractive term was still too simple to determine vapor pressures. Also, liquid volumes had insufficient accuracy [46]. Further research in this field sought to improve the temperature dependence of the attractive term for the calculation of vapor pressures, and to enhance the functional form of the equation for better prediction of volumetric properties.

Trying to improve the accuracy of Redlich-Kwong equation of state, Soave proposed a more general temperature-dependent term in the equation by making the parameter *a* change with temperature [47],

$$p = \frac{RT}{v-b} - \frac{a(T)}{v(v+b)} \tag{9}$$

$$a(T) = 0.4274\frac{R^2T_c^2}{p_c}\left\{1+m\left[1-\left(\frac{T}{T_c}\right)^{0.5}\right]\right\}^2 \tag{10}$$

$$m = 0.480 + 1.57\omega - 0.176\omega^2 \tag{11}$$

$$b = 0.08664 \frac{RT_c}{p_c} \tag{12}$$

this is the so called Soave-Redlich-Kwong equation of state, in which ω is the acentric factor of the fluid. For the validation of his equation, Soave calculated vapor pressures for a variety of hydrocarbons and their binary mixtures and demonstrated that his new equation could fit phase equilibrium data and critical behavior better than the simple Redlich-Kwong equation. The Soave-Redlich-Kwong equation of state (SRK) played a relevant role in the progress of cubic state and represented a vote of confidence to these equations as tools for vapor-liquid equilibrium calculations.

Peng and Robinson in 1976 redefined *a(T)* as well as the denominator of the attractive term [48]

$$p = \frac{RT}{v-b} - \frac{a(T)}{v(v+b)+b(v-b)} \tag{13}$$

$$a(T) = 0.45724 \frac{R^2 T_c^2}{p_c} \left\{ 1 + k \left[1 - \left(\frac{T}{T_c} \right)^{0.5} \right] \right\}^2 \tag{14}$$

$$b = 0.07780 \frac{RT_c}{p_c} \tag{15}$$

Peng-Robinson equation of state improves the prediction of liquid volumes and the critical compressibility factor compared to previous cubic equations of state. Later in 1977, Peng and Robinson showed how to use their equation to calculate saturation and critical properties for pure components and mixtures [49]. The results suggested the Peng-Robinson equation of state performs as well or better than Soave-Redlich-Kwong.

Since then, the Peng-Robinson equation of state has found wide use in academia and industry because it offers relatively accurate results with practical computational usage.

Other cubic equations of state have appeared following the same idea of including empirical expressions in the attractive term of van der Waals that allow better accuracy. Some good examples are the equations from Patel-Teja [50] and Stryjek-Vera-Peng-Robinson [51-53]. The results of several studies indicate that cubic equations of state need at least three parameters for an acceptable representation of liquid and vapor volumes (3 - 4 %). Also, a certain temperature dependence is necessary to predict vapor pressures within 1 - 2 % when the fluid parameters come from the critical constraints, or 0.5 % when the parameters come from fitting pure component data [46]. The most accurately derived property from these equations is the heat of vaporization. This result might lead one to expect accurate vapor pressures predictions when using the heat of vaporization with the Clasius-Clapeyron equation. Cubic equations predict critical behavior poorly because of the rigidity of their form. They also predict second-order derivatives, such as caloric properties, with very low accuracy. However, despite these difficulties, cubic equations of state are a good balance between accurate volumetric properties prediction and computational cost, and they still find use in semi-quantitative calculations of equilibrium phenomena, process design and fluids simulation. Another advantage is that cubic equations of state can be adjusted in several ways to estimate acceptable results for the majority of practical applications [54], so cubic equations of state have a stable position in the field.

2.2 VAN DER WAALS AND NONCUBIC EQUATIONS OF STATE

As shown in section 1.1, most cubic equations of state are only empirical modifications of the attractive term in the van der Waals equation. This section focuses upon non-cubic equations of state that originate from modifications of the van der Waals repulsive term or both the repulsive and the attractive term. These equations are more useful at higher temperatures and pressures where the repulsive term is more important than the attractive interactions. These equations fit well to hard-sphere fluid system, which treats molecules as spheres with finite volume and are defined by a potential of interaction that considers only repulsive forces [55].

The non-cubic equations that involve only modification of the repulsive term of van der Waals have the following form

$$p = \frac{RT}{v} Z^{hs} - \frac{a}{v^2} \tag{16}$$

in which Z^{hs} is the hard-sphere compressibility factor, which is a function of the packing fraction of the system, η, defined by $\eta=b/4v$. In this definition, b the molecular covolume from the van der Waals equation of state.

Some famous expressions for the hard-sphere compressibility factor are:

Reiss-Frisch-Lebowitz [56],

$$Z^{hs} = \frac{1+\eta+\eta^2}{(1-\eta)^3} \tag{17}$$

Thiele [57],

$$Z^{hs} = \frac{1+2\eta+3\eta^2}{(1-\eta)^2} \tag{18}$$

Ree-Hoover [58],

$$Z^{hs} = \frac{1+1.75399\eta+2.31704\eta^2+1.108928\eta^3}{1-2.246004\eta+1.301056\eta^2} \tag{19}$$

Guggenheim [59],

$$Z^{hs} = \frac{1}{(1-\eta)^4} \tag{20}$$

Carnahan-Starling [60],

$$Z^{hs} = \frac{1+\eta+\eta^2-\eta^3}{(1-\eta)^3} \tag{21}$$

Hall [61],

$$Z^{hs} = \frac{1+\eta+\eta^2-0.67825\eta^3-\eta^4-0.5\eta^5-1.7\eta^6}{1-3\eta+3\eta^2-1.04305\eta^3} \tag{22}$$

Boublik [62]

$$Z^{hs} = \frac{1+(3\alpha-2)\eta+(3\alpha^2-3\alpha+1)\eta^2-\alpha^2\eta^3}{(1-\eta)^3} \tag{23}$$

Erpenbeck-Wood [63],

$$Z^{hs} = \frac{1+1.7227128\eta+2.2532688\eta^2+0.89244864\eta^3-0.34302926\eta^4}{1-2.2772872\eta+1.32624176\eta^2} \tag{24}$$

Malijevsky-Veverka [64],

$$Z^{hs} = \frac{1 + 1.056\eta + 1.6539\eta^2 + 0.3262\eta^3}{(1-\eta)^3\left(1 + 0.056\eta + 0.5979\eta^2 + 0.3076\eta^3\right)} \tag{25}$$

An article by Mulero [55] is an extended review of hard-sphere models for fluids. In general, the Guggeheim equation of state (Eq. (16) combined with Eq. (20)) was the first relatively accurate hard-sphere model, and it can calculate reasonable equilibria close to the critical region. The parameters *a* and *b* come from critical properties. Perhaps the most widely used replacement of van der Waals repulsive term is the equation published by Carnahan and Starling in 1969 (Eq. (16) combined with Eq. (21)). This equation also follows the same predictions obtained from molecular dynamics calculations, and it is accurate for systems composed of nonpolar substances. Also, Carnahan and Starling used virial coefficients to develop their equation, which makes it popular among proponents of statistical mechanics [65]. The equation published for hard-sphere solids by Hall in 1972 (Eq. (16) combined with Eq. (22)) corresponds to an empirical modification of the model proposed by Carnahan and Starling. It agrees well with simulation data and finds use in solid-liquid equilibrium calculations of hard-sphere systems [55]. Boublik in 1981 used the hard-spheres model proposed by Carnahan and Starling as a basis for his equation extended to molecules with arbitrary geometry. He included a nonsphericity parameter α defined as $\alpha = R_o S_o / V_o$, where R_o, S_o and V_o are the mean curvature, mean surface and mean volume of the hard convex molecule respectively. Erpenbeck and Wood [63] fit their own computer simulations and proposed a van der Waals type equation of state with the hard-sphere compressibility factor stated in Eq. (24). The advantage of this equation lies in avoiding singularities for

pressure for some real values of the packing fraction, a problem that has occurred with some empirical equations. However, the Erpenbeck-Wood equation of state cannot reproduce simulation date from other authors. Finally, Malijevsky and Veverka published what is today the most acceptable modern equation for hard-sphere (Eq. (16) combined with Eq. (25)). Its accuracy is slightly better than Carnahan-Starling equation of state, although its functional form is more complex.

Non-cubic equations of state whose only modification to the van der Waals equation of state is in the repulsive term generally do a better job of reproducing volumetric properties at high temperatures and pressures and near the critical region than normal cubic equations of state. However, they are not very good at predicting vapor pressures because their attractive term lacks temperature dependence.

Other equations of state have appeared that change both the attractive and repulsive terms in van der Waals equation, or combine a hard-sphere formulation with an empirical temperature dependence for the attractive part. Carnahan and Starling combined their hard-sphere model with the Redlich-Kwong temperature dependent term

$$p = \frac{RT\left(1+\eta+\eta^2-\eta^3\right)}{v\left(1-\eta\right)^3} - \frac{a}{v\left(v+b\right)T^{0.5}} \tag{26}$$

the results from Eq. (26) revealed that it improved the calculation of hydrocarbon densities and phase equilibria [65]. De Santis in 1976 proved that Eq. (26) fits pure components well from ideal gases to saturated liquid states.

Chen and Kreglewski in 1977 [66] were able to predict phase behavior of fluids by combining the hard-spheres model proposed by Boublik in Eq. (23) with an attractive

term that consists of a power series correlation of simulation data for square-well fluids published by Alder in 1972 [67]. This new formulation is the so-called BACK equation of state [65]

$$p = \frac{RT}{v}\left[\frac{1+(3\alpha-2)\eta+(3\alpha^2-3\alpha+1)\eta^2-\alpha^2\eta^3}{(1-\eta)^3}-\sum_i\sum_j jD_{ij}\left(\frac{u}{kT}\right)^i\left(\frac{v^o}{v}\right)^j\right] \tag{27}$$

in which u is the characteristic energy, v^o is the hard-core volume and D_{ij} are numerical coefficients. They estimated D_{ij} from volumetric data of Argon and treated them as universal constants. The BACK equation assumes the characteristic energy and the hard-core volume are temperature-dependent, and use representations for them from the literature [46, 68]. Finally, experimental data are necessary to determine three parameters.

Christoforakos and Franck in 1986 added a temperature dependent repulsive term to a modified version of the hard-sphere model of Carnahan and Starling [69]:

$$p = \frac{RT}{v}\left[\frac{1+\beta/v+\beta^2/v^2-\beta^3/v^3}{(1-\beta/v)^3}-\frac{4\beta(\lambda^3-1)(\exp(\varepsilon/kT)-1)}{v}\right] \tag{28}$$

in which $4\beta=b(T_c/T)^{0.3}$. The attractive term relates to the virial coefficients of gases from a square-well potential. The parameters ε and λ represent the depth of the well and the width of the well respectively. They applied this equation to high-pressure phase behavior for some binary aqueous mixtures.

Three years later in 1989, Heilig and Franck [70] published a modification of the Carnahan-Starling equation of state with a different attractive term based upon virial coefficients

$$p = \frac{RT}{v}\left[\frac{1+\beta/v+\beta^2/v^2-\beta^3/v^3}{(1-\beta/v)^3}-\frac{B}{v+C/B}\right] \tag{29}$$

in which B and C are the second and third virial coefficients respectively of a square-well fluid.

Another well-known non-cubic equation that enhances both the repulsive and the attractive terms in van der Waals equation is the one developed by Deiters [71]. He proposed a semi-empirical approach with three adjustable parameters a, b, and c,

$$p = \left\{1+cc_0\left[4y-2y^2/(1-y)^3\right]\right\}\frac{RT}{\rho}-aI\left[\exp\left(1/T_{eff}\right)-1\right]\frac{R\rho^2T_{eff}}{b} \tag{30}$$

in which $\rho=b/v$, $y=0.7404\rho$, $c_o=0.6887$, $\lambda=-0.06911c$ and $T_{eff}=(cT/a+\lambda\rho)/\eta$. I is a hard-sphere constant, and packing fractions range from 1 for a dilute gas to 0.46 for dense fluids. The parameter c_o is useful to adjust the Carnahan-Starling model to fit better experimental vapor pressures for Ar, while values of c greater than 1 take into account deviations from spherical geometries. Eq. (30) can predict reasonably accurate vapor-liquid properties for binary mixtures.

2.3 THE VIRIAL EQUATION OF STATE

Almost 30 years after van der Waals published his equation of state, Kammerlingh Onnes [72] introduced in 1901 the virial equation of state,

$$\frac{p}{\rho RT} = Z = 1 + B\rho + C\rho^2 + D\rho^3 + \ldots \tag{31}$$

Eq. (31) is also known as the virial expansion. B is the second virial coefficient, C is the third virial coefficient, D is the fourth, and so on. For pure components, virial coefficients are only function of temperature and hence completely independent of density and pressure. The real advantage of the virial equation of state over other empirical or semi-empirical equations of state is that there is a theoretical relation between the virial coefficients and intermolecular potentials [73]. Statistical thermodynamics provides a way to estimate the virial coefficients as a function of interaction between molecules in isolated clusters. B depends on the interactions between pairs of molecules, C upon interactions in a cluster of three molecules, D upon interactions in a cluster of four molecules, and so on.

Another advantage of virial equations is the possibility of estimating the virial coefficients from experimental data. B is appropriately found from low pressure P-ρ-T data by definition,

$$B = \lim_{\rho \to 0} \left(\frac{\partial Z}{\partial \rho} \right)_T \tag{32}$$

similarly, the third virial coefficient can also be found from low pressure P-ρ-T data,

$$C = \lim_{\rho \to 0} \frac{1}{2!} \left(\frac{\partial^2 Z}{\partial \rho^2} \right)_T \tag{33}$$

this emphasizes the fact that the virial coefficients are properties of the fluid in the limit of zero density. From isothermal data, B can be found as the intercept on the ordinate of $(Z-1)/\rho$ versus ρ, and C as the slope as ρ goes to zero.

It has been observed for several fluids that the virial expression when truncated after the third term gives good representation of the compressibility factor to about half the critical density and fair results up to the critical density. For much higher densities, the virial equation of state provides poor predictions given the lack of experimental and theoretical capabilities to estimate the fourth and higher order coefficients. However, the virial expression is applicable for moderate densities and the study of vapor-liquid equilibria problems [74].

As mentioned before, the importance of the virial expression lies in its relation to intermolecular interactions. In an ideal gas, molecules do not exert any force upon each other. A similar situation occurs for a real gas at low density where all the molecules are so far apart that they do not interact significantly with one another. However, as density increases, molecules interact more frequently. The virial coefficients account for these effects.

From a statistical thermodynamics perspective, virial coefficients are linked to intermolecular potential functions [73]. Consider a simple case of a gas composed of spherically symmetric molecules such as argon or helium. Let $\Gamma(r)$ be the potential energy between such molecules, and r is the distance between molecular centers. The second and third virial coefficients are given as functions of the potential energy and the temperature by,

$$B = 2\pi N_A \int_0^\infty \left[1 - \exp\left(-\Gamma(r)/kT\right)\right] r^2 dr \tag{34}$$

$$C = \frac{-8\pi^2 N_A^2}{3} \int_0^\infty \int_0^\infty \int_{|r_{12}-r_{13}|}^{r_{12}+r_{13}} \left[f_{12} f_{13} f_{23} r_{12} r_{13} r_{23} \right] dr_{12}\, dr_{13}\, dr_{23} \tag{35}$$

where f_{ij}=exp(-Γ_{ij}/kT)-1, k is Boltzmann's constant and N_A is Avogadro's constant. Analogous expressions exist for the fourth and higher virial coefficients. In this context, the virial equation of state applies to stable and electrically neutral molecules. For complex molecules, not only the distance between molecular centers affects the potential function, but aspects such as the spatial geometry and orientation. The accuracy of the virial equation of state from statistical thermodynamics increases as the level of theory becomes deep enough to generate a potential model able to take into account all kinds of interactions [74].

2.4 MOLECULAR-BASED EQUATIONS OF STATE

Improvements in statistical mechanics and advances in computer power have allowed the development of equations of state based upon molecular theories that are accurate for real fluids and their mixtures. Most of the models presented in the previous sections refer to simple molecules, for which the most significant intermolecular forces are repulsion and dispersion (van der Waals forces), with weak electrostatic forces. However, many fluids and mixtures do not fall within this category, for instance polar solvents, electrolytes, hydrogen-bonded fluids, polymers and liquid crystals. For such fluids, new intermolecular forces must be considered (coulombic, strong polar activity, chain flexibility forces, induction and association). For these cases the typical predictions fail given their inadequate functional form.

Two key concepts that most of the molecular-based equations of state have in common are: chain-like molecules [75] and perturbation theory [76]. Many studies have assumed non-spherical molecules to be chains of freely jointed spherical segments [77]. Despite its simplicity, this molecular model accounts for many size and shape effects of molecules and has been applied successfully to small molecules and large polymeric fluids and mixtures. Essentially, the chains form from covalent-like bonds, and the model can approximate a broad range of molecules, from non-associating near-spherical (for example methane and n-pentane) and non-spherical (chain alkanes and polymers) to associating near-spherical (methanol) and non-spherical (alkanols). Each molecule is characterized by the number of segments, m, and the segment diameter, σ. These parameters are estimated using Barker-Henderson theory and fitting liquid densities [78]. The number of segments (m) gives an idea of the sphericity of the molecule, for spherical molecules $m = 1$.

The use of thermodynamic perturbation theory makes it possible to express the properties of a complex system as a function of a simpler reference system and then add "correction terms" that depend upon the types of interactions in that system of molecules. Although this is the basic idea, the theory behind these interactions is what makes molecular-based equations of state a challenging topic.

A very detailed review on molecular-based equations of state, including their progress in theories and complexity throughout the past 30 years appears in the works of Beret and Prausnitz [76], Nezbeda [79] and Wei [65]. In general, these theoretical models are important because they bring physical meaning to their terms. However, their

accuracy and consistency when predicting any thermodynamic property is still debatable.

An example is the SAFT (Statistical Associating Fluid Theory) equation of state developed by Jackson, Chapman and Gubbins [77]. SAFT is a method that combines Wertheim's thermodynamic perturbation theory (TPT) for associating fluids with modern ideas for formulating molecular-based equations of state. SAFT considers a fluid composed of chain-like molecules. These molecular units associate to form relatively long-lived dimers or higher *n*-mers. Such fluids could be those with hydrogen bonding and charge transfer.

The SAFT equation of state generally is expressed in terms of the Helmholtz energy of the system with other thermodynamic properties derived from it. The perturbed form of the Helmholtz energy approximation is,

$$A[\rho,T] = A^{id}[\rho,T] + A^{ex,hs}[\rho,T] + A^{att}[\rho,T] + A^{ex,Totalassoc}[\rho,T] \tag{36}$$

the first term corresponds to the ideal gas Helmholtz energy. The ideal gas contribution to the energy does not include intra-molecular interactions. Those appear in the association term. The second incremental term is the hard-spheres term and represents the change in energy caused by excluded volume/short-range repulsion. The excess energy for hard spheres can be approximated by a weighted segment density formalism originally postulated by Rosenfeld and known as fundamental measure theory (FMT) [80]. The third term is the long-range attraction based upon the mean field approximation [81] in which a many-body problem is converted into a single-body problem by considering an average of interactions. A pair potential model is necessary

in this term, and the Lennard-Jones potential is the most common one. Along with the number of segments and the segment diameter, the final parameter needed to fully describe the molecules is the intermolecular interaction parameter, ε, which appears in the expression for the pair potential.

The excess energy caused by association accounts for the intramolecular interactions. To explain the theory of association, it is necessary to understand first the basis of chain formation (linear or branched) and the concept of sites. One can picture the system as a mixture of hard spheres that undergo two kinds of bonding, covalent-like bonds to form chains and association interactions. For the association terms, the type of interaction is hydrogen bonding, which is a short-range and highly orientation-dependent site-site interaction. The theory allows branched or chain-like associated clusters as depicted in Figure 7.

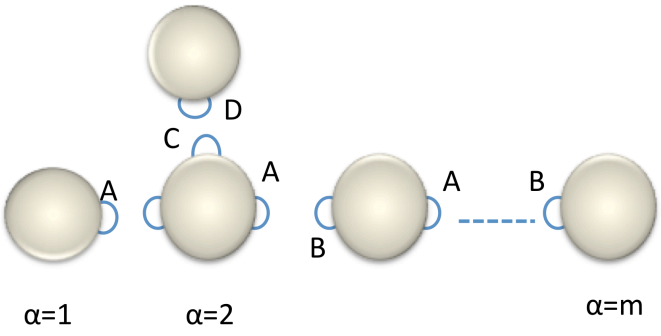

Figure 7. Formation of branched sites from associating hard spheres.

For the case of a linear chain of *m* segments, the segment number 1 has a single associating site (known as A). Segments 2 to *m*-1 have two associating sites A and B,

and segment *m* has an associating site B. To extend this model to branched systems, the segments to which the branches are attached at the backbone must have additional associating sites. It is important to keep in mind that the mixture of spheres must be stoichiometric.

As opposed to associated clusters, multisegmented chain molecules form via strong covalent-like bonds occurring through bonding sites. The procedure for formation of chains is similar to the one presented in Figure 1, retaining the constraint that the ratio of spheres is stoichiometric.

Figure 8 summarizes the principles of association and chain formation in the SAFT EoS. The final representation of the molecule is in Figure 2(a). Initially, the fluid consists of hard spheres (b), then a dispersive potential such as Lennard-Jones or square-well accounts for attraction among the spheres (c). Next, the formation of chains occurs in (d). It is mandatory to notice that the chain formation is related to bonding sites, which mathematically is treated as the limit of complete association. Finally, interaction sites are introduced at certain positions along the chain, which enable the chains to associate through some attractive interaction like hydrogen bonding (e).

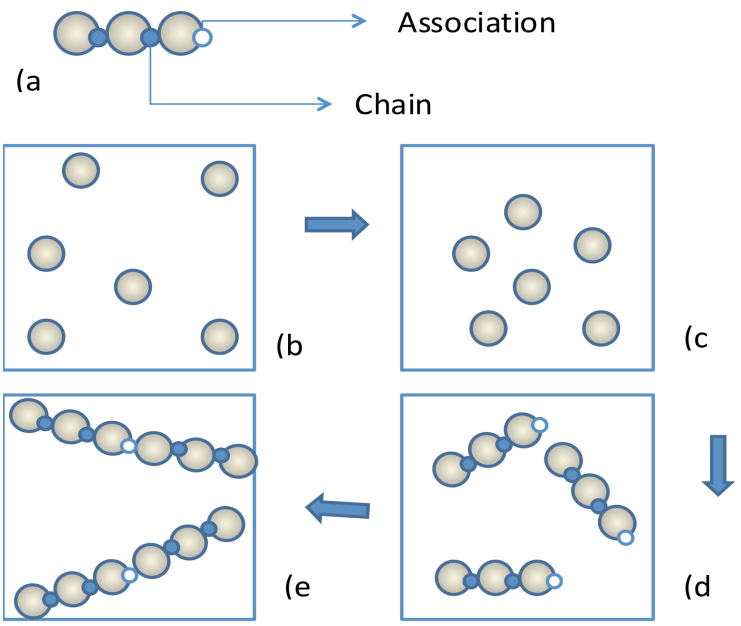

Figure 8. Path to form a molecule in the SAFT model. (a) final molecule containing chain and associating sites; (b) initially the fluid is a mixture of hard spheres; (c) attractive forces involved; (d) chains are formed by means of complete association; (e) association sites are responsible for association complexes.

3. MULTI-PARAMETER EQUATIONS OF STATE FOR PURE FLUIDS

This section presents detailed information about current formulations of empirical, multi-parameter equations of state. Well-developed multi-parameter equations of state can reproduce thermodynamic properties of fluids within the accuracy of experimental data. As a consequence, a multi-parameter equation of state can become a thermodynamic reference equation for the fluid under study. As a result of improved computational power, highly accurate multi-parameter equations of state are common in several engineering exercises and are the most practical source of thermodynamic information for challenging and demanding applications and for internationally agreed upon reference tables for fluids. It is relevant to clarify that a multi-parameter equation of state is not a thermodynamic correlation. Correlations provide relatively accurate thermodynamic information for a specific property but usually fail to reproduce other derived properties, and their performance is poor outside the range considered during the fit. This is the main advantage of multi-parameter equations of state over the equations of state studied in Section 2. Although accuracy might be comparable for a specific property, for example p-ρ-T data, most of the Section 2 equations of state cannot predict other properties with the same level of accuracy as they do for the p-ρ-T points. The beauty of a multi-parameter equation of state, and what makes it a thermodynamic reference, is consistency and extrapolation capabilities. Consistency relates to being an accurate source for all thermodynamic properties of the fluid (including properties that cannot be measured directly), and extrapolation capabilities relate to reproducing relatively accurate and well-behaved properties in regions where no data are available.

The beginnings of current multi-parameter equations of state date from the virial equation of state. The observations that a polynomial series seems to work properly for gases and gaseous-like supercritical states, and the fact that the virial coefficients have a molecular meaning represent an attraction for the scientific community. However, a functional form for the virial coefficients is necessary and, although statistical thermodynamics offers a feasible solution to that problem, simple empirical correlations for the virial equation avoid the complexity of unknown intermolecular potential models. Later, Benedict, Webb and Rubin proposed adding an exponential term to a truncated virial expansion. This is the BWR equation of state [82, 83]

The development of multi-parameter equations of state accelerated with the availability of more sophisticated computational systems. Then, two main classifications of multi-parameter equations of state appeared: the first branch corresponds to simple modifications of the BWR equation of state, equations for several fluids and specifically for mixtures with a variety of mixing rules. A good example is the equation developed by Starling in 1975 [84] that applies to mixtures of light hydrocarbons. These formulations apply in engineering applications for selected properties. The other branch corresponds to deeper modifications of the BWR equations of state that led to accurate thermodynamic descriptions for specific fluids. Examples are the equations proposed by Altunin [85, 86] and the MBWR equation by Jacobsen and Stewart [87]. In this regard, an important step in the development of "reference equations of state for pure substances" was the implementation of phase equilibrium data along with the typical p-ρ-T data. These equations were not only applicable in the

homogeneous region, but also could define accurately the boundary of the two-phase region. This was the birth of multiproperty fitting.

Two factors impacted the development of highly accurate multi-parameter equations of state within the last 20 years: the enhancement of optimization algorithms and better formulations of functional forms. With increased multi-property fitting, the numerical aspect became a problem. One of the best initial solutions to this problem was the stepwise regression analysis proposed by Wagner [88]. This procedure seemed to work properly for several study cases, and it used a bank of terms to reduce the number of final optimized parameters. Along with numerical improvement, one major change impacted the design of equations of state. Most equations of state were explicit in terms of pressure or compressibility factor. Such equations require integration to calculate caloric properties, and they require expressions for the ideal heat capacity and saturation properties. Furthermore, the integration process has numerical issues. New formulations of equations of state are based upon fundamental expressions. The term "fundamental equation" in this section refers to the use of thermodynamic potentials (internal energy, enthalpy, Gibbs energy, and Helmholtz energy) as models for the equation. The advantage of fundamental equations offer is the ability to obtain all thermodynamic properties from their derivatives without additional equations for saturation properties and without integrating to calculate another property (the integration procedure involves more numerical issues than a simple differentiation). Recently, the most common fundamental equation used in the design of multi-parameter equations of state is the Helmholtz energy as a function of density and temperature. This

formulation is successful because its independent variables are observables and, unlike Gibbs energy, do not present a discontinuity when moving between the single- and two-phase regions.

Development of a multi-parameter equation of state implies analysis and rigorous selection of data. Essentially, data with lower uncertainty, no outliers and trusted experimental techniques are preferred. Data with systematic errors can affect the performance of the equation, so such data should be avoided. Some data, reference states and molecular information are essential. They are the temperature, pressure and density at the critical point and triple point, the molecular weight, the acentric factor, the molar gas constant, and the enthalpy and entropy reference values. Also, some types of data are fundamental for the design of the equation of state such as $p\rho T$ covering the entire thermodynamic surface, vapor pressure, saturated liquid and vapor densities, ideal-gas heat capacities and speed of sound measurements. It is clear that the accuracy of the equation improves if other data are available, such as energies, caloric properties and virial coefficients.

Subsequently, the choice of the thermodynamic property formulation is in order. Generally, it is a pressure-based model or a fundamental equation. Then, the process of finding the optimum set of parameters for the thermodynamic formulation involves science and knowledge of thermodynamics of fluids, experience, and art to some extent. The general goal of correlation is to develop a consistent thermodynamic model able to reproduce data within experimental uncertainty with good extrapolation capabilities. This goal implies the following [89]:

1. All thermodynamic properties can be reproduced within their experimental uncertainty by integrating or differentiating the equation of state.
2. The equation of state satisfies ideal gas behavior in the limit of zero density.
3. The equation of state satisfies the Maxwell criterion, that is, equal Gibbs energy for both saturated liquid and vapor states at a given vapor pressure and temperature.
4. The critical behavior is consistent with theoretical constraints and experimental behavior. However, the critical region representation deviates from the real behavior because of complexity and the lack of current functional forms that allow more accuracy in this region without adding numerical difficulties.
5. The behavior of constant property lines (*e.g.* isotherms, isochores, isobars) is consistent with theoretical calculations and experimental data.
6. The behavior of properties at extreme conditions or in regions with no data must be smooth and coherent with any thermodynamic information.

Another important point regarding the resulting equation of state is its simplicity, which affects the computational cost of the equation. Following this idea, one more goal is to minimize the number of parameters in the final optimization without compromising the accuracy and consistency of the model.

3.1 PRESSURE-EXPLICIT EQUATIONS OF STATE

Despite the fact that most of the current reference equations of state are based upon Helmholtz energy formulations, pressure-explicit forms still dominate technical

applications. Following are some of the most common thermodynamic property formulations in terms of pressure.

3.1.1 The Benedict-Webb-Rubin Equation of State

The BWR equation of state, published in 1940, represents a breakthrough in the prediction of volumetric properties of fluids, even at relative high densities [82]. The general form is

$$p = RT\rho + \left(B_0 RT - A_0 - \frac{C_0}{T^2} \right)\rho + \left(bRT - a \right)\rho^3 + a\alpha\rho^6 + \frac{c\rho^3\left(1+\gamma\rho^2\right)\exp\left(-\gamma\rho^2\right)}{T^2} \tag{37}$$

A_0, B_0, C_0, a, b, c, α and γ are parameters of the equation. The exponential term allows reasonable calculations of: liquid fugacities in equilibrium calculations, high-density data reproduction and improved calculation of the critical region [82].

Eq. (37) was clearly superior to cubic equations of state for pure fluids. Several modifications of the BWR equation of state have appeared to study pure fluids and are still important in technical applications.

In 1962, Strobridge [90] modified the BWR equation of state for nitrogen using

$$p = \rho RT + \left(n_1 RT + n_2 + \frac{n_3}{T} + \frac{n_4}{T^2} + \frac{n_5}{T^4} \right)\rho^2 + \left(n_6 RT + n_7 \right)\rho^3 + n_8 T\rho^4 + \rho^3\left(\frac{n_9}{T^2} + \frac{n_{10}}{T^3} + \frac{n_{11}}{T^4} \right)\exp\left(-n_{16}\rho^2\right) + \rho^5\left(\frac{n_{12}}{T^2} + \frac{n_{13}}{T^3} + \frac{n_{14}}{T^4} \right)\exp\left(-n_{16}\rho^2\right) + n_{15}\rho^6 \tag{38}$$

In 1973, Starling generalized a BWR-type equation of state for light hydrocarbon systems with 11 adjustable coefficients [84].

The BWR equation of state and its modifications remain significant in several technical applications as a result of accurate predictions for the gas phase and moderate densities. However, results for energetic properties at liquid or liquid-like supercritical states may be in error by more than ±10 %.

3.1.2 The Martin-Hou Equation of State

Martin and Hou [89] released an equation of state that has been useful for mixtures containing halocarbons refrigerants. Its form is:

$$p = \frac{RT}{v-b} + \sum_{i=2}^{5} \frac{A_i + B_i T + C_i \exp(-\gamma)}{(v-b)^i} \tag{39}$$

where $\gamma = \kappa T / T_c$. The constants A_i, B_i, C_i and κ come from treating experimental data. To improve the accuracy of the equation, they add an additional term for refrigerants,

$$p = \frac{RT}{v-b} + \sum_{i=2}^{5} \frac{A_i + B_i T + C_i \exp(-\gamma)}{(v-b)^i} + \frac{A_6 + B_6 T + C_6 \exp(-\gamma)}{\exp(uv)\left(1 + C' \exp(uv)\right)} \tag{40}$$

in which the additional parameters are fluid dependent constants. The Martin-Hou equation of state performs similarly to the BWR equation of state [89].

3.1.3 The Bender Equation of State

Bender published another modification of the BWR equation of state [91]

$$p = \rho T\left[R + B\rho + C\rho^2 + D\rho^3 + E\rho^4 + F\rho^5 + \left(G + H\rho^2\right)\rho^2 \exp\left(-a_{20}\rho^2\right)\right] \tag{41}$$

in which the coefficients of the equation are polynomial functions of temperature that need 19 parameters for a total of 26 coefficients. The Bender equation of state was one

of the first modifications of the BWR equation that aimed to describe vapor-liquid phase equilibria as well as energetic properties in the liquid phase with results that represent the measured values with accuracy suitable for technical applications.

3.1.4 The Jacobsen-Stewart Equation of State

The equation developed by Jacobsen and Stewart, known as the mBWR equation of state, would become the most successful and sophisticated modification of the BWR equation of state. It has the form

$$p = \sum_{n=1}^{9} a_n \rho^n + \exp\left(-\gamma\rho^2\right) \sum_{n=10}^{15} a_n \rho^{2n-17} \tag{42}$$

in which $\gamma = 1/\rho_c^2$. 32 constants accompany 15 different polynomial forms for a_n [87]. This functional form upgraded the reference equation for nitrogen, and it has found wide use for the thermodynamic characterization of other fluids such as refrigerants and cryogens.

3.1.5 Thermodynamic properties from pressure-explicit equations of state

Given a functional model, the next step is to identify the necessary equations to predict other thermodynamic properties. For that purpose, several thermodynamic relations are necessary, but they appear in any thermodynamics textbook need not be repeated here.

Several thermodynamic properties based upon pressure-explicit equations of state appear in this section. Ancillary equations are necessary for the vapor pressure,

saturated liquid density, saturated vapor density, and the ideal isobaric heat capacity. Example for ancillary equations for the vapor pressure, saturated liquid density, and saturated vapor density are:

$$\ln\left(\frac{p}{p_c}\right)=\frac{T}{T_c}\sum_i N_i\theta^{t_i} \tag{43}$$

$$\ln\left(\frac{\rho^{sl}}{\rho_c}\right)=\sum_i N_i\theta^{t_i} \tag{44}$$

$$\ln\left(\frac{\rho^{sv}}{\rho_c}\right)=\frac{T}{T_c}\sum_i N_i\theta^{t_i} \tag{45}$$

in which $\theta=1-T/T_c$. N_i, t_i and the number of terms vary for each property and fluid.

Integral representations for properties pass through the two-phase region to estimate liquid properties. Properties that require integration often encounter numerical complications during the calculations. That is the case of entropy, enthalpy, internal energy and heat capacities.

The entropy of a thermodynamic state is

$$s(T,\rho)=s^0_{T_0}+\int_{T_0}^{T}\left(\frac{c_p^0}{T}\right)\mathrm{d}T-R\ln(RT\rho)+\int_0^{\rho}\left[\frac{R}{\rho}-\left(\frac{1}{\rho^2}\right)\left(\frac{\partial p}{\partial T}\right)_{\rho}\right]_T\mathrm{d}\rho \tag{46}$$

in which c_p^0 is the ideal isobaric heat capacity. The reference entropy of the ideal gas at T_0 and p_0 depends only upon the fluid under study. The enthalpy is

$$\begin{aligned}h(T,\rho)=h^0_{T_0}+T\int_0^{\rho}\left[\left(\frac{R}{\rho}\right)-\left(\frac{1}{\rho^2}\right)\left(\frac{\partial p}{\partial T}\right)_{\rho}\right]_T\mathrm{d}\rho+\int_0^{\rho}\left[\left(\frac{p}{\rho^2}\right)-\left(\frac{RT}{\rho}\right)\right]_T\mathrm{d}\rho\\+\left(\frac{p}{\rho}-RT\right)+\int_{T_o}^{T}c_p^0\,\mathrm{d}T\end{aligned} \tag{47}$$

the reference state of the ideal gas also depends upon the fluid under investigation. The internal energy is

$$u(T,\rho) = h(T,\rho) - \frac{p}{\rho} \tag{48}$$

and the isochoric and isobaric heat capacities are

$$c_v(T,\rho) = \left(c_p^0 - R\right) - \int_0^\rho \left[\left(\frac{T}{\rho^2}\right)\left(\frac{\partial^2 p}{\partial T^2}\right)_\rho\right]_T d\rho \tag{49}$$

$$c_p(T,\rho) = c_v(T,\rho) + \left[\left(\frac{T}{\rho^2}\right)\left(\frac{\partial p}{\partial T}\right)_\rho^2\left(\frac{\partial \rho}{\partial p}\right)_T\right] \tag{50}$$

3.2 EQUATIONS OF STATE IN TERMS OF THE HELMHOLTZ ENERGY

The principal advantage of fundamental equations of state is that they contain the necessary thermodynamic information to obtain all thermodynamic properties from their derivatives. The four typical fundamental expressions are the internal energy *u(s,ρ)*, enthalpy *h(s,p)*, Helmholtz energy *a(T, ρ)* and Gibbs energy *g(T,p)*. The first two formulations are not useful for equations of state development because entropy is not measurable. The Gibbs free energy might be useful because temperature and pressure are easy to measure. However, it has a discontinuity in slope at the phase boundaries, which would impair the performance of the equation in the two-phase region [89]. Hence, the Helmholtz energy is the most suitable option for the design of equations of state for the whole fluid region.

Sections 3.2.1 to 3.2.5 include examples of equations of state based upon the Helmholtz energy. Jacobsen *et al* [89] recommended this approach. Section 3.2.6 shows the modern functional form used for this work. Given the model, section 3.2.7 shows how to calculate thermodynamic properties from the Helmholtz energy.

3.2.1 The equation of Keenan, Keyes, Hill and Moore

The equation published by Keenan in 1969 was the first thermodynamic formulation in terms of the Helmholtz energy [92]. This equation covers the liquid, vapor and solid regions of water. The formulation is

$$a(\rho,T) = a_0(T) + RT\ln\rho + RT\rho Q(\rho,\tau) \tag{51}$$

$$a_0(T) = \sum_{i=1}^{6}\frac{C_i}{\tau^{i-1}} + C_7\ln T + \frac{C_8\ln T}{\tau} \tag{52}$$

$$Q(\rho,\tau) = (\tau-\tau_c)\sum_{j=1}^{7}(\tau-\tau_{aj})^{j-2}\left[\sum_{i=1}^{8}A_{ij}(\rho-\rho_{aj})^{j-1} + e^{-E\rho}\sum_{i=9}^{10}A_{ij}\rho^{i-9}\right] \tag{53}$$

in which $\tau = 1000\ \mathrm{K}/T$, $a_0(T)$ is the ideal gas behavior of the fluid and $Q(\rho,\tau)$ corresponds to the residual part of the Helmholtz energy. This equation of state is no longer used, but it represents an important contribution to the study of Helmholtz energy formulation for equations of state.

3.2.2 The equation of Pollak

Pollak released a new Helmholtz energy formulation for water in 1975 [93]. His expression was,

$$\frac{a(\rho,T)}{RT} = \alpha(\delta,\tau) = \alpha^0(\tau) + \ln\frac{\delta}{\delta_t} + \alpha^r(\delta,\tau) \tag{54}$$

$$\alpha^r(\delta,\tau) = \sum_{i=1}^{24} a_i \delta^{r_i} \tau^{t_i} + \exp\left(-A_1\delta^2\right) \sum_{i=25}^{40} a_i \delta^{r_i} \tau^{t_i} \tag{55}$$

where $\delta = \rho/\rho^+$, $\tau = T_t/T$, T_t is the temperature at the triple point, δ_t is 0.9997602 and ρ^+ is simply 1 g cm^{-3}. $\alpha(\delta,\tau)$ is the reduced Helmholtz energy and is the most common notation of Helmholtz energy in the field of equations of state. $\alpha^0(\tau)$ is the ideal contribution to the dimensionless Helmholtz energy, and $\alpha^r(\delta,\tau)$ is the residual part. This equation of state has 40 parameters, and it is more accurate than the equation developed by Keenan and his colleagues. An unfortunate feature of this equation is that it cannot be integrated analytically to obtain caloric properties.

3.2.3 The equations of Haar and Gallagher, Haar, and Gallagher and Kell

The equations developed by Haar and Gallagher in 1978 [94] along with the one published in 1984 by Haar, Gallagher and Kell became international standards for ammonia and water respectively. However, other equations currently serve as standards. Nonetheless, the original versions still are useful in technical applications.

The equation of state for ammonia is

$$a(\rho,T) = a^0(T) + a^r(\rho,T) \tag{56}$$

$$a^0(T) = RT\left[a_1 \ln T + \sum_{i=2}^{11} a_i T^{i-3} - 1 + \ln(4.818T)\right] \tag{57}$$

$$a^r(\rho,T) = RT\left[\ln(\rho) + \rho\left(\sum_{i=1}^{9}\sum_{j=1}^{6} a_{ij}\rho^{i-1}(\tau-\tau_c)^{j-1}\right)\right] \tag{58}$$

where τ=500 *K/T* and τ_c=1.2333498. The equation of state for water has three different terms: an ideal gas contribution, a residual part and a base function. The base function term provides more accurate predictions in the dilute-gas region [89].

$$a(\rho,T) = a^0(T) + a_{\text{base}}(\rho,T) + a^{\text{r}}(\rho,T) \tag{59}$$

$$a^0(T) = -RT\left[1 + \left(\frac{C_1}{T_R} + C_2\right)\ln T_R + \sum_{i=3}^{18} C_i T_R^{i-6}\right] \tag{60}$$

$$a_{\text{base}}(\rho,T) = RT\left[-\ln(1-y) - \frac{\beta-1}{1-y} + \frac{\alpha+\beta+1}{2(1-y)^2} + 4y\left(\frac{B}{b} - \gamma\right) - \frac{\alpha-\beta+3}{2} + \ln\frac{\rho RT}{p_0}\right] \tag{61}$$

$$a^{\text{r}}(\rho,T) = \sum_{i=1}^{36} \frac{a_i}{k_i}\left(\frac{T_0}{T}\right)^{l_i}\left(1-e^{-\rho}\right)^{k_i} + \sum_{i=37}^{40} a_i \delta_i^{l_i} \exp\left(-\alpha_i \delta_i^{k_i} - \beta_i \tau_i^2\right) \tag{62}$$

T_R=*T*/100 K, y=$b\rho$/4, and α, β, γ, a_i, k_i, and l_i are determined from experimental data. The parameters *B* and *b* are temperature-dependent and contain eight more parameters. The variables δ_i and τ_i depend on specific density and temperature values. The expressions are

$$\delta_i = \frac{\rho - \rho_i}{\rho_i} \tag{63}$$

$$\tau_i = \frac{T - T_i}{T_i} \tag{64}$$

3.2.4 The equation of Schmidt and Wagner

The equation of state from Schmidt and Wagner is the first modern multi-parameter equation of state [95]. It was developed for oxygen, and its success mostly

relies upon utilization of better optimization techniques and faster computers. The equation of state in terms of the reduced Helmholtz energy is

$$\frac{a(\rho,T)}{RT} = \alpha(\delta,\tau) = \alpha^0(\delta,\tau) + \alpha^r(\delta,\tau) \tag{65}$$

in which $\tau = T_c/T$, $\delta = \rho/\rho_c$, T_c is the critical temperature and ρ_c is the critical density. The Helmholtz energy of the ideal gas is

$$a^0 = h^0 - RT - Ts^0 \tag{66}$$

in which the ideal gas enthalpy and entropy are,

$$h^0 = h_0^0 + \int_{T_0}^{T} c_p^0 \mathrm{d}T \tag{67}$$

$$s^0 = s_0^0 + \int_{T_0}^{T} \frac{c_p^0}{T} \mathrm{d}T - R\ln\left(\frac{\rho T}{\rho_0 T_0}\right) \tag{68}$$

$c_p{}^0$ is the ideal gas heat capacity, ρ_0 is the ideal gas density at T_0 and p_0, and T_0 and p_0 are arbitrary reference states. Combining these equations results in the following equation for the Helmholtz energy of an ideal gas,

$$a^0 = h_0^0 + \int_{T_0}^{T} c_p^0 \mathrm{d}T - RT - T\left[s_0^0 + \int_{T_0}^{T} \frac{c_p^0}{T} \mathrm{d}T - R\ln\left(\frac{\rho T}{\rho_0 T_0}\right)\right] \tag{69}$$

this equation requires an extra expression for the ideal gas heat capacity either from experimental data or statistical mechanics. The dimensionless form of the ideal Helmholtz energy is

$$\alpha^0(\delta,\tau) = \frac{h_0^0 \tau}{RT_c} - \frac{s_0^0}{R} - 1 + \ln\frac{\delta\tau_0}{\delta_0\tau} - \frac{\tau}{R}\int_{\tau_0}^{\tau} \frac{c_p^0}{\tau^2} d\tau + \frac{1}{R}\int_{\tau_0}^{\tau} \frac{c_p^0}{\tau} d\tau \tag{70}$$

in which the state (τ_0,δ_0) is $\tau_0=T_c/T_0$, $\delta_0 = p_0/\left(RT_0\rho_c\right)$ and T_0, p_0, h_0^0 and s_0^0 are reference values.

The equation for the residual part, optimized using a bank of suitable terms, for oxygen is

$$\alpha^{\mathrm{r}}(\delta,\tau)=\sum_{i=1}^{13} a_i\delta^{d_i}\tau^{t_i} + \exp(-\delta^2)\sum_{i=14}^{24} a_i\delta^{d_i}\tau^{t_i} + \exp(-\delta^4)\sum_{i=25}^{32} a_i\delta^{d_i}\tau^{t_i} \tag{71}$$

Eq. (71) contains 13 polynomial terms and 8 exponential terms. Exponential terms are necessary for the representation of the critical region.

3.2.5 The equation of Jacobsen, Stewart, Jahangiri and Penoncello

This formulation developed in 1986 was used successfully for nitrogen [96] and ethylene [97]. It used the same expression for the reduced Helmholtz energy and essentially the same ideal gas term as presented in Eq. (65) and Eq. (70). The residual term was different though

$$\alpha^{\mathrm{r}}(\delta,\tau) = \sum_{k=1}^{m} a_k\delta^{i_k}\tau^{j_k}\exp\left(-\gamma\delta^{l_k}\right) \tag{72}$$

γ=1 for all cases except when l_k=0 then γ=0. All density exponents are positive integers while the temperature exponents can be any real number.

3.2.6 Modern functional form

The modern functional form for the reduced Helmholtz energy is the one used to develop the reference equation of state for helium 4. This modern functional form

corresponds to the one implemented for other fluids by Span and Wagner [31] and Lemmon [30]. The general form is identical to Eq. (65). All temperature values in kelvins, and the temperature scale must be taken into consideration for applications that require high levels of accuracy. Preston-Thomas [5] established the current temperature scale ITS-90. All property values in different temperature scales are previously converted to ITS-90 for equation of state development. Also, Mohr and Taylor [98] produced the current internationally accepted gas constant, which is R=8.314472 J mol^{-1} K^{-1} with a standard uncertainty of ±0.000015 J mol^{-1} K^{-1}.

The partition of the reduced Helmholtz energy into two terms obeys statistical mechanics concepts. The dimensionless ideal gas term, α^0, accounts for the effects of translation, rotation and vibration of the molecules, but ignores the presence of other molecules. The dimensionless residual term, α^r must account for all interactions among molecules. Models exist for α^0 that yield good results depending on the information available for the heat capacities. However for the residual Helmholtz energy, the situation is more complicated. Molecular simulation may be a possible future solution to this problem. However, while this approach enhances physical understanding of the fluid, the current state-of-the-art for computers makes the approach far from being a replacement for empirical equations of state. In other words, the greatest importance of molecular simulations in this matter is to impart understanding of physical effects, and the possibility of obtaining thermodynamic information in regions where it is not possible to collect experimental data. In general, accurate formulations for α^r still require empirical representations of experimental data.

The expression for the dimensionless ideal Helmholtz energy is Eq. (70), in which the reference values for helium are $T_0 = 100$ K, $p_0 = 0.101325$ MPa, $h_0^0 / RT_0 = 2.5$ and $s_0^0 / R = 12.4284$ [1]. The thermodynamic functions for helium 4 in the ideal gas limit are relatively simple to calculate given that helium is a monatomic gas and statistical thermodynamics offers a feasible solution. The isobaric heat capacity of helium is not a function of temperature,

$$c_p^0 = \frac{5}{2} R \tag{73}$$

Details of this derivation appear in any statistical thermodynamics textbook [73]. Thus, Eq. (70) rewritten for helium is

$$\alpha^0(\delta,\tau) = \frac{h_0^0 \tau}{RT_c} - \frac{s_0^0}{R} - 1 + \ln\frac{\delta\tau_0}{\delta_0\tau} + \frac{\tau}{R} c_p^0 \left(\frac{1}{\tau} - \frac{1}{\tau_0} \right) + \frac{c_p^0}{R} \ln\frac{\tau}{\tau_0} \tag{74}$$

Span [28] provides more information for other fluids that require sophisticated expressions for the ideal heat capacity term.

Most of the modern Helmholtz energy-based equations of state treat the residual contribution as Eq. (72), inspired by the use of polynomial terms along with exponential terms from the BWR equation of state and its modifications. This equation has as independent variables the inverse of the reduced temperature and the reduced density; as a matter of fact, the inverse temperature is also a statistical thermodynamics concept, in which the analogous independent variable is $\beta = 1/k_B T$.

The new functional form for the residual Helmholtz energy used in this work contains additional terms with exponentials of both temperature and density. These

terms are the Gaussian-bell shaped terms or critical-region terms that correspond to the last terms in Eq. (75).

$$\alpha^{\mathrm{r}}(\delta,\tau)=\sum_{k=1}^{I_{pol}} N_k \delta^{d_k}\tau^{t_k}+\sum_{k=I_{pol}+1}^{I_{pol}+I_{\exp}} N_k \delta^{d_k}\tau^{t_k}\exp\left(-\delta^{l_k}\right) + \sum_{k=I_{pol}+I_{\exp}+1}^{I_{pol}+I_{\exp}+I_{crit}} N_k \delta^{d_k}\tau^{t_k}\exp\left(-\eta_k\left(\delta-\varepsilon_k\right)^2-\beta_k\left(\tau-\gamma_k\right)^2\right) \tag{75}$$

The parameters N_k, d_k, t_k, l_k, I_{pol}, I_{exp} I_{crit}, η_k, β_k, ε_k, and γ_k are the *functional form.* Equations of state that use only exponential and polynomial terms can describe a fluid with high accuracy except in the critical region, although the exponential terms provide an improvement. The Gaussian-bell shaped terms can mimic the crossover from classical to non-classical behavior close to the critical point, but they disappear rapidly away from the critical point. This functional form has appeared in current worldwide-accepted reference equations of state such as methane [99], carbon dioxide [31], water [100], nitrogen [29], argon [101], ethylene [102] and propane [30].

Common problems observed in multi-parameter equations of state come from "irregular values" in the parameters of Eq. (75) that, although they might reproduce data with low deviations, cause incorrect behavior of derived properties. These irregularities affect the determination of phase boundaries, the calculation of metastable states within the two-phase region, and the shapes of isotherms in the low temperature vapor phase [103]. These problems can be traced to the magnitude of t in τ^t in Eq. (75). As the temperature goes to zero, τ^t goes to infinity for values of $t > 1$, causing the pressure to increase rapidly to infinity. The effect is more pronounced for higher values of t. The primary use of terms with high values of t is for modeling the area around the critical

region, where the properties change rapidly. Outside the critical region, this influence balances with the δ^d term in the vapor phase and the $\exp(-\delta^l)$ term in the liquid phase. Hence, at temperatures close to the triple point temperature in the vapor phase, where the density is very small, higher values of d in the δ^d part of each term result in a smaller influence of the exponential increase in temperature. Likewise, in the liquid region at similar temperatures, a higher value of l dampens the effect of the τ^t part in the term. At densities near the critical density, $\delta^d \exp(-\delta^l)$ is close to 0.39, and the shape of the τ^t contribution can greatly affect the critical region behavior of the model. Regarding the numeric values of the parameters in the functional form, all t_k should be greater than zero, and d_k and l_k should be integers greater than zero to satisfy zero derivatives at zero density [28].

3.2.7 Calculating thermodynamic properties from the Helmholtz energy model

The functions used to calculate pressure (p), compressibility factor (Z), internal energy (u), enthalpy (h), entropy (s), Gibbs energy (g), isochoric heat capacity (c_v), isobaric heat capacity (c_p), and the speed of sound (w) from Eq. (65) are:

$$p = \rho^2 \left(\frac{\partial a}{\partial \rho} \right)_T = \rho RT \left[1 + \delta \left(\frac{\partial \alpha^{\mathrm{r}}}{\partial \delta} \right)_\tau \right] \tag{76}$$

$$Z = \frac{p}{\rho RT} = 1 + \delta \left(\frac{\partial \alpha^{\mathrm{r}}}{\partial \delta} \right)_\tau \tag{77}$$

$$\frac{u}{RT} = \frac{a + Ts}{RT} = \tau \left[\left(\frac{\partial \alpha^0}{\partial \tau} \right)_\delta + \left(\frac{\partial \alpha^{\mathrm{r}}}{\partial \tau} \right)_\delta \right] \tag{78}$$

$$\frac{h}{RT}=\frac{u+pv}{RT}=\tau\left[\left(\frac{\partial\alpha^0}{\partial\tau}\right)_\delta+\left(\frac{\partial\alpha^{\mathrm{r}}}{\partial\tau}\right)_\delta\right]+\delta\left(\frac{\partial\alpha^{\mathrm{r}}}{\partial\delta}\right)_\tau+1 \tag{79}$$

$$\frac{s}{R}=-\frac{1}{R}\left(\frac{\partial a}{\partial T}\right)_\rho=\tau\left[\left(\frac{\partial\alpha^0}{\partial\tau}\right)_\delta+\left(\frac{\partial\alpha^{\mathrm{r}}}{\partial\tau}\right)_\delta\right]-\alpha^0-\alpha^{\mathrm{r}} \tag{80}$$

$$\frac{g}{RT}=\frac{h-Ts}{RT}=1+\alpha^0+\alpha^{\mathrm{r}}+\delta\left(\frac{\partial\alpha^{\mathrm{r}}}{\partial\delta}\right)_\tau \tag{81}$$

$$\frac{c_v}{R}=\frac{1}{R}\left(\frac{\partial u}{\partial T}\right)_\rho=-\tau^2\left[\left(\frac{\partial^2\alpha^0}{\partial\tau^2}\right)_\delta+\left(\frac{\partial^2\alpha^{\mathrm{r}}}{\partial\tau^2}\right)_\delta\right] \tag{82}$$

$$\frac{c_p}{R}=\frac{1}{R}\left(\frac{\partial h}{\partial T}\right)_p=\frac{c_v}{R}+\frac{\left[1+\delta\left(\frac{\partial\alpha^{\mathrm{r}}}{\partial\delta}\right)_\tau-\delta\tau\left(\frac{\partial^2\alpha^{\mathrm{r}}}{\partial\delta\partial\tau}\right)\right]^2}{\left[1+2\delta\left(\frac{\partial\alpha^{\mathrm{r}}}{\partial\delta}\right)_\tau+\delta^2\left(\frac{\partial^2\alpha^{\mathrm{r}}}{\partial\delta^2}\right)_\tau\right]} \tag{83}$$

$$\frac{w^2M}{RT}=\frac{M}{RT}\left(\frac{\partial p}{\partial\rho}\right)_s=1+2\delta\left(\frac{\partial\alpha^{\mathrm{r}}}{\partial\delta}\right)_\tau+\delta^2\left(\frac{\partial^2\alpha^{\mathrm{r}}}{\partial\delta^2}\right)_\tau-\frac{\left[1+\delta\left(\frac{\partial\alpha^{\mathrm{r}}}{\partial\delta}\right)_\tau-\delta\tau\left(\frac{\partial^2\alpha^{\mathrm{r}}}{\partial\delta\partial\tau}\right)\right]^2}{\tau^2\left[\left(\frac{\partial^2\alpha^0}{\partial\tau^2}\right)_\delta+\left(\frac{\partial^2\alpha^{\mathrm{r}}}{\partial\tau^2}\right)_\delta\right]} \tag{84}$$

the fugacity coefficient and second, third and fourth virial coefficients are

$$\phi=\exp\left[Z-1-\ln(Z)+\alpha^{\mathrm{r}}\right] \tag{85}$$

$$B(T)=\lim_{\delta\to0}\left[\frac{1}{\rho_c}\left(\frac{\partial\alpha^{\mathrm{r}}}{\partial\delta}\right)_\tau\right] \tag{86}$$

$$C(T)=\lim_{\delta\to0}\left[\frac{1}{\rho_c^{\,2}}\left(\frac{\partial^2\alpha^{\mathrm{r}}}{\partial\delta^2}\right)_\tau\right] \tag{87}$$

$$D(T)=\lim_{\delta\to0}\left[\frac{1}{\rho_c^{\,3}}\left(\frac{\partial^3\alpha^{\mathrm{r}}}{\partial\delta^3}\right)_\tau\right] \tag{88}$$

other derived properties, given below, include the first derivative of pressure with respect to density at constant temperature $(\partial p/\partial \rho)_T$, the second derivative of pressure with respect to density at constant temperature $(\partial^2 p/\partial \rho^2)_T$, and the first derivative of pressure with respect to temperature at constant density $(\partial p/\partial T)_\rho$,

$$\left(\frac{\partial p}{\partial \rho}\right)_T = RT\left[1 + 2\delta\left(\frac{\partial \alpha^{\mathrm{r}}}{\partial \delta}\right)_\tau + \delta^2\left(\frac{\partial^2 \alpha^{\mathrm{r}}}{\partial \delta^2}\right)_\tau\right] \tag{89}$$

$$\left(\frac{\partial^2 p}{\partial \rho^2}\right)_T = \frac{RT}{\rho}\left[2\delta\left(\frac{\partial \alpha^{\mathrm{r}}}{\partial \delta}\right)_\tau + 4\delta^2\left(\frac{\partial^2 \alpha^{\mathrm{r}}}{\partial \delta^2}\right)_\tau + \delta^3\left(\frac{\partial^3 \alpha^{\mathrm{r}}}{\partial \delta^3}\right)_\tau\right] \tag{90}$$

$$\left(\frac{\partial p}{\partial T}\right)_\rho = R\rho\left[1 + \delta\left(\frac{\partial \alpha^{\mathrm{r}}}{\partial \delta}\right)_\tau - \delta\tau\left(\frac{\partial^2 \alpha^{\mathrm{r}}}{\partial \delta\, \partial \tau}\right)\right]. \tag{91}$$

Lemmon *et al* [104] provide equations for additional thermodynamic properties.

The derivatives of the ideal Helmholtz energy do not appear because of their simplicity. The derivatives of the residual Helmholtz energy necessary for most of the calculations are:

$$\begin{aligned}\delta\frac{\partial \alpha^{\mathrm{r}}}{\partial \delta} = &\sum_{k=1}^{5} N_k \delta^{d_k} \tau^{t_k} d_k \\ &+ \sum_{k=6}^{11} N_k \delta^{d_k} \tau^{t_k} \exp\left(-\delta^{l_k}\right)\left[d_k - l_k \delta^{l_k}\right] \\ &+ \sum_{k=12}^{18} N_k \delta^{d_k} \tau^{t_k} \exp\left(-\eta_k(\delta - \varepsilon_k)^2 - \beta_k(\tau - \gamma_k)^2\right) \\ &\quad \times\left[d_k - 2\eta_k \delta(\delta - \varepsilon_k)\right]\end{aligned} \tag{92}$$

$$\delta^2 \frac{\partial^2 \alpha^{\mathrm{r}}}{\partial \delta^2} = \sum_{k=1}^{5} N_k \delta^{d_k} \tau^{t_k} \left[d_k (d_k - 1) \right] + \sum_{k=6}^{11} N_k \delta^{d_k} \tau^{t_k} \exp\left(-\delta^{l_k}\right) \left[\left(d_k - l_k \delta^{l_k}\right)\left(d_k - 1 - l_k \delta^{l_k}\right) - {l_k}^2 \delta^{l_k} \right] + \sum_{k=12}^{18} N_k \delta^{d_k} \tau^{t_k} \exp\left(-\eta_k (\delta - \varepsilon_k)^2 - \beta_k (\tau - \gamma_k)^2\right) \times \left\{ \left[d_k - 2\eta_k \delta (\delta - \varepsilon_k) \right]^2 - d_k - 2\eta_k \delta^2 \right\} \tag{93}$$

$$\delta^3 \frac{\partial^3 \alpha^{\mathrm{r}}}{\partial \delta^3} = \sum_{k=1}^{5} N_k \delta^{d_k} \tau^{t_k} \left[d_k (d_k - 1)(d_k - 2) \right] + \sum_{k=6}^{11} N_k \delta^{d_k} \tau^{t_k} \exp\left(-\delta^{l_k}\right) \left\{ d_k (d_k - 1)(d_k - 2) + l_k \delta^{l_k} \left[-2 + 6d_k - 3d_k^2 - 3d_k l_k + 3l_k - l_k^2 \right] + 3l_k^2 \delta^{2l_k} \left[d_k - 1 + l_k \right] - l_k^3 \delta^{3l_k} \right\} + \sum_{k=12}^{18} N_k \delta^{d_k} \tau^{t_k} \exp\left(-\eta_k (\delta - \varepsilon_k)^2 - \beta_k (\tau - \gamma_k)^2\right) \times \left\{ \begin{array}{l} \left[d_k - 2\eta_k \delta (\delta - \varepsilon_k) \right]^3 - 3d_k^2 + 2d_k \\ -6d_k \eta_k \delta^2 + 6\eta_k \delta (\delta - \varepsilon_k)\left(d_k + 2\eta_k \delta^2\right) \end{array} \right\} \tag{94}$$

$$\tau \frac{\partial \alpha^{\mathrm{r}}}{\partial \tau} = \sum_{k=1}^{5} N_k \delta^{d_k} \tau^{t_k} t_k + \sum_{k=6}^{11} N_k \delta^{d_k} \tau^{t_k} \exp\left(-\delta^{l_k}\right) t_k + \sum_{k=12}^{18} N_k \delta^{d_k} \tau^{t_k} \exp\left(-\eta_k (\delta - \varepsilon_k)^2 - \beta_k (\tau - \gamma_k)^2\right) \left[t_k - 2\beta_k \tau (\tau - \gamma_k) \right] \tag{95}$$

$$\tau^2 \frac{\partial^2 \alpha^r}{\partial \tau^2} = \sum_{k=1}^{5} N_k \delta^{d_k} \tau^{t_k} \left[t_k (t_k - 1) \right] + \sum_{k=6}^{11} N_k \delta^{d_k} \tau^{t_k} \exp\left(-\delta^{l_k}\right) \left[t_k (t_k - 1) \right] + \sum_{k=12}^{18} N_k \delta^{d_k} \tau^{t_k} \exp\left(-\eta_k (\delta - \varepsilon_k)^2 - \beta_k (\tau - \gamma_k)^2\right) \times \left\{ \left[t_k - 2\beta_k \tau (\tau - \gamma_k) \right]^2 - t_k - 2\beta_k \tau^2 \right\} \tag{96}$$

$$\tau\delta \frac{\partial^2 \alpha^r}{\partial \tau \, \partial \delta} = \sum_{k=1}^{5} N_k \delta^{d_k} \tau^{t_k} \left[d_k t_k \right] + \sum_{k=6}^{11} N_k \delta^{d_k} \tau^{t_k} \exp\left(-\delta^{l_k}\right) \left[t_k \left(d_k - l_k \delta^{l_k} \right) \right] + \sum_{k=12}^{18} N_k \delta^{d_k} \tau^{t_k} \exp\left(-\eta_k (\delta - \varepsilon_k)^2 - \beta_k (\tau - \gamma_k)^2\right) \times \left[d_k - 2\eta_k \delta (\delta - \varepsilon_k) \right] \left[t_k - 2\beta_k \tau (\tau - \gamma_k) \right] \tag{97}$$

$$\delta\tau^2 \frac{\partial^3 \alpha^r}{\partial \delta \, \partial \tau^2} = \sum_{k=1}^{5} N_k \delta^{d_k} \tau^{t_k} \left[d_k t_k (t_k - 1) \right] + \sum_{k=6}^{11} N_k \delta^{d_k} \tau^{t_k} \exp\left(-\delta^{l_k}\right) \left[t_k (t_k - 1) \left(d_k - l_k \delta^{l_k} \right) \right] + \sum_{k=12}^{18} N_k \delta^{d_k} \tau^{t_k} \exp\left(-\eta_k (\delta - \varepsilon_k)^2 - \beta_k (\tau - \gamma_k)^2\right) \times \left[d_k - 2\eta_k \delta (\delta - \varepsilon_k) \right] \left\{ \left[t_k - 2\beta_k \tau (\tau - \gamma_k) \right]^2 - t_k - 2\beta_k \tau^2 \right\} \tag{98}$$

3.3 FITTING PROCEDURES

Designing a multi-parameter equation of state involves correlating high quality data using least-squares methods to develop a model (Helmholtz energy in this case) that ultimately reproduces the data within its experimental uncertainty and exhibit proper behavior in the ideal gas and low density regions as well as in zones that require extrapolation from data. One important task of the correlator is to select a set of data

that is representative of all available data because fitting all data points is very time consuming and, for many cases, does not make any difference on the result. Selecting a subset of data may be a function of the accuracy of the experimental values, the availability of data in a specific region, and the reliability of the methods and procedures used in the laboratory.

Once a representative set of data is available, the next step is to choose the appropriate numerical procedure to minimize the resulting least-squares problem. The type of fitting procedure (e.g., nonlinear versus linear fits of the parameters) determines the use of the experimental data. Even though linear fitting procedures have been useful for several fluids, such as argon and carbon dioxide [28] [31] [101], they fail when the coefficients of the linear approximation of the residuals with respect to the parameters vector is not linear [28]. Another disadvantage of these algorithms is that they are constrained to linear and linearized data. Hence, not all properties are fit properly, such as sound speed, which is highly nonlinear. In linear fits, only equalities can be used. Thus in regions with no data, the curves of the experimental values usually are extrapolated by hand and subsequently those "new values" become input data. The fact that linear fit procedures must deal with linearized data (not raw data) can directly affect the accuracy of the equation of state because the solution would also have an implied error from the previous linearization. Nonlinear fitting has many advantages over linear fitting, such as the capability to fit any type of experimental data. Shock-wave measurements of the Hugoniot curve are an example in which nonlinear fitting can use (p, ρ, h) measurements. Another advantage in nonlinear fitting is the ability to use

"greater than" or "less than" operators for controlling the extrapolation behavior of properties in regions with no data. Curves can be controlled by ensuring that a calculated value along a constant property path is always greater (or less) than a previous value. Thus, only the shape is specified not the magnitude. The nonlinear fitter then determines the optimal magnitude for the properties based upon other information in a specific region. Having said this, the numerical procedure for the development of the new helium equation of state was based on nonlinear fitting algorithms. Also considering both that McCarty's helium equation of state was developed using linear optimization techniques and the aforementioned extrapolation abilities inherent to nonlinear fittings, the use of nonlinear algorithms is a way to avoid unreasonable behavior in regions with no data and improve significantly the behavior of the standard for helium 4.

Regarding nonlinear methods, a good preliminary equation is necessary as a starting point. All of the coefficients and exponents in the advanced functional form described in Eq. (75) were fit simultaneously. Thus, with $Ipol + Iexp + Icrit = 18$, approximately 90 parameters are fit at the same time. The nonlinear methods followed for the development of this project appear in a powerful nonlinear optimization solver that will be used for development of the equation of state. Lemmon [103] created this solver. Essentially the minimization is a constrained minimization with initial line-search and Lagrange multipliers. Lemmon has dedicated more than 15 years to the continuous improvement of formulations and numerical methods with regard to multi-parameter equations of state. This work includes a collaboration with the National

Institute of Standards and Technology, and the equation of state presented in this document should be the next worldwide thermodynamic standard for helium.

The goal of the nonlinear algorithm is to find the set of parameters of the equation of state that minimizes the overall sum of squares of the deviations of calculated properties from the input data, in which the residual sum of squares is

$$S = \sum W_\rho F_\rho^2 + \sum W_p F_p^2 + \sum W_{c_v} F_{c_v}^2 + \ldots \tag{99}$$

W is the weight assigned to each datum, and F is the function that minimizes the deviations. The equation of state is fit to $p\rho T$ data for instance with either deviations in pressure $F_p = (p_{\text{data}} - p_{\text{calc}})/p_{\text{data}}$ for vapor-phase and critical-region data, or deviations in density, $F_\rho = (\rho_{\text{data}} - \rho_{\text{calc}})/\rho_{\text{data}}$, for liquid phase data. Other experimental data are fit in a similar manner.

The weighting process is crucial when fitting an equation; it varies with region, type of data, and experimental uncertainty. The critical point is a characteristic state of any substance; given this importance, its weight is large (~10^7). Regarding $p\rho T$ data, the saturation region is relevant, and a weight on a saturation point is generally greater than a regular $p\rho T$ point. Also, between two experimental sets covering the same property with different uncertainty, the one with lower deviations receives a higher weight than that for the set with higher uncertainties. The nature of the property is also a factor to take into account. For example, $p\rho T$ data are less affected by the weight than heat capacities. Hence to cause a change in the equation, a heat capacity point generally has a lower weight than a $p\rho T$ point. Typical values of W are 1 for $p\rho T$ and vapor pressure values, 0.05 for heat capacities, and 10 to 100 for vapor sound speeds. In

addition of reflecting experimental uncertainties, the weighting allows the correlator to emphasized certain kinds of data during the equation development.

Constraining the fitting problem may assure proper behavior in regions with no data. One can constrain the actual value of a property (positive, negative or zero), or its slope, curvature, third and fourth derivative. These constraints are purely subject to thermodynamic knowledge of the correlator and appear throughout the development of the equation. At the end, the results will not only be a set of parameters, but also a set of constraints that led to a proper set of parameters. As an example, the second virial coefficient goes to zero when the temperature goes to infinity, and the curvature of the third virial coefficient is positive from about 3 times the critical temperature to infinity. The equation of state was constrained to the critical parameters by adding the values of the first and second derivatives of pressure with respect to density at the critical point, multiplied by some arbitrary weight, to the sum of squares. In this manner, the calculated values of these derivatives would be zero at the selected critical point.

Although one may think that fitting a massive amount of data with many constraints from the start of the process is a way to hasten the fit, by doing so all calculations might fail. Nonlinear optimization techniques are very sensitive and can be very time consuming if the correlator does not follow an appropriate path. The entire fitting process is progressive. It must start with the most accurate data and the basic constraints (conditions at extremes). Subsequently more data can be added and, considering preliminary results, new constraints also.

To reduce the number of terms in the equation, terms were eliminated in successive fits by either deleting the term that contributed least to the overall sum of squares or by combining two terms that presented similar values of the exponents (resulting in analogous contributions to the equation of state). After eliminating a term, the fit was repeated until the sum of squares for the resulting new equation was of the same order of magnitude as the previous equation.

Because non-integer numbers for the density exponents resulted from the nonlinear fitting methods, each density exponent was rounded to the nearest integer, followed by refitting the other parameters to minimize the overall sum of squares, until all of the density exponents in the final form were positive integers. A similar process was used for the temperature exponents to reduce the number of significant figures to one or two decimal places.

4. DEVELOPING AN EQUATION OF STATE FOR HELIUM-4

This section explains the basic steps and recommendations that led to the development of a multiparameter reference equation of state for helium-4. Initially, the presentation consists of establishing the equations and the fitter along with initial values for the parameters. Then, a rigorous data selection process is necessary along with a distribution of weights for the data. For development of the equation, it was crucial to define constraints on thermodynamic properties, especially in regions that lack data. Assigning constraints is a key step during the fitting process. Besides using common thermodynamic properties for constraints, this work uses, for the first time, two additional parameters to constraint equations of state: the Gruneisen parameter and the Phase Identification Parameter (PIP). This section ends with basic elements of the transition to superfluid; it was necessary to conclude the design of the equation by matching the behavior of the normal fluid with the onset of helium-II. These characteristics definitely add a challenging new aspect to the development of multiparameter equations of state for pure fluids.

4.1 INITIAL SETUP

This project was a collaboration with the National Institute of Standards and Technology (NIST). Dr. Eric Lemmon is the principal investigator at NIST in charge of developing reference equations of state for fluids, thermodynamic correlations and technical equations of state for mixtures. NIST provided the program used during this project, which they have developed over the past decade. This program, written in

Fortran, is specifically applicable to development of equations of state. The new functional form for the Helmholtz free energy used for helium presented by Eq. (65), Eq. (74) and Eq. (75) in Section 3, as well as the derivatives and formulas to determine the rest of thermodynamic properties (Eq. (76) to Eq. (98) in Section 3) are in the program. The fitting procedures explained in section 3.3 cover the numerical aspects of the algorithm. In addition to the Helmholtz energy-based equations related to thermodynamic properties, the initial setup also requires a built-in subroutine for unit conversions and update of temperature scales to ITS-90. This is necessary to establish accurate formulations for designing a reference equation of state. Relations between previous temperatures scales and ITS-90 appear in Preston [5].

Another crucial aspect is to select initial values for all parameters in the equation. A new equation of state for propylene provided a starting point. Usually, a recent equation of state contains a good bank of terms to develop a correlation for another fluid. The equation contains six terms for the polynomial part of Eq. (75), six terms for the exponential part and nine critical region terms. Thus, the preliminary equation of state consists of 21 terms.

4.2 DATA AND WEIGHTING PROCESS

Significant new experimental data have become available since the development of the current standard equation of state for helium [32]. Whereas McCarty and Arp had available only 10 data sets featuring three different properties ($p\rho T$, isochoric heat

capacity and sound speed), after a rigorous literature review on measured properties of helium identified 145 data sets covering 15 different thermodynamic properties.

An important contribution for the current work is the data published after the release of the current standard for helium. Donnelly *et al.* [33] published a relevant compendium of saturation data for helium along with new, accurate $p\rho T$ at high temperatures [105, 106]. These data were part of the representative set of data for the final equation.

A new feature in this upgrade of the equation of state is the implementation of theoretical data. Taking advantage of new computational technology, it is possible to use quantum mechanical calculations to predict thermodynamic properties of substances. Sandler et al. [107] recently showed how to calculate intermolecular potentials that would lead to thermophysical properties. Other important works have treated interatomic potentials of helium from different perspectives and have estimated virial coefficients for helium [106, 108-111]. These calculations along with the data employed for the development of the equation appear in Table **2**.

Table 2. Total sets of experimental and theoretical data combined.

Author	**Type of data**	**Reference**
Barrufet	2^{nd} Virial coefficient	[9]
Berman and Mate	Latent heat of vaporization Saturated vapor density	[112]

Table 2. Continued

Author	Type of data	Reference
Berry	2^{nd} Virial coefficient 3^{rd} Virial coefficient	[113]
Blancett *et al.*	2^{nd} Virial coefficient	[114]
Blancett *et al.*	PVT* 2^{nd} Virial coefficient 3^{rd} Virial coefficient	[115]
Blancett *et al.*	PVT*	[116]
Briggs	PVT*	[117] [118]
Buchmann	PVT*	[119]
Canfield *et al.*	PVT*	[120]
Canfield *et al.*	PVT* 2^{nd} Virial coefficient 3^{rd} Virial coefficient	[121]
Cataland and Plumb	Sound speed	[122]
Cramer	PVT* 2^{nd} Virial coefficient 3^{rd} Virial coefficient 4^{th} Virial coefficient	[123]
Dillard and Robinson	2^{nd} Virial coefficient	[124]
Donnelly and Barenghi	PVT* Saturation heat capacity Sound speed Latent heat of vaporization Vapor pressure Saturated liquid density	[33]

Table 2. Continued

Author	Type of data	Reference
Dugdale and Franck	Isochoric heat capacity	[125]
Edeskuty and Sherman	PVT*	[126]
Edwards and Woodbury	PVT*	[127]
Edwards and Woodbury	Saturated vapor density Saturated liquid density	[128]
El Hadi	Saturated liquid density Saturated vapor density PVT*	[129]
El Hadi *et al.*	PVT*	[130]
Evers *et al.*	PVT*	[131]
Gaisser and Fellmuth	2^{nd} Virial coefficient 3^{rd} Virial coefficient	[110]
Garberoglio *et al.*	3^{rd} Virial coefficient	[108]
Gibby *et al.*	PVT* 2^{nd} Virial coefficient	[132]
Glassford and Smith	PVT* Internal Energy	[133]
Grilly and Mills	PVT*	[134]
Grilly and Mills	PVT*	[135]
Gugan and Michel	2^{nd} Virial coefficient 3^{rd} Virial coefficient	[136]

Table 2. Continued

Author	Type of data	Reference
Hall and Canfield	2^{nd} Virial coefficient	[13]
Hall and Canfield	2^{nd} Virial coefficient PVT*	[137]
Hill and Lounasmaa	Isochoric heat capacity PVT* $(\delta P/\delta T)v$	[138]
Holborn and Otto	2^{nd} Virial coefficient PVT*	[139]
Holste *et al.*	2^{nd} Virial coefficient	[140]
Hoover *et al.*	2^{nd} Virial coefficient 3^{rd} Virial coefficient	[141]
Hurly *et al.*	Sound speed PVT*	[10]
Hurly and Moldover	2^{nd} Virial coefficient	[111]
Keesom and Kraak	2^{nd} Virial coefficient PVT*	[142]
Keesom and Walstra	PVT* 2^{nd} Virial coefficient 3^{rd} Virial coefficient	[142]
Keesom and Walstra	PVT* 2^{nd} Virial coefficient	[143]
Kell *et al.*	2^{nd} Virial coefficient	[144]
Keller	PVT* 2^{nd} Virial coefficient 3^{rd} Virial coefficient	[145]

Table 2. Continued

Author	Type of data	Reference
Kerr	PVT*	[146]
Kessler and Osborne	Sound speed Vapor pressure 2nd Virial coefficient	[147]
Kierstead	Critical point	[148]
Kistemaker and Keesom	PVT* 2nd Virial coefficient 3rd Virial coefficient	[149]
Kramer and Miller	2nd Virial coefficient 3rd Virial coefficient	[150]
Ku and Dodge	2nd Virial coefficient 3rd Virial coefficient PVT*	[151]
Liebenberg *et al.*	PVT* Sound speed	[152]
Linshits	PVT*	[153]
Linshits *et al.*	PVT* 2nd Virial coefficient	[154]
Lounasmaa	Isochoric heat capacity Saturation heat capacity	[155]
Lounasmaa	Isochoric heat capacity	[156]
Lounasmaa	$(\delta P/\delta T)v$ PVT*	[157]
Lounasmaa and Kaunisto	PVT* $(\delta P/\delta T)v$	[158]

Table 2. Continued

Author	Type of data	Reference
McLinden et al.	PVT*	[105]
Mallu *et al.*	2nd Virial coefficient	[159]
Mansoorian *et al.*	2nd Virial coefficient 3rd Virial coefficient	[160]
Mehl	2nd Virial coefficient 3rd Virial coefficient	[109]
Michels and Wouters	PVT* 2nd Virial coefficient 3rd Virial coefficient	[161]
Miller *et al.*	PVT*	[162]
Moldover	Critical point	[163]
Moldover	Isochoric heat capacity	[164]
Moldover	Isochoric heat capacity	[165]
Moldover and McLinden	2nd Virial coefficient 3rd Virial coefficient 4th Virial coefficient PVT*	[106]
Nijhoff	PVT*	[166]
Patel *et al.*	2nd Virial coefficient 3rd Virial coefficient	[167]
Pfefferle *et al.*	2nd Virial coefficient 3rd Virial coefficient	[168]
Prasad *et al.*	2nd Virial coefficient PVT*	[169]

Table 2. Continued

Author	Type of data	Reference
Provine and Canfield	PVT*	[170]
Roach	Saturated liquid density Saturated vapor density Vapor pressure PVT*	[171]
Sengers and Hastings	2nd Virial coefficient	[172]
Stewart.	PVT*	[173]
Stroud *et al.*	2nd Virial coefficient PVT*	[174]
Suh and Storvick	2nd Virial coefficient	[175]
Sullivan and Sonntag	2nd Virial coefficient PVT*	[176]
Tanner and Masson	2nd Virial coefficient	[177]
Tsederberg *et al.*	PVT*	[178]
Tsiklis *et al.*	PVT*	[179]
Tsiklis *et al.*	PVT*	[180]
Vogl and Hall	PVT* 2nd Virial coefficient	[181]
White *et al.*	PVT* 2nd Virial coefficient 3rd Virial coefficient	[182]
Wiebe *et al.*	PVT*	[183]

Table 2. Continued

Author	Type of data	Reference
Zelmanov	Isochoric heat capacity	[184]
	Enthalpy	
Zhang *et al.*	PVT*	[185]
	2^{nd} Virial coefficient	
	3^{rd} Virial coefficient	

*PVT data refers generally to pressure- temperature-density data; or replacing either density or pressure by compressibility factor, *pv* values, or compression ratio.

A few data sets were not used in this project as recommended by McCarty and Arp [32]. The data by Sullivan [176] was classified as suspect by Sychev *et al.* [1], and because new data covered the same conditions, the Sullivan *et al.* publication was not used. The $p\rho T$ data by Wiebe *et al.* [183] was replaced in this work by more recent data with less scatter. Also, the data by Glassford and Smith [133] were not considered because they appear to be inconsistent. Finally Briggs et al. [118] were not used because of more trustworthy data being available at the same conditions.

One of the most common problems encountered with data during the fitting process was inconsistent data. The problem was easy to solve when dealing with outliers because they are obvious either from deviation plots or because they contribute most to the sum of squares compared to other data points in the same set. The solution for outliers is to assign zero weight to them. The situation is much more complicated when dealing with inconsistencies between data sets that have no obvious deficiencies.

Most of the data reported in Table **2** lack uncertainty statements therefore it is difficult to determine which data set is more "accurate." In reality, no a specific list of solutions can help you overcome such problems, but from experience the next steps might facilitate this process.

- The first step is to identify that there is an actual problem with inconsistent data. Symptoms are that either the sum of squares remains static or there is a systematic behavior with some data when plotting deviations. The sum of squares is in fact a sign of inconsistent data when it does not change by switching initial values for the parameters or when all the thermodynamic properties look reasonable. Systematic deviations indicate a problem with data that requires further checking of the data involved.
- After identifying a problem with data, the next step is to determine which data sets are implicated. One should estimate the contribution of each data point to the sum of squares. Generally, a data set is doubtful when several of its points have high contributions to the sum of squares. Also, if a data set presents systematic behavior, it is suspect.
- In order to find out which other data set is in conflict with the one found in the previous step, the suspicious data set should be removed and the minimization should proceed. Elimination of an incorrect data set causes a relatively drastic decrease of the sum of squares for most cases.
- Once the conflicting data sets are identified, the next step is to determine why they conflict and which set is better. For the majority of situations, both data sets

share either the same conditions of temperature and density and/or the type of property. The best defining factor is the uncertainty statement, but this seldom is available. Other factors for consideration include: the reliability of the researchers who made the measurements, the quality of the experimental techniques, the availability of other data sets at similar conditions that might provide useful comparisons and the age of the data.

- Finally, whenever there is an idea about which data set might be more "accurate," the most suspicious data set can be removed from the fitting or assigned lower weights than the set believed to be correct.

4.2.1 Weighting data points

Weighting is a process during fitting that gives direction to the development of the equation. A measurement assigned a higher weight influences the minimization of the sum of squares more than a measurement with lesser weight. If the uncertainty of a measurement is known, the first step is to assign an experimental uncertainty σ_j to each measurement j; then calculate a weighted residual. If the experimental value is, for example, a pressure point measured as a function of temperature and density, the relative residual ζ is defined as,

$$\zeta_j = \frac{p_{j,\mathrm{calc}}\left(T_{\mathrm{meas}},\rho_{\mathrm{meas}},\mathbf{n}\right) - p_{j,\mathrm{meas}}\left(T_{\mathrm{meas}},\rho_{\mathrm{meas}}\right)}{\sigma_{p,j}}. \tag{100}$$

in which **n** is the parameter vector.

The relative residual is equal to unity when deviation of the prediction from the experimental value is the same as the experimental uncertainty. Thus, for a reference equation of state, the residuals should be less than unity for almost all data (typically > 95 % of the points, if *s* is twice the standard deviation for an expanded uncertainty at a confidence interval of 0.95). In this equation the calculated pressure depends upon **n**, thus upon the fitted coefficients of the equation of state.

For the sum of squares in Eq. (99) from section 3.3, the weight is

$$W_j = 1/\sigma_j^2 \tag{101}$$

which supports the idea that if a data point has low uncertainty its weight should be higher.

However, for the case of helium, the majority of the data collected did not have uncertainty statements. Accuracy was determined by comparisons to data from other authors or by calculating deviations from a thermodynamic correlation that was believed to be very accurate at the time the data were collected. Hence, the weighting process became subject to the expertise of the correlator rather than information from the original researchers. From experience, the aspects considered when assigning weights were:

- The laboratory that took the measurements. The best way to predict future performance is from past performance. If the laboratory is known to be trustworthy, the measurements are likely to be accurate, and the assigned weights are larger. Authors included in this category are for instance, McLinden, Hall, Holste, Moldover, Canfield, Blancett, Provine, Lounasma, Keesom, Vogl, Hill,

Donnelly, Wagner, Span and Catalan. Nonetheless, this criterion is subjective. As the equation development progresses, one may find that individual data sets reported by a highly regarded laboratory is not correct.

- Another important aspect is the type of property fitted, because the weights are chosen to reflect the accuracy of the measurement technique. Typical values of W are 1 to 1000 for $p\rho T$, 0.05 to 1 for heat capacities, 10 to 100 for vapor sound speeds, 1 to 100 for virial coefficients and 1 for energies. An exception in the $p\rho T$ weight is data from McLinden [105], whose uncertainty is 0.04% deviation in density. The weights on those data points was 10000, which forced the equation to fit them almost exactly.
- The thermodynamic conditions also affect the weights. Because accurate representation of the critical point is extremely important, within $p\rho T$ data the measurements in this region generally are weighted at 10^7 or higher even though the accuracies are not significantly greater. Vapor pressure and saturated densities also require higher weights, generally around 10^5.
- During the development process, it is often necessary to increase temporarily weights on data points in regions where the fit is not satisfactory. Once the deviations are within expectations, the weights may be decreased.

4.3 CONSTRAINTS

Constraints are key elements to avoid unreasonable behavior in regions with no data, and they ensure proper thermodynamic behavior for lines of constant temperature,

density and pressure (for instance, preventing their crossing). One could constraint the actual value of a property (positive, negative or zero), or its slope, curvature, third and fourth derivatives. These constraints come from principles of thermodynamics and appear throughout the development of the equation. It is rare that sufficient measurements exist for a fluid that such constraints are not necessary. More often, insufficient data are available and regions exist where the equation can deviate from real behavior when overfitting available data produces what appears to be very good results. The overfitting causes incorrect slopes that give the appearance of a good fit to the limited data but a bad fit in the region where data are not available. The first and most important constraint forces is the correct slope and curvature at the critical point, that is $\partial p/\partial \rho = 0 = \partial^2 p/\partial \rho^2$. Also, it is mandatory that the virial coefficients to go to zero at infinite temperature.

Many other constraints can be added to the fit. Three inputs are necessary to construct a constraint. The first one indicates the property being constrained, the second indicates which variables to hold constant and which to vary, and the third indicates what attribute of the property should be constrained: the line, the slope, the acceleration, the third derivative, the fourth derivative, or all of these derivatives. These values can be negative, positive or close to zero. Besides typical thermodynamic properties, recognized properties also include the first and second derivatives of pressure with respect to density, $(Z-1)/\rho$, which is important to study virial coefficients, and the Gruneisen and phase identification parameter. The phase identification parameter is

used for the first time in the development of equations of state in this work. Analogous to data points, weights assigned to constraints govern their relative influence on the fit.

Adding and deleting constraints is also a frequent task. The behavior of thermodynamic properties always should be checked for unreasonable behavior, even at extreme conditions or in the two-phase region. Constraints come and go to ensure that the data are fit within expected performance.

4.4 GRUNEISEN AND PHASE IDENTIFICATION PARAMETERS

Two new parameters have recently become key tools for evaluating equations of state. These are the Gruneisen parameter and the phase identification parameter (PIP). These new parameters, along with the isochoric and isobaric heat capacities and speed of sound, can help identify problems during the development of an equation. In particular, the new parameters are more sensitive than those that have been used for decades, and can identify areas needing improvement that otherwise would go unnoticed. With these, the extrapolation behavior of an equation can be fashioned so that the equation predicts results as well as possible in the absence of data. Thermodynamic definitions of the Gruneisen parameter and PIP appear in this section in context with definitions of related derivatives of the Helmholtz potential.

4.4.1 The Gruneisen parameter

The Gruneisen parameter, Γ, appeared in the literature about 100 years ago [186] in discussions of thermodynamic equations for solid materials. This work shows that attention to $\Gamma(\rho,T)$ can provide valuable smoothing of derivatives of the Helmholtz

potential $A(\rho,T)$ for fluids. The thermodynamic equations that govern the Gruneisen parameter follow.

The original definition of Γ is [186]:

$$\Gamma = (1/\rho)\, dp/dU \tag{102}$$

This definition applied to solids, which means that the derivative is essentially at constant density. This definition was extended to fluids [187] [188] by recognizing density as a variable. The internal energy change at constant density is $\mathrm{d}U = C\mathrm{v}\ \mathrm{d}T$. The definition of Γ becomes,

$$\Gamma = \left(\partial p/\partial T\right)_{\rho} \Big/ \rho C_{v}\,. \tag{103}$$

Using the Maxwell relation $\partial p/\partial T|_{v} = \partial s/\partial v|_{T}$, an alternative definition is,

$$\Gamma = \left(v/T\right)\left(\partial T/\partial v\right)_{s} \tag{104}$$

thus, conceptually Γ is the inverse of the dimensionless isentropic thermal expansivity.

The Gruneisen parameter is also a derivative of the Helmholtz Energy. Consider the thermodynamic "tree" of the Helmholtz energy in Figure **9**. At the top of the tree is the Helmholtz energy $A(v,T)$ in the first level. Temperature derivatives are diagonally downward to the left, and volume derivatives are diagonally downward to the right.

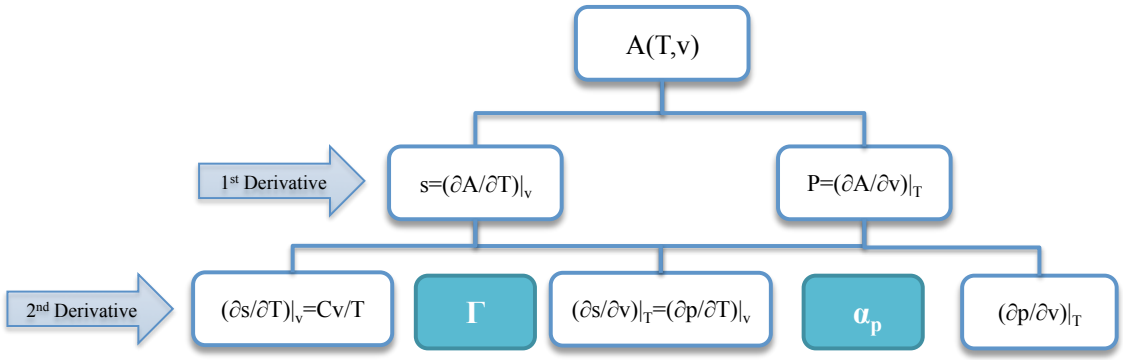

Figure 9. Helmholtz energy tree – Gruneisen

The highlighted boxes on the third level correspond to the Gruneisen (Γ) parameter and the isobaric expansivity (α_p). What is very interesting is that these two quantities equal the ratio of the properties on either side of the corresponding box: $\Gamma = \partial p/\partial T|_\rho / \rho C_v$ and $\alpha_p = (T/V)(\partial p/\partial T)_V / (\partial p/\partial V)_T$ (the quantities were multiplied by ρ and T to create dimensionless quantities). The basic conclusion is that Γ and α_p occupy complementary positions in the tree of Helmholtz energy derivatives. The isobaric expansivity is familiar when dealing with fluids but the Gruneisen is not, and it deserves at least commensurate attention in thermodynamic studies.

The Gruneisen parameter is very sensitive to constraints, and it is very useful to resolve improper behavior for the isochoric heat capacity and speed of sound, even at very low temperatures near the lambda line transition and at high densities near the limit of the solid region.

4.4.2 The phase identification parameter (PIP)

The phase identification parameter is a property defined in terms of partial derivatives of pressure, volume and temperature that can determine the phase of a fluid without using saturated properties as a reference. Venkatarathnam and Oellrich [189] introduced the term in 2011 as a handy tool in phase equilibria calculations, particularly for liquid–liquid or vapor–liquid–liquid equilibria calculations. The authors previous work on the isothermal compressibility [190] led to the definition:

$$PIP = v\left[\frac{\left(\partial^2 p/\partial v\,\partial T\right)}{\left(\partial p/dT\right)_v} - \frac{\left(\partial^2 p/dv^2\right)_T}{\left(\partial p/dv\right)_T}\right]. \tag{105}$$

PIP is a dimensionless parameter that states that a liquid or liquid-like phase should have a PIP value greater than 1, and a vapor-like phase a PIP value less than or equal to 1.

PIP is a dimensionless parameter that should have a PIP value greater than unity for a liquid or liquid-like phase, and less than or equal to unity for a vapor-like phase. Figure **10** shows a plot of PIP versus temperature at constant densities for the equation of state for nitrogen [29].

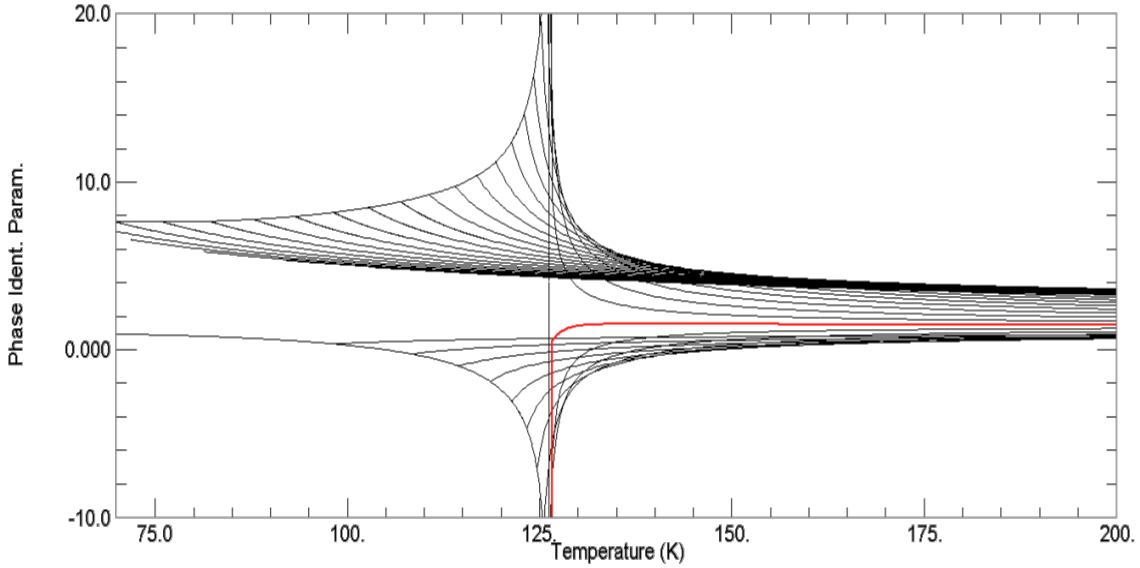

Figure 10. Phase identification parameter versus temperature at different densities for nitrogen. The red curve is a density slightly less than the critical density. The critical temperature for nitrogen is 126.19 K.

As it is presented in Figure **10**, the PIP parameter splits both liquid and vapor phases drastically around the critical point and reveals possible problems that otherwise would have not been observed. The same situation happens along the lambda line for helium, where each point on the line behaves as a critical point. The PIP for helium helped fix slope and curvature problems of isochores, isobars and isotherms near the critical point and the transition to superfluid.

The PIP parameter represents an additional level of the Helmholtz energy tree presented in Figure **9**. Figure **11** shows that extension.

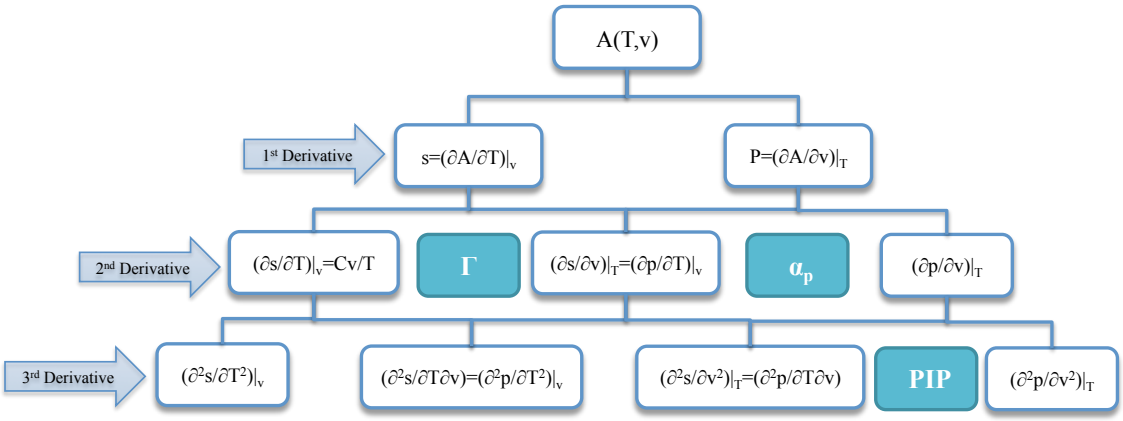

Figure 11. Helmholtz energy tree – Phase identification parameter.

The PIP parameter is a combination of branches on the fourth level. This leaves open a door to new combinations of derivatives that might lead to new parameters of use in developing equations of state in the future. Like the PIP parameter, they might add novel features regarding the thermodynamic behavior of fluids.

4.5 LAMBDA TRANSITION

The two isotopes of helium have the lowest normal boiling points of all known elements, 4.21 K for ^{4}He and 3.19 K for ^{3}He. In addition, when the temperature drops, both isotopes remain liquid under their own vapor pressures and only become solid at high pressures (≥25 atm). However, liquid ^{4}He, below approximately 2.2 K behaves as a superfluid with unusual characteristics described in Section 1. The superfluid liquid phase is known as helium II and the normal liquid phase as helium I. The line that separates these phases is the lambda transition curve or simply λ-line. These important features appear in Figure 12.

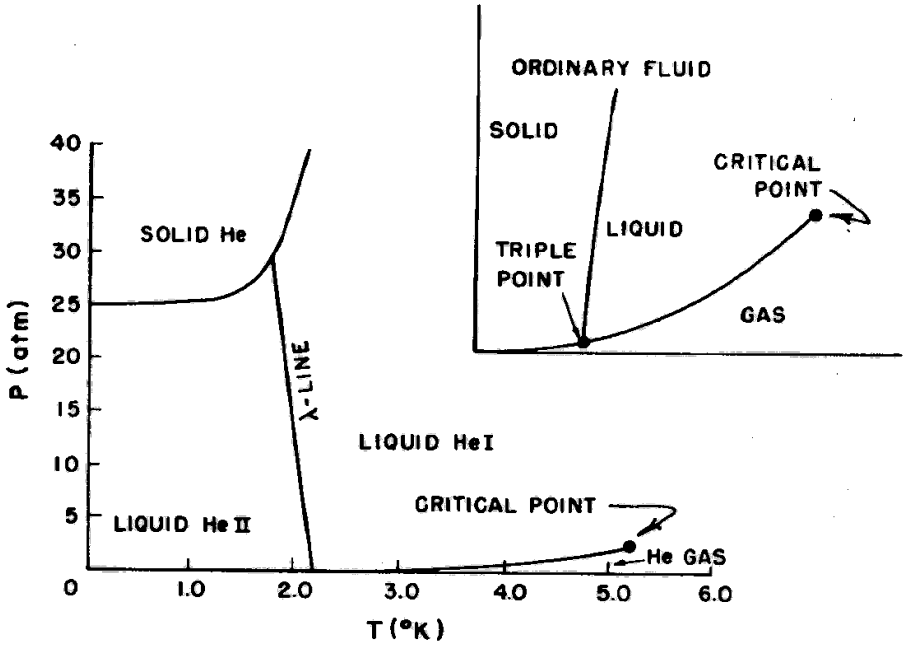

Figure 12. Pressure-temperature for helium-4 compared to that for an ordinary fluid (upper right). *Acknowledgement:* W.E. Keller, Helium-3 and helium-4 [191].

Aside from the λ-line that separates two liquid phases (one of them superfluid), Figure 12 also reveals another remarkable characteristic of helium: the absence of a triple point at which liquid, vapor and solid coexist at equilibrium. Because there is no triple point, the characteristics points for helium are the critical point (discussed in section 5) and the λ-line points. The lower λ-point is $T_\lambda^l = 2.1720$ K, $p_\lambda^l = 5.040 \times 10^{-3}$ MPa and $\rho_\lambda^l = 146.15$ kg m^{-3}; whereas the upper λ-point is $T_\lambda^u = 1.7633$ K, $p_\lambda^u = 3.013$ MPa and $\rho_\lambda^u = 180.44$ kg m^{-3} [1].

One of the goals of this equation of state is to represent qualitatively correctly the characteristics of the lambda transition. Some volumetric characteristics of this transition appear in Figure 13, where T_λ represents an estimated average of both the λ-point temperatures. The density of the saturated liquid (upper plot of Figure 13) passes through the λ-point and has a maximum slightly above the λ temperature; the density curve then decreases and presents a discontinuity of slope at the λ-point. The isobaric expansion coefficient and the isothermal compressibility (middle and bottom plots in Figure 13 respectively) reflect and even magnify the variations in density. The latter quantity presents a cusp-like behavior at the λ-point and is positive everywhere as expected.

The behavior of some thermal properties appear in Figure 14. The entropy of liquid helium (upper plot in Figure 14) is continuous everywhere but presents remarkably different behavior above and below the λ-point, which causes the entropy to have a discontinuous slope. Although the curve always decreases moving toward absolute zero, the dependence of entropy with temperature is much higher in the helium-II region. Considering that entropy is a direct function of the organization and molecular configuration, such a change in the curve suggests that the λ transition marks a significant change in the configuration of the system.

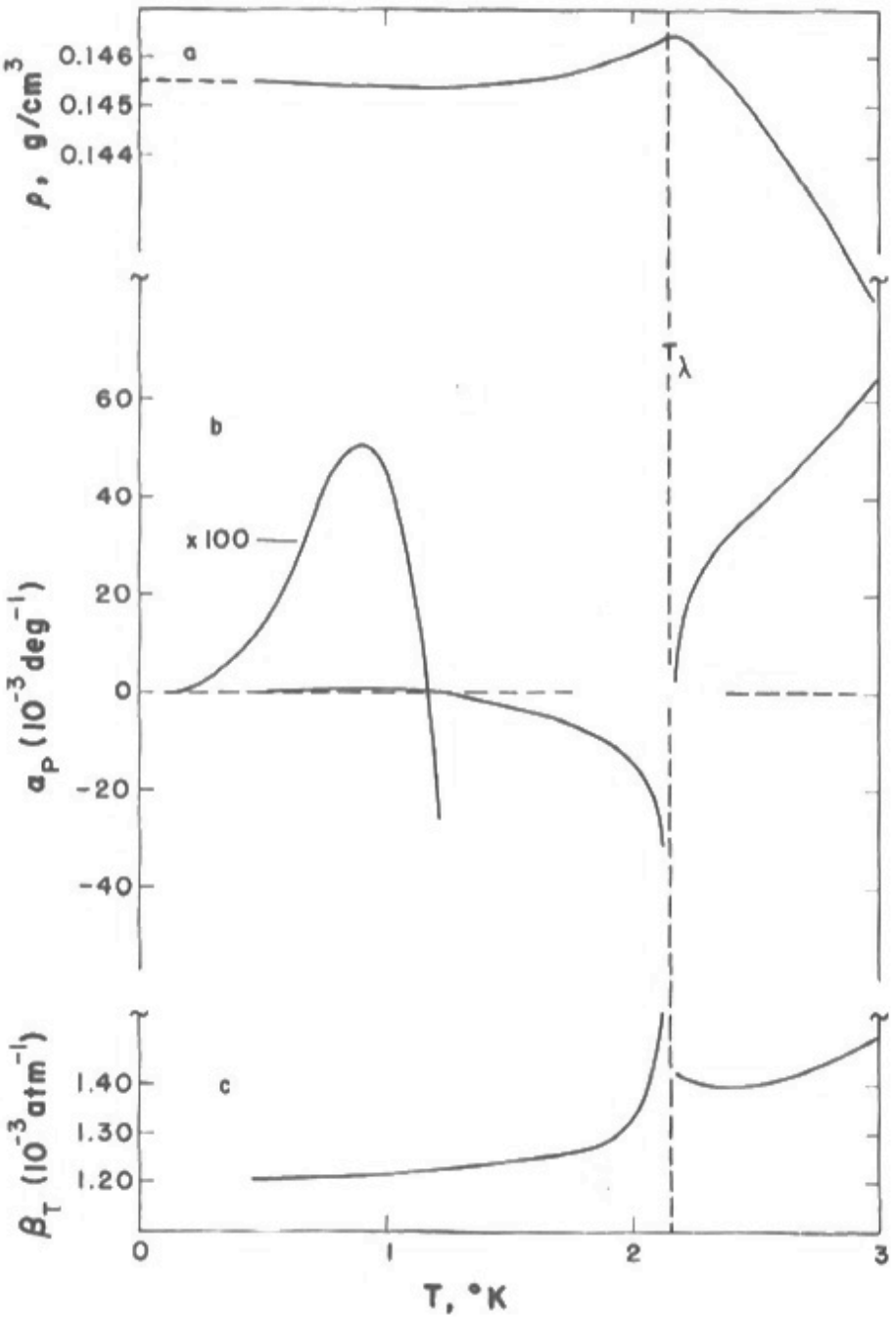

Figure 13. Schematics of some volumetric properties of liquid helium-4 along the saturation curve. Upper plot is density, middle plot is expansion coefficient at constant pressure, and bottom plot is compressibility coefficient at constant temperature. *Acknowledgement:* W.E. Keller, Helium-3 and helium-4 [191].

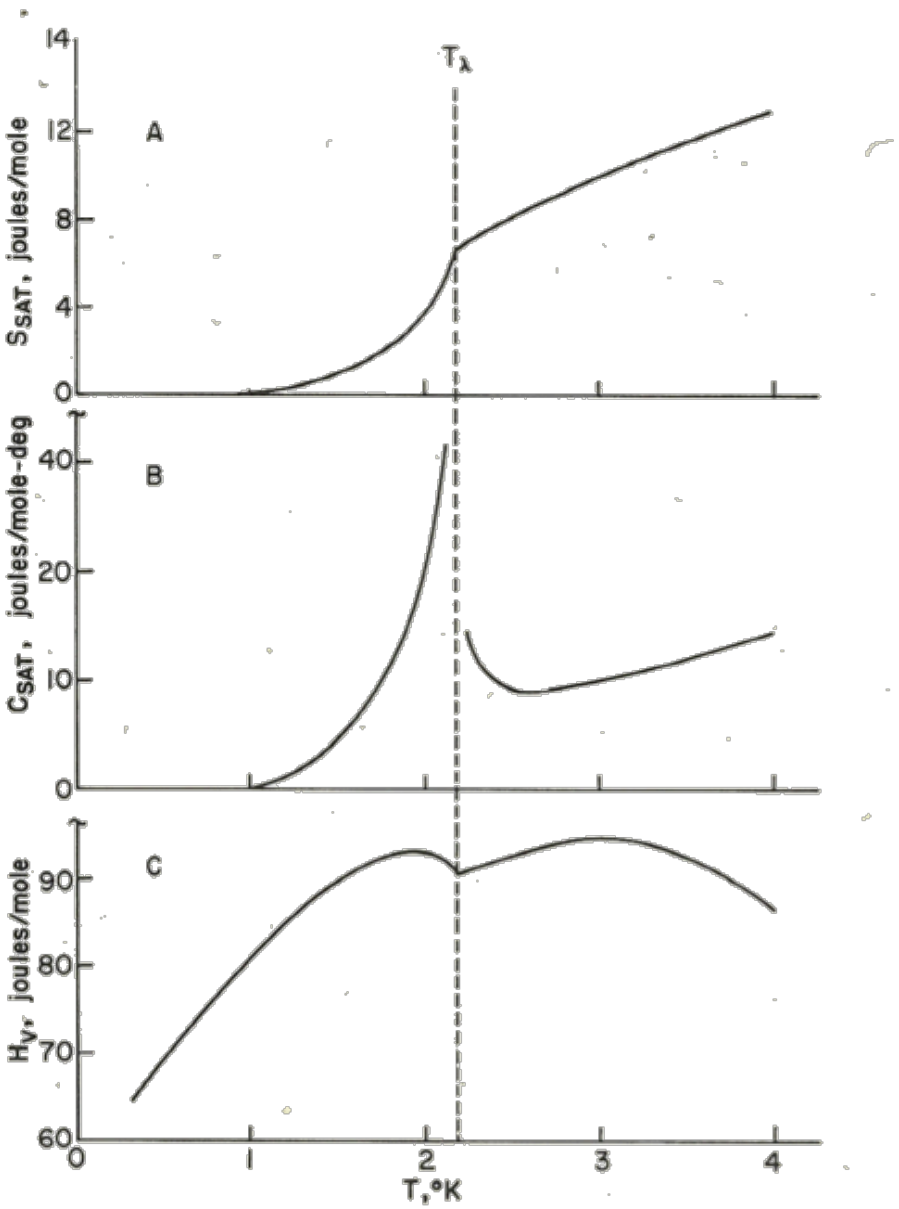

Figure 14. Schematics of some thermal properties of liquid helium-4 along the saturation curve. Upper plot is entropy, middle plot is specific heat and bottom plot is heat of vaporization. *Acknowledgement:* W.E. Keller, Helium-3 and helium-4 [191].

Although entropy is a primary thermodynamic property, it results from experimental measurements of specific heat. The middle plot in Figure 14 shows the behavior of the specific heat with temperature around the λ-point. The most relevant observation is the singularity at the λ-point similar to the behavior of the specific heat at the critical point. Finally, the bottom plot of Figure 14 depicts the performance of the heat of vaporization (calculated using the Clausius-Clapeyron equation).

In order to predict the abnormal and unique behavior of helium at the λ-point, it is necessary to utilize Gaussian-bell shaped terms similar to those used for the critical point. This is novel implementation of such terms proves very useful to mimic the critical point-like characteristics observed along the λ-line.

5. RESULTS

This section contains the results of developing the equation of state for ^{4}He. It begins with a brief summary of characteristic constants and the parameters of the equation of state. The section proceeds with phase equilibrium parameters and ancillary equations that provide a quick method to determine volumetric properties along the saturation curve. The section then focuses upon comparisons to experimental data and explanations of deviation plots. The data associated with the deviations appeared in Table **2** of section 4. All relative deviation plots presented in this section show the value calculated from the equation of state subtracted from the experimental value and divided by the experimental value. Finally, this section covers comparisons between the current standard for helium and the new equation of state for helium presented in this dissertation together with some results showing the capabilities of the new equation to predict properties around the lambda line.

5.1 THE NEW FUNCTIONAL FORM FOR HELIUM

It is necessary to define the reducing parameters and characteristic constants of helium before proceeding with fitting. The reducing parameters correspond to the critical properties, which appear in Table 3 along with other important parameters.

Table 3. Physical constants and characteristic properties of helium.

Symbol	Quantity	Value
R	Molar gas constant	8.314 472 J·mol^{-1}·K^{-1}
M	Molar mass	4.002602 g·mol^{-1}
T_c	Critical temperature	5.1953 K
p_c	Critical pressure	0.22746 MPa
ρ_c	Critical density	17.3887 mol·dm^{-3}
T_λ^l	Lower λ-point temperature	2.1720 K
p_λ^l	Lower λ-point pressure	0.005040 MPa
ρ_λ^l	Lower λ-point density	36.5137 mol·dm^{-3}
T_λ^u	Upper λ-point temperature	1.7633 K
p_λ^u	Lower λ-point pressure	3.013 MPa
ρ_λ^u	Lower λ-point density	45.0807 mol·dm^{-3}
T_{nbp}	Normal boiling point temperature	4.23 K
T_0	Reference temperature for ideal gas properties	100 K
p_0	Reference pressure for ideal gas properties	0.101325 MPa
h_0^0/RT_0	Reference ideal gas enthalpy at T_0	2.5
s_0^0/R	Reference ideal gas entropy at T_0 and p_0	12.4284

The functional form contains the parameters defined in Eq. (75) of Section 3.

The rounded values and final equation that is part of Refprop 9.1 [192] are in Table 4.

Table 4. Coefficients of the equation of state. (Eq. (75), Section 3).

k	N_k	t_k	d_k	l_k	η_k	β_k	γ_k	ε_k
1	0.014799269	1	4	-				
2	3.06281562	0.426	1	-				
3	-4.25338698	0.631	1	-				
4	0.05192797	0.596	2	-				
5	-0.165087335	1.705	2	-				
6	0.087236897	0.568	3	-				
7	2.10653786	0.9524	1	1				
8	-0.6283503	1.471	1	2				
9	-0.28200301	1.48	3	2				
10	1.04234019	1.393	2	1				
11	-0.07620555	3.863	2	2				
12	-1.35006365	0.803	1	1				
13	0.11997252	3.273	1	2	-8.674	-8.005	1.1475	0.912
14	0.107245	0.66	1	2	-4.006	-1.15	1.7036	0.79
15	-0.35374839	2.629	1	2	-8.1099	-2.143	1.6795	0.90567
16	0.75348862	1.4379	2	2	-0.1449	-0.147	0.9512	5.1136
17	0.00701871	3.317	2	2	-0.1784	-0.154	4.475	3.6022
18	0.226283167	2.3676	2	2	-2.432	-0.701	2.7284	0.6488
19	-0.22464733	0.7545	3	2	-0.0414	-0.21	1.7167	4.2753
20	0.12413584	1.353	2	2	-0.421	-0.134	1.5237	2.744
21	0.00901399	1.982	2	2	-5.8575	-19.256	0.7649	0.8736

The final equation contains 6 polynomial terms, 6 exponential and 9 Gaussian-bell shaped terms. This equation minimizes the combination of data and constraints

selected in Section 4. Reducing the number of terms in the equation requires eliminating terms in successive fits by either deleting the term that contributed least to the overall sum of squares in a previous fit or by combining two terms that had similar values of the exponents (resulting in similar contributions to the equation of state). After having eliminated a term, the fit was repeated until the sum of squares for the new iteration was of the same order of magnitude as the previous one. This combination was the one that provided significant results in terms of deviations and thermodynamic behavior with the least number of terms. Several combinations with fewer total terms were tested but none were fulfilled the expectations of a reference equation of state. As the minimization proceeded, several parameters were fixed if they were essentially integers, then the number of variables in the minimization was reduced gradually.

The exponents on density in the equation of state must be positive integers so that the derivatives of the Helmholtz energy with respect to density have the correct behavior near the ideal gas limit [103]. Because non-integer values for the density exponents resulted from the nonlinear fitting methods, a sequential process of rounding each density exponent to the nearest integer, followed by refitting the other parameters to minimize the overall sum of squares, was implemented until all of the density exponents in the final form were positive integers. A similar process used for the temperature exponents reduced the number of significant figures to one or two decimal places.

5.2 PHASE EQUILIBRIUM OF HELIUM

The single most important state of any fluid in the development of equations of state is the critical point. This point becomes the reducing parameter for the equation and defines liquid and vapor states, as well as supercritical states that behave like gases (when the density is less than the critical density) and like liquids (when the density exceeds the critical density). Nearly all fluids show similar behavior when their properties are scaled by the critical parameters. The law of corresponding states uses this observation to predict properties for any fluid by mapping the surface of an unknown substance onto that of a well-known substance. The prediction can improve after incorporating additional experimental data.

The λ-line defines the boundary between helium I and superfluid helium II. As discussed in Section 4, the equation of state should describe qualitatively the behavior of the fluid along the transition. The melting (or freezing) line describes the boundary between the liquid and solid states for temperatures above the triple point. Equations of state such as the one described here can calculate the properties at the melting point in the liquid phase, but cannot calculate properties of the solid phase. Both the λ-line and the melting curve are boundaries of the equation of state and constrain the applicability of the equation. Characteristic values of the λ-line are in table 1 whereas melting curve information is in the review released by Sychev, *et al.* [1].

5.2.1 Critical point

Numerous authors [112, 128, 130, 146, 148, 163, 165, 171, 193] report critical parameters for helium. Difficulties in the experimental determination of the critical parameters and impurities in the samples cause considerable differences among the results obtained by the various investigators. The critical density is difficult to determine accurately by experiment because of the infinite compressibility at the critical point and the associated difficulty of reaching thermodynamic equilibrium. Therefore, reported values for the critical density are often calculated by extrapolation of rectilinear diameters with measured saturation densities, or by correlating single-phase data close to the critical point.

The critical density and temperature adopted in this project are the values used by McCarty and Arp [32] but adjusted to the ITS-90 temperature scale. The critical parameters come from the work done by Moldover in determining the behavior of heat capacities in the critical region [163]. The critical pressure usually results from extrapolating vapor pressures to the assumed critical temperature. The critical point values recommended by McCarty and Arp appear in Table 3. However, with the availability of new high accuracy vapor pressure and saturated liquid data [33] in the critical region, the reducing pressure (critical pressure) of the equation of state was determined simultaneously with the other coefficients and exponents in the equation, while the critical temperature and density remain almost exactly the experimental values by using a large weight for them. The resulting critical point from the equation of state is

$T_c = 5.1953$ K (106)

$\rho_c = 17.38379$ mol·dm^{-3} (107)

$p_c = 0.22761$ MPa (108)

These values agree within experimental errors with those adopted by McCarty and Arp but differ slightly because more accurate saturation data now are available. Figure 15 shows the critical point along with both the reference lambda line and melting curve that represent the limits of the equation.

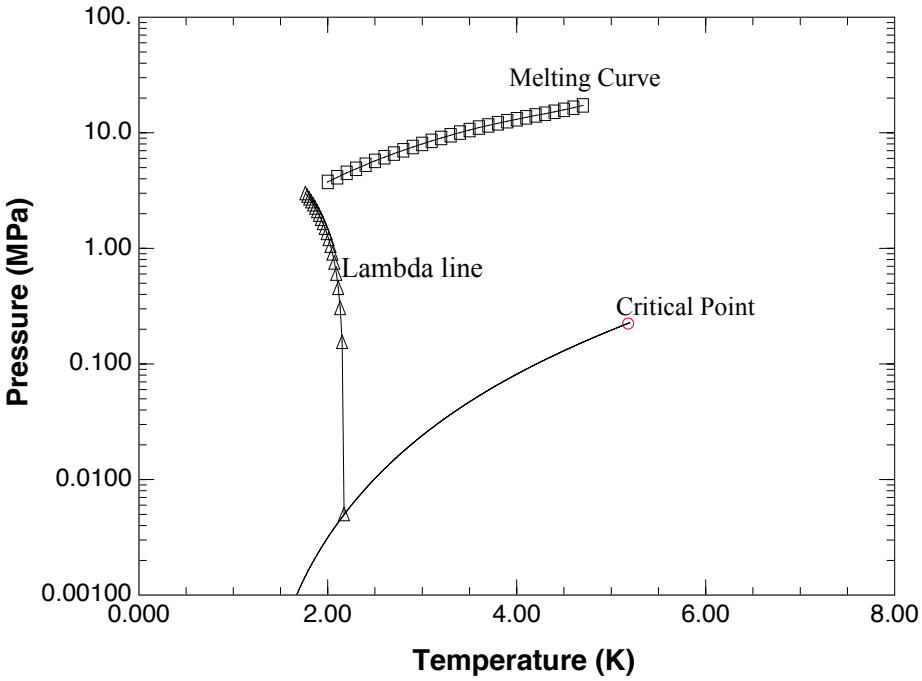

Figure 15. Critical point and boundaries of the equation.

5.2.2 Vapor pressures

Saturation states define the boundaries between liquid and vapor, and ancillary equations can give good estimates. These ancillary equations are not necessary when a full equation of state is available because application of the Maxwell criteria to the equation of state can provide the saturation states. This criterion for a pure fluid requires finding a state in the liquid and a state in the vapor that have the same temperature, pressure, and Gibbs energy. The ancillary equations can provide good estimates for the pressure and densities required in the iterative procedure to find the saturation states.

Figure 16 summarizes the available vapor pressure data for helium.

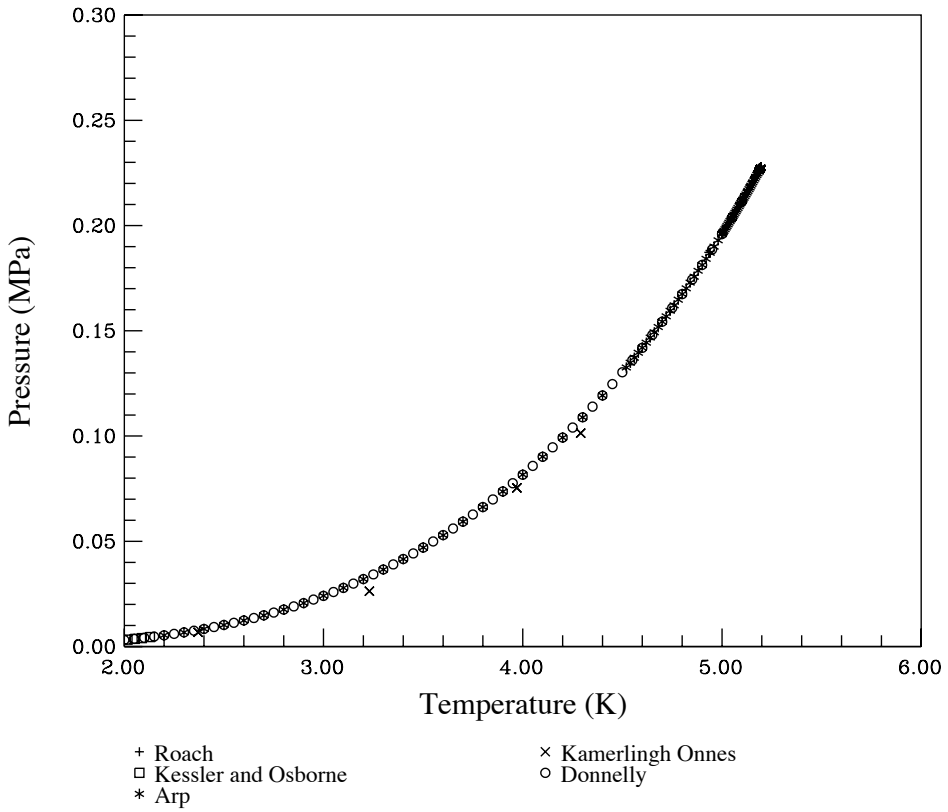

Figure 16. Vapor pressure data.

The points identified as Arp correspond to calculations from the current standard equation of state for helium. The Donnelly data received higher weights given their current relevance and accuracy. The ancillary equation used to represent the vapor pressure is

$$\ln\left(\frac{p_\sigma}{p_c}\right) = \frac{T_c}{T}\left[N_1\theta + N_2\theta^{1.5} + N_3\theta^{1.25} + N_4\theta^{2.8}\right] \tag{109}$$

where $N_1 = -3.8357$, $N_2 = 1.7062$, $N_3 = -0.71231$, $N_4 = -1.0862$, $\theta = (1 - T/T_c)$, and p_σ is the vapor pressure. This equation is a modification of the equation first proposed by Wagner [88]. The original form of the equation has been used to model the vapor pressures for a large number of substances.

Figure 17 shows the deviations of the equation of state from experimental vapor pressures. Although the deviations are systematic, they fit the Donnelly data within its experimental uncertainty. These measurements are very recent (1998) and are the most reliable source of experimental, saturated data of liquid helium.

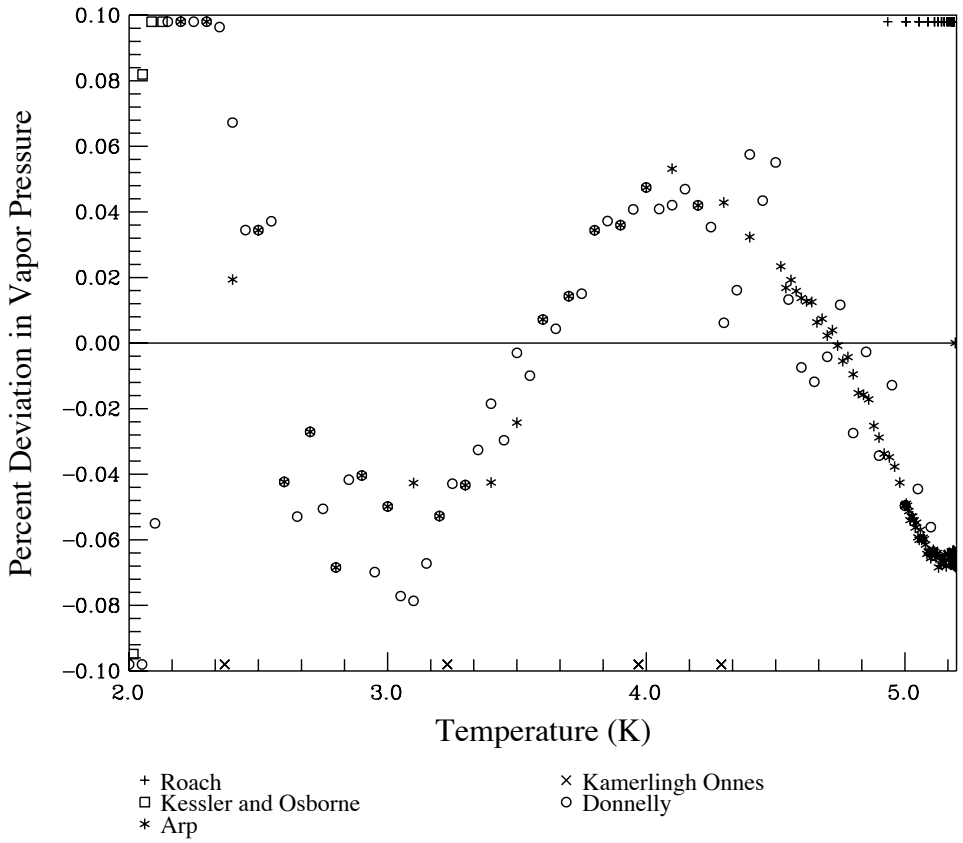

Figure 17. Deviation in vapor pressure.

5.2.3 Saturated densities

Figure 18 summarizes the available saturated densities data for helium. An unexpected curvature appears on the vapor side of the graph (lower right) around 2.0 K. This strange behavior is a result of the superfluid influence close to the transition.

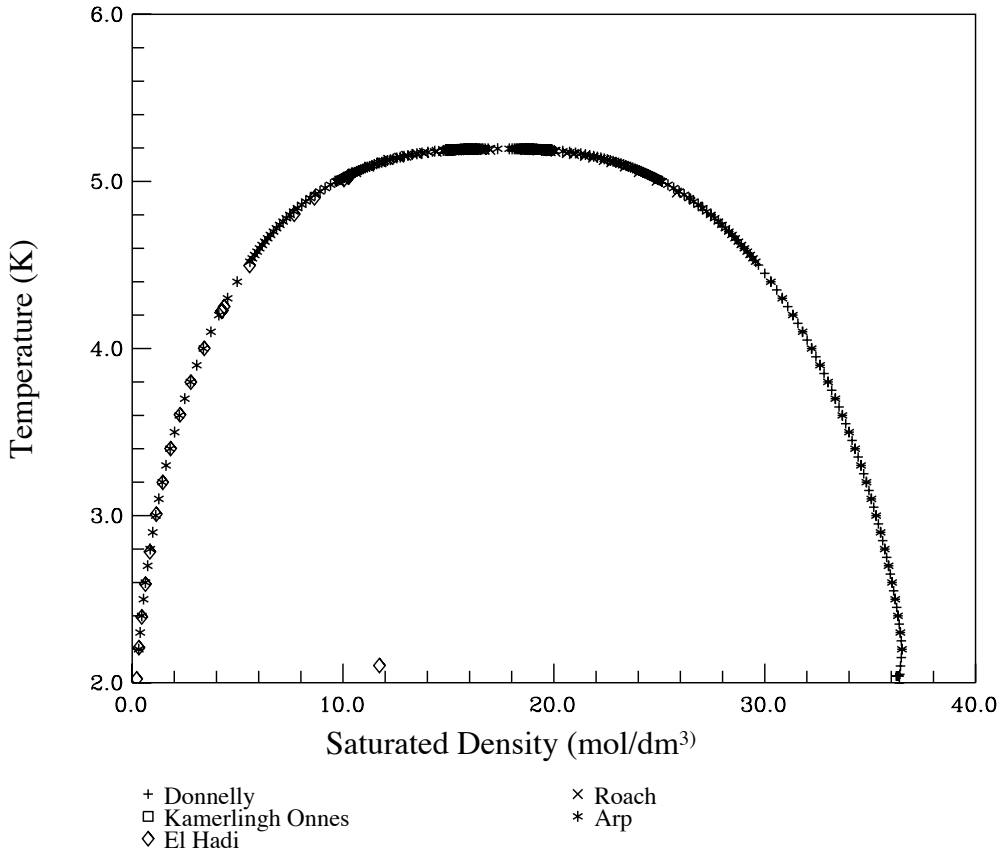

Figure 18. Saturated densities data.

The points identified as Arp correspond to calculations from the current standard equation of state for helium. Donnelly's data are also available for the liquid region. The for the ancillary equation for the saturated liquid density is

$$\frac{\rho'}{\rho_c} = 1 + N_1\theta^{0.286} + N_2\theta^{1.2} + N_3\theta^{2.0} + N_4\theta^{2.8} + N_5\theta^{6.5} \qquad (110)$$

in which $N_1 = 1.0926$, $N_2 = 1.6584$, $N_3 = -3.6477$, $N_4 = 2.7440$, $N_5 = -2.3859$, $\theta = (1 - T/T_c)$, and ρ' is the saturated liquid density. Eq. (111) represents the saturated vapor density

$$\ln\left(\frac{\rho''}{\rho_c}\right) = N_1\theta^{0.333} + N_2\theta^{1.5} + N_3\theta^{2.1} + N_4\theta^{2.7} + N_5\theta^{9.0} \tag{111}$$

in which $N_1 = -1.5789$, $N_2 = -10.749$, $N_3 = 17.711$, $N_4 = -15.413$, $N_5 = -14.352$, and ρ'' is the saturated vapor density. Values calculated from the equation of state using the Maxwell criteria were used in developing Eq. (111), along with the rectilinear diameter criterion (the average of the saturated liquid and vapor densities). The values of the coefficients and exponents for Eq. (110) and Eq. (111) resulted from nonlinear least squares fitting techniques.

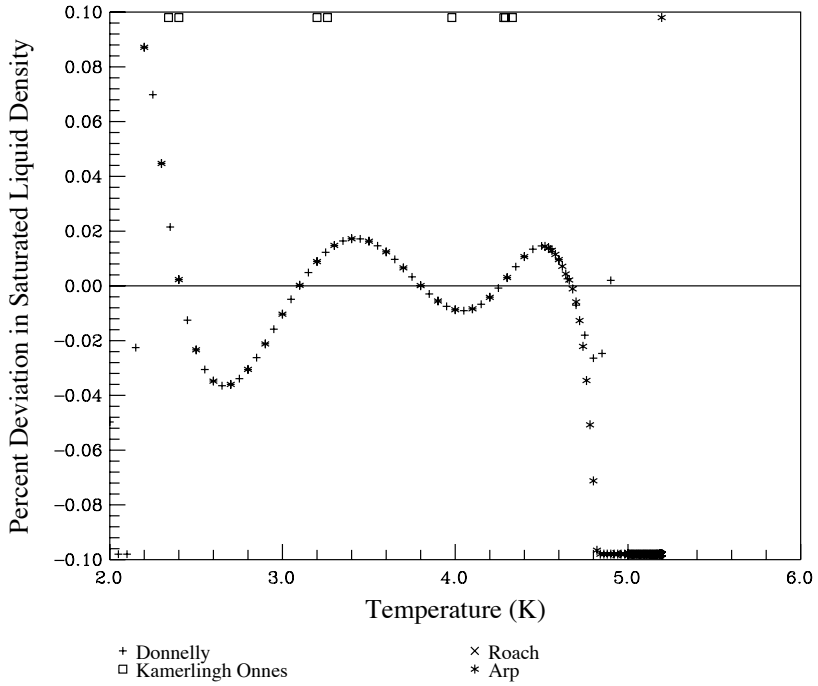

Figure 19. Deviation in saturated liquid density.

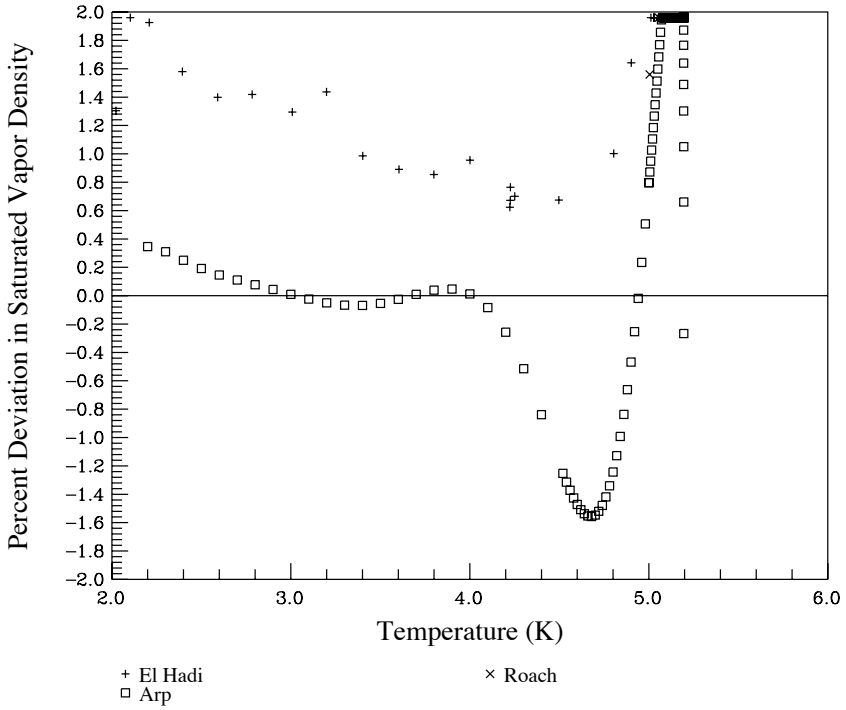

Figure 20. Deviation in saturated vapor density.

Figure 19 and Figure 20 illustrate the deviations of the equation of state from experimental data for saturated liquid density and saturated vapor density respectively. Similar to the vapor pressure, the saturated liquid density from Donnelly is fit very well. Arp's correlation has similar behavior, except in the critical region where it behaves differently. The deviations are larger near the critical temperature and the lambda line temperature because of the complexity of the physics in these regions. The situation is different for the saturated vapor pressure represented in Figure 20. The values of saturation along the vapor side come from the Maxwell criteria and the rectilinear diameter criterion using reliable saturated liquid densities. Therefore, the high deviations reflect limited experimental capabilities at the time of the measurements. As

a recommendation, new saturated vapor measurements would be useful for further tuning of the equation of state.

5.3 $p\rho T$ DATA AND VIRIAL COEFFICIENTS

Figure 21 presents experimental $p\rho T$ data for helium. Figure 22 shows the $p\rho T$ data measured recently by McLinden during the past five years [105, 106]. He reports a maximum experimental uncertainty of 0.04% in density, so these measurements represent an important new source of data for the current equation. Figure 23 and Figure 24 compare densities calculated from the equation of state with experimental data; Figure 25 shows detailed comparisons with the highly accurate data taken by McLinden. In Figure 23 and Figure 24, the deviations appear in groups classified by temperature. The temperature listed at the top of each small plot is the nearest temperature to the measured value.

Lounasma [157], Keller [145], Grilly [135], Hill [138], El Hadi [129], Roach [171] and Edwards [127] gave special attention to low temperature data (T<20 K). Most of the data can be fit within 0.2 % deviation in density, except in the critical region where the deviations are higher.

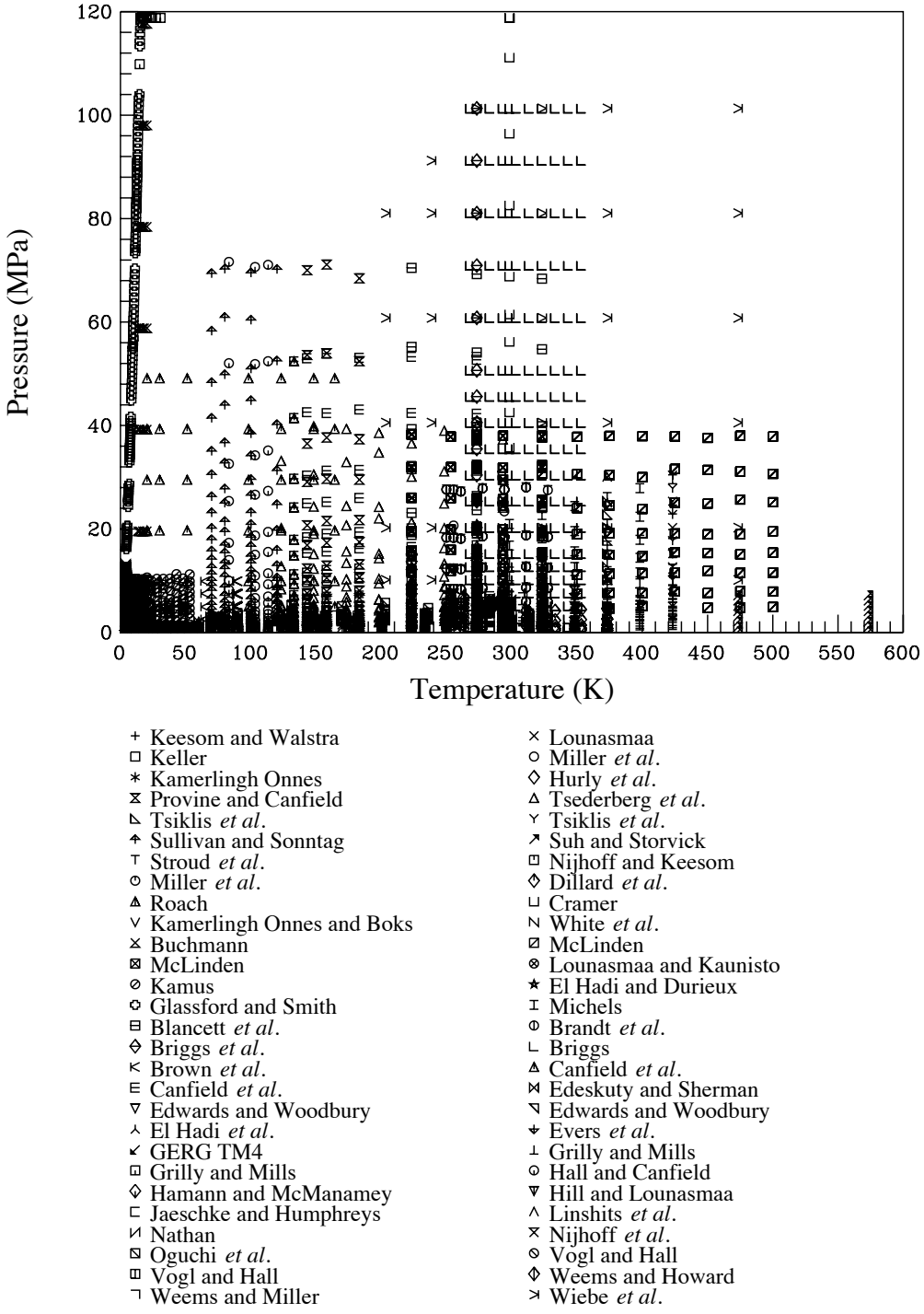

Figure 21. Overall $p\rho T$ data for helium.

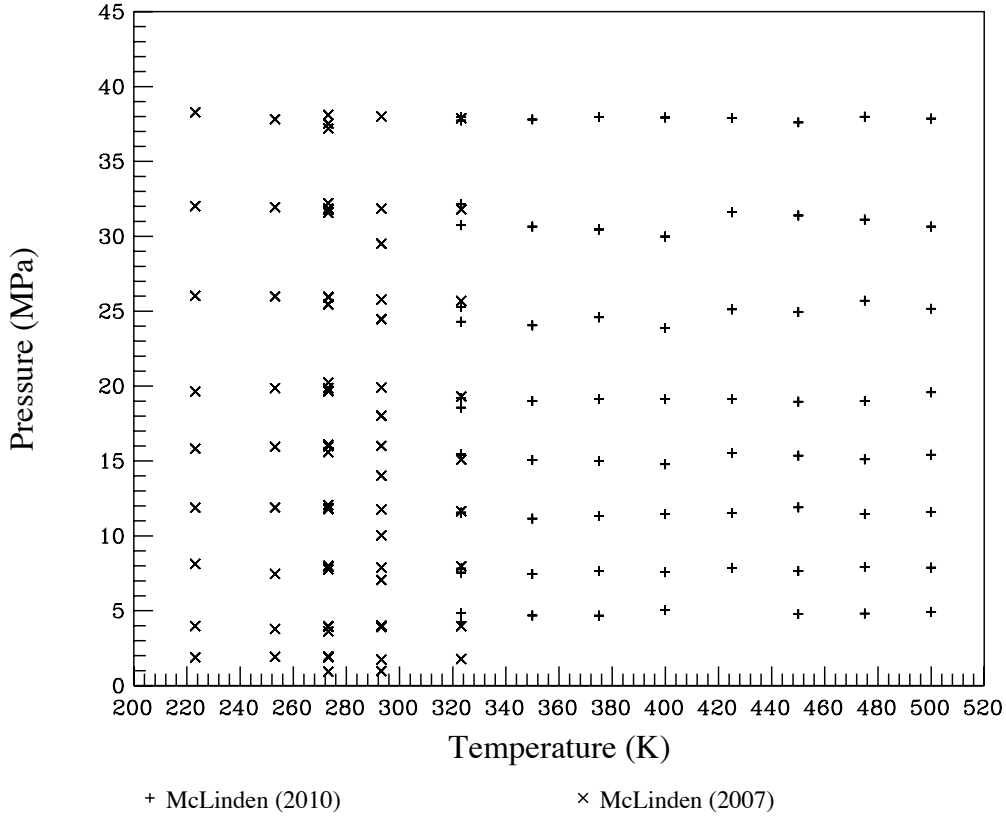

Figure 22. McLinden's $p\rho T$ data for helium [105, 106].

Two cases of inconsistent data exist in this range. One of them is the data published by Edeskuty [126] that presents a systematic deviation close to the critical temperature. Apparently, Donnelly's saturated liquid densities cause this problem, but given the relevance of the latter, the former receives lower weights. The other problem is between the data of Keller and those of Keesom [143], but the Keller data are more recent and cover a wider range of conditions, so they have been chosen.

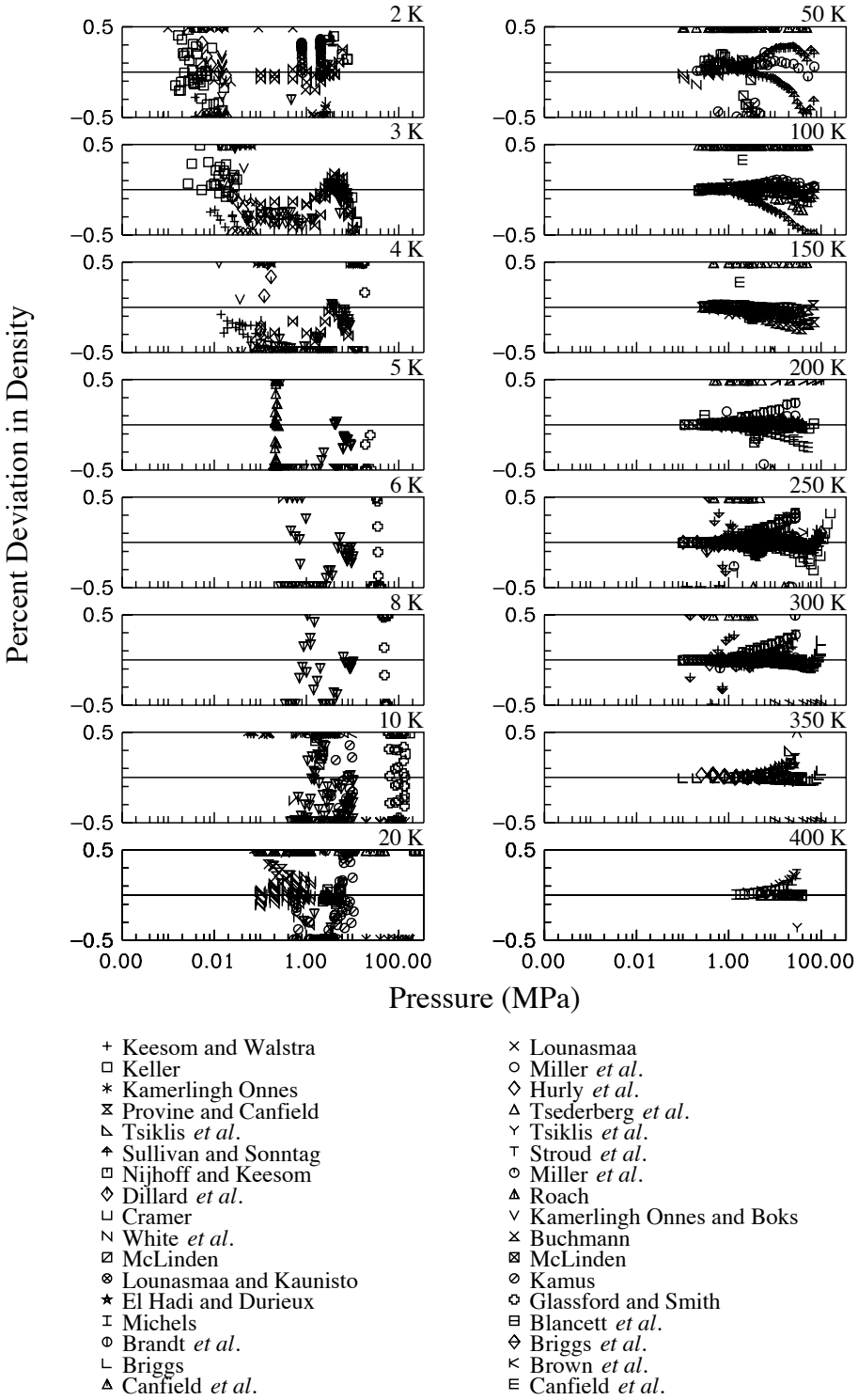

Figure 23. Deviation in $p\rho T$ data from 2 K to 400 K.

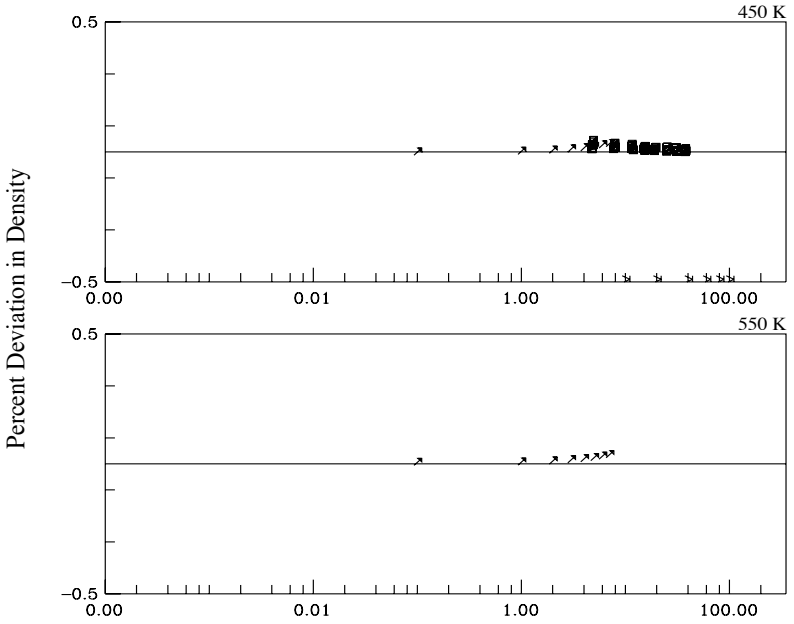

Figure 24. Deviation in $p\rho T$ data from 450 K to 550 K.

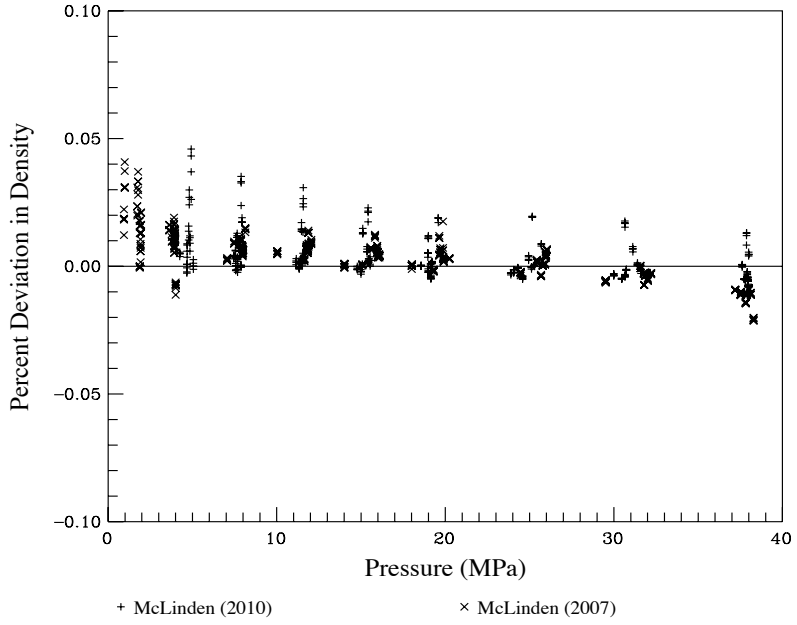

Figure 25. Deviation from McLinden $p\rho T$ data.

Hill's data are relevant because they are close to the critical area. Roach's importance lies in having high-pressure measurements (~ 40 MPa) at low temperature, and El-Hadi's relevance derives from the McCarty and Arp recommendation. Also, as McCarty and Arp suggested in their equation, Glassford's high-pressure data deviate significantly around 10 K.

The data by White [182], Boks [114], Nijhoff [166] and Hall [137] received higher weights from 20 K to 50 K. The density deviations for these data are up to 0.05 % below 20 MPa and 0.07% up to 70 MPa. As commented by McCarty and Arp, Sullivan's data are strongly systematic.

For medium temperatures (100 K to 150 K), the deviations are much lower. For instance, from 100 K to 150 K, the density deviations for Canfield [120], Provine [170], Hall [13] and Tsederberg [178] are up to 0.02 % up to 20 MPa, increase to 0.05 % around 40 MPa and go back down to 0.02% at 70 MPa. Sullivan's data were separate and systematic, as expected. For 200 K a systematic problem exists for one data set by Canfield [121] and Stroud [174] and the deviations go up to 0.2 % around 70 MPa. On the other hand, data taken by McLinden, Tsederberg, Blancett [116] and Vogl [181] yielded deviations of about 0.03 % up to 60 MPa.

New systematic problems appeared from 250 K to 300 K for Brandt, Stroud and Michels [181] with deviations as high as 0.2 %. Data from Evers [131] have significant deviations as well, even though they are more recent than other data. However, data by Vogl, McLinden, Miller [162], Weems [185], Blancett and Dillard [124] are fit well at

around 0.02 % in density deviation. Finally, 0.01 % for 95% confidence interval exists for all data sets at temperatures from 350 K to 550 K.

The McLinden data receive special attention. The apparatus is a two-sinker, magnetic suspension densimeter, and the most accurate measuring technique for density currently available. The deviation in density of the equation of state from the experimental data is 0.02 % at 2σ. This value is lower than the experimental uncertainty he reports (0.04 %).

Differences between experimental values and calculations from the equation of state for the second and third virial coefficients appear in Figure 26 and Figure 27 respectively. Virial coefficients plots mostly present absolute rather than relative deviations [31] [30] because they show more clearly difficulties associated with the data.

The results are impressive for both the second and third virial coefficients. The equation is consistent with values determined both experimentally and theoretically. For experimental measurements, good agreement appears for values reported by Holste [30], Barrufet [9], Blancett [114-116], Canfield [116], Cramer [123], Dillard [124], Gugan [124], Holborn [139], Hoover [141], Keesom [141],

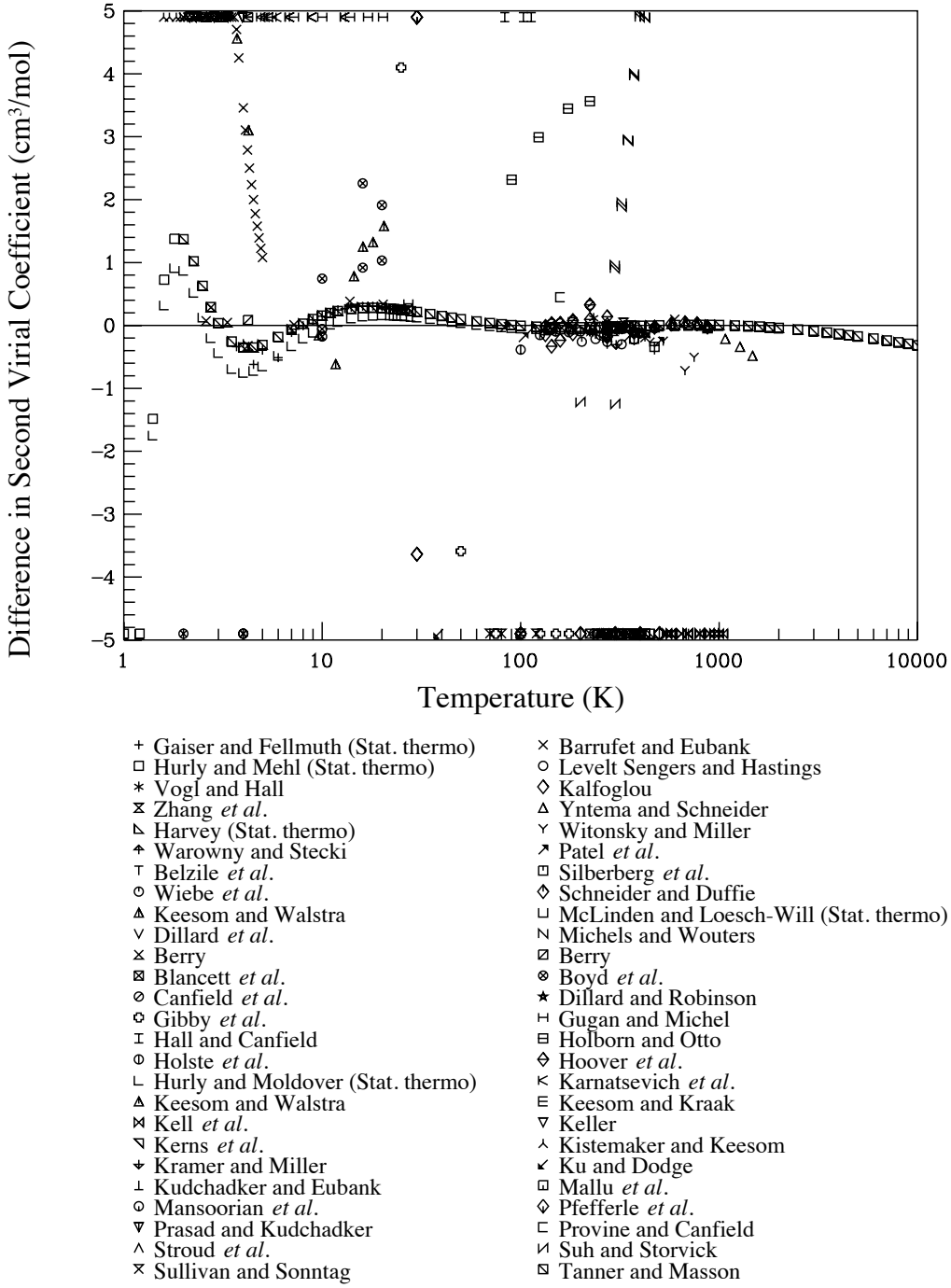

Figure 26. Difference in second virial coefficient.

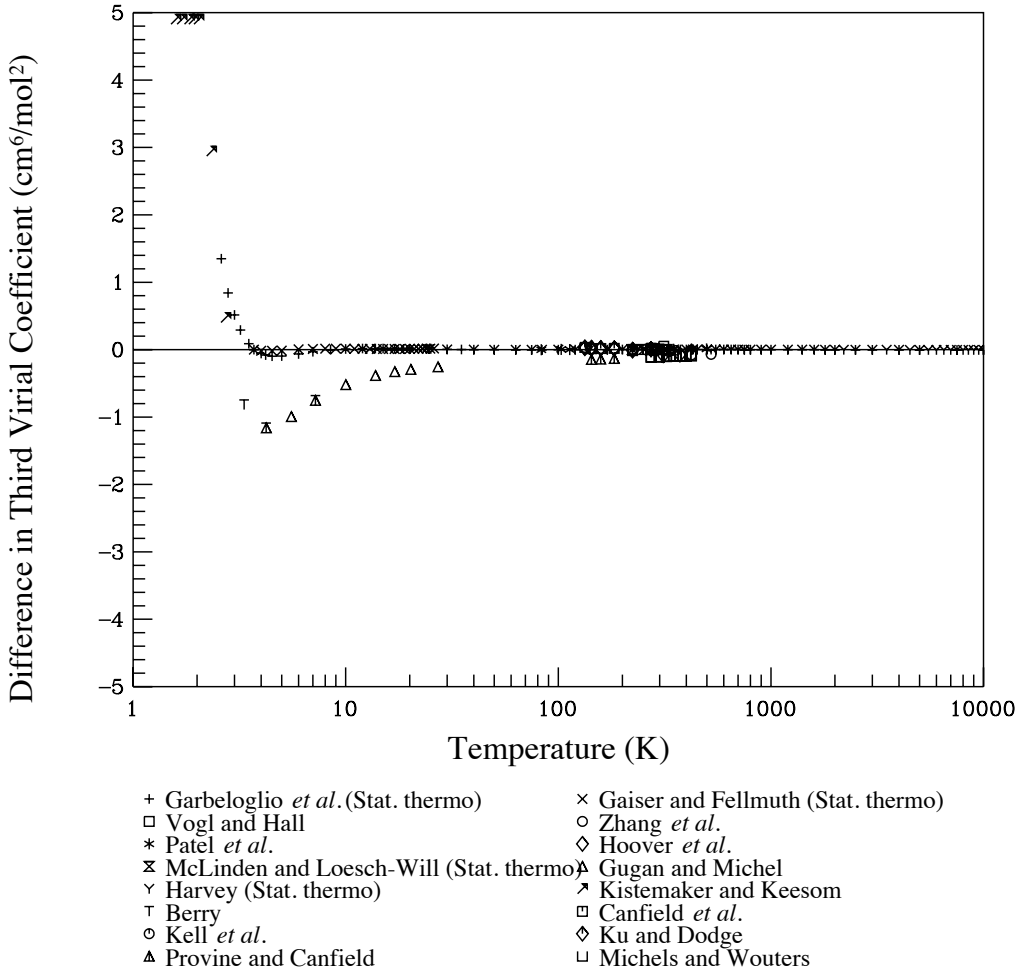

Figure 27. Difference in third virial coefficient.

Patel [167] and White [182] among others. On the theoretical side, Moldover [106], Hurly [10], Gaiser [10], Sengers [172], and Harvey and Garberoglio [108] performed important calculations.

New theoretical calculations have appeared for the fourth virial coefficient of helium [106], however this information is not useful for this equation of state. Currently, no multiparameter equation of state can describe the fourth virial coefficient.

Solving this problem this problem remains one of the main challenges in the field of multiparameter equations of state.

5.4 CALORIC DATA

The sources of experimental data for the caloric properties of helium are in Table **2** in section 4. Comparisons of values calculated from the equation of state for the enthalpy of vaporization are in Figure 28. Only two data sets are available, and only one of them has low deviations. These data are part of Donnelly's paper. He claimed an experimental uncertainty of up to 0.2 %, which suggests that the equation of state is capable of reproducing enthalpies of vaporization within the experimental error, except in the vicinity of the critical region and the lambda transition. The accurate values for vapor pressure, and saturated liquid and vapor densities demonstrate that the equation will provide accurate heats of vaporizations.

Figure 29 shows the deviations for saturated liquid heat capacity with respect to Donnelly's values. Donnelly reported experimental uncertainties of about 2 %. The numbers predicted by the equation of state lie within the experimental uncertainty, except for the critical and the lambda transition regions, where the experimental uncertainty is higher.

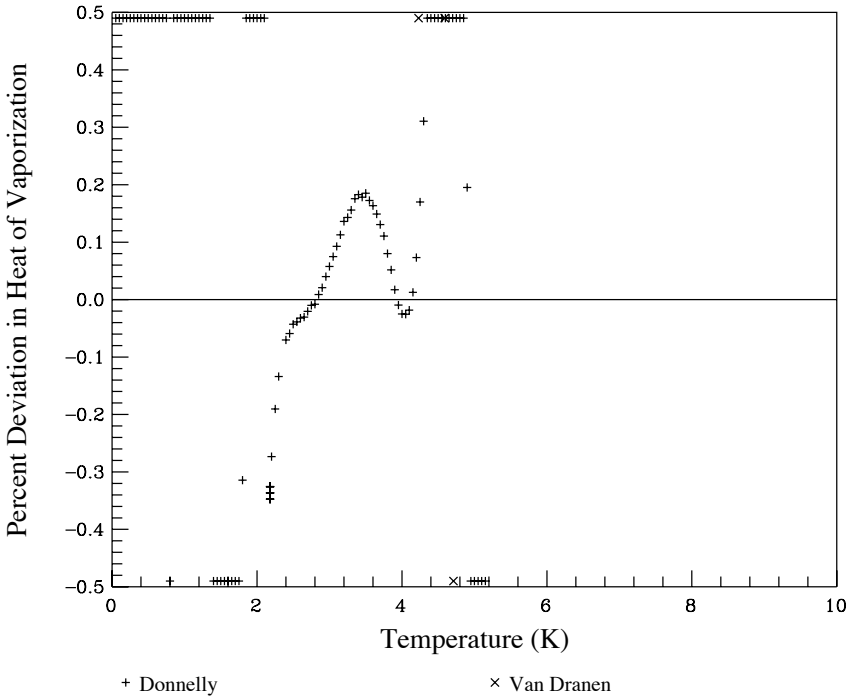

Figure 28. Deviation in heat of vaporization.

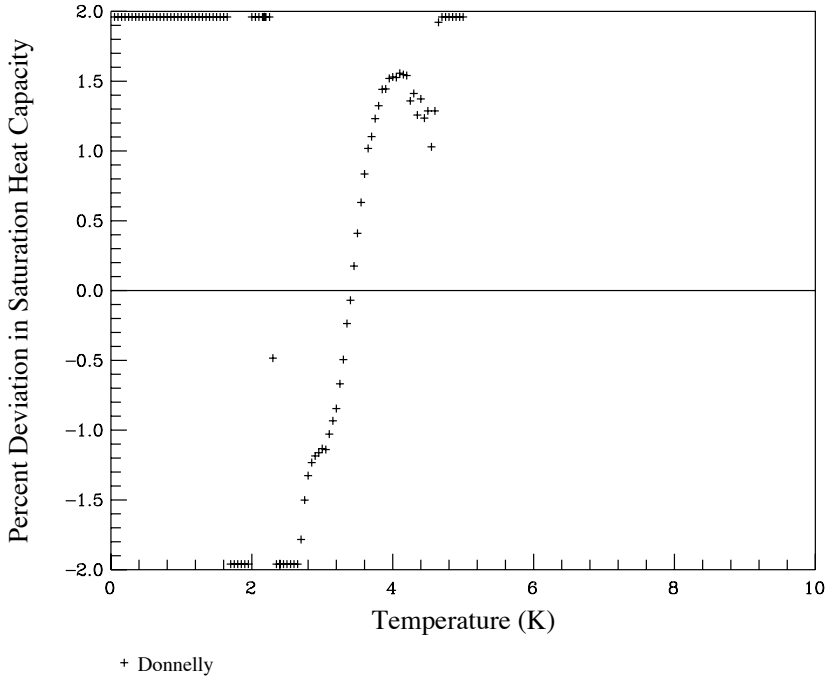

Figure 29. Deviation in saturation heat capacity.

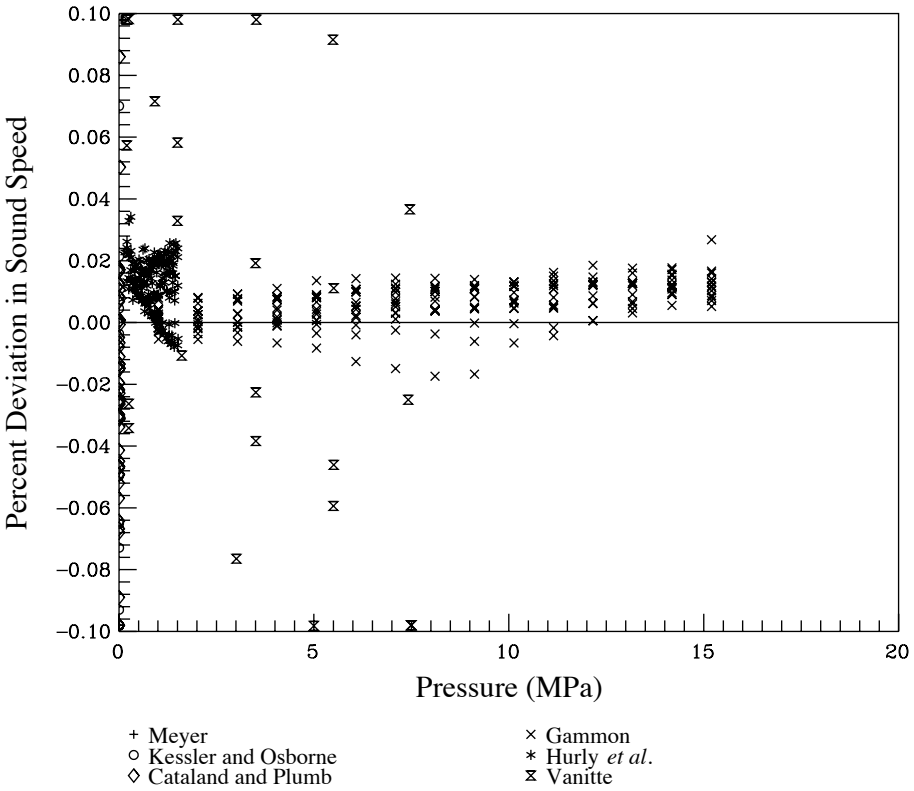

Figure 30. Deviation in sound speed.

Comparisons of values calculated from the equation of state for the speed of sound are in Figure 30. The calculations are accurate considering that at least for Hurly [10] the experimental uncertainty increases to 0.035 %. Speed of sound measurements at low pressure are necessary for developing an equation of state because they help balance the lack of low experimental uncertainty of $p\rho T$ data at such conditions.

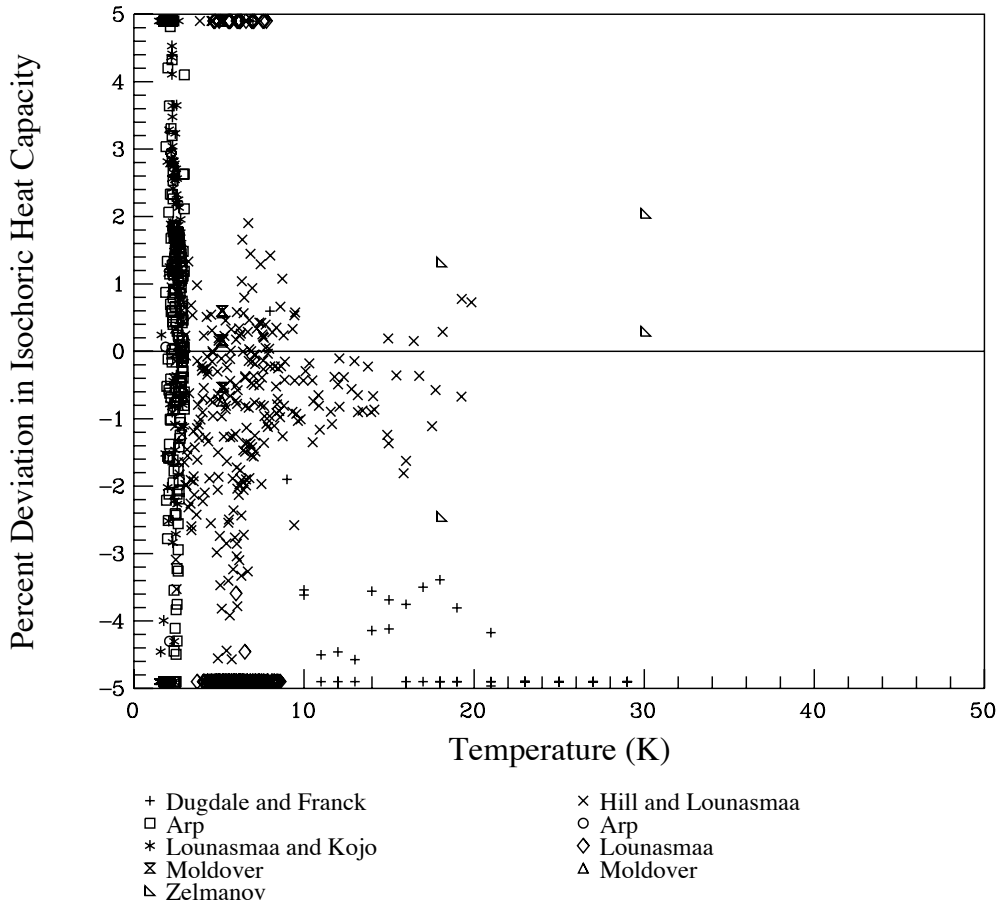

Figure 31. Deviation in isochoric heat capacity.

Figure 31 shows the equation with experimental isochoric heat capacity values Special attention was given to the data of Lounasmaa [156] and Moldover [163-165]. Lounasmaa's data are important considering the number of points he collected, and Moldover's are relevant because of his work in the critical region. For areas different from the critical region and the lambda line, the experimental uncertainty is no worse than 5 %. In the difficult regions, the uncertainty can as much as 10 %. This suggests

that most of the predicted isochoric heat capacities are inside the experimental uncertainty limit. Good predictions of thermodynamic properties indicates internal consistency of the equation of state. For instance, good fits to accurate density, speed of sound and saturation heat capacity data also result in accurate descriptions of the isobaric and isochoric heat capacities

Using several Gaussian-bell shaped terms for the equation helped tremendously to decrease the deviations of the isochoric heat capacity in the critical region and near the lambda transition because they are more capable of describing the sharpness of the isochoric heat capacity in these areas.

5.5 IDEAL CURVES

An ideal curve for any property of a real fluid is the curve of the hypothetical ideal gas at the same temperature and density. Ideal curves can be defined for any property, but in the field of multiparameter equations of state they specifically refer to the compressibility factor and its first derivatives. The characteristic curves are the Boyle curve, given by the equation

$$\left(\frac{\partial Z}{\partial v}\right)_T = 0 \tag{112}$$

the Joule-Thomson inversion curve,

$$\left(\frac{\partial Z}{\partial T}\right)_p = 0 \tag{113}$$

the Joule inversion curve,

$$\left(\frac{\partial Z}{\partial T}\right)_v = 0 \tag{114}$$

and the ideal curve,

$$\frac{p}{\rho RT} = 1. \tag{115}$$

They are useful because their shapes are essentially the same for any pure fluid, and because the available data for most fluids are insufficient to cover the conditions where the ideal curves reside. So, knowing their expected behavior is useful in shaping the extrapolation behavior of the fluid. Unfortunately, for helium no data exist for the ideal curves region, so only the shape, but not the actual numeric values can be specified accurately.

The temperature at which the Boyle and ideal curves begin (at zero pressure) is also known as the Boyle temperature, or the temperature at which the second virial coefficient is zero. The point at which the Joule inversion curve begins (at zero pressure) corresponds to the temperature at which the second virial coefficient is a maximum. Thus, in order for the Joule inversion curve to extend to zero pressure, the second virial coefficient must pass through a maximum value, a constraint that not all equations of state satisfy. Figure 32 shows the ideal curves for helium predicted by the new equation of state. They look reasonable as was found for other fluids [29] [101] [30].

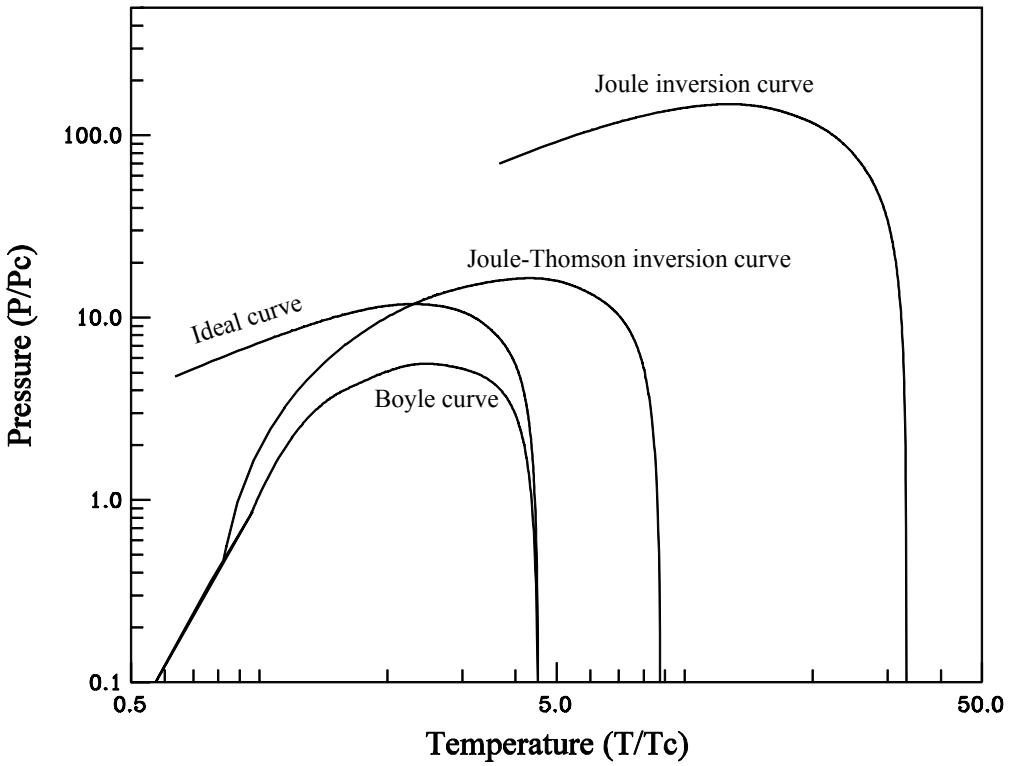

Figure 32. Ideal curves of the equation of state for helium as a function of temperature and pressure.

Equations of state with temperature exponents less than zero do not provide reasonable shapes for the ideal curves. The effects of all terms should decrease at high temperatures, but the contribution of terms with $t < 0$, increases as the temperatures rises. Therefore, negative temperature exponents should never be allowed in an equation of state of the form presented in this work.

5.5 COMPARISONS WITH MCCARTY'S EQUATION OF STATE

One of the main difficulties found with McCarty's equation of state was the lack of ability to obtain reasonable thermodynamic behavior upon extrapolation.

Extrapolation capabilities are important for two reasons: (1) if the extrapolation is correct, then state points in normal regions should be more accurate (because bad extrapolations outside the normal range result from incorrect derivatives in normal regions, with adverse effects on derivative properties such as heat capacities; and (2) mixture models can access regions outside the range of validity of the equation of state depending upon composition and non-ideality of the mixture.

Constraints are a key element in enhancing the extrapolation behavior. For example, additional plots of constant property lines on various thermodynamic coordinates were made to assess other behavior of the equation of state, and constraints helped to avoid having these constant property lines cross. Typical constraints avoid abnormal positive or negative values in slopes, curvatures, third and fourth derivatives.

One consequence that arises from poor extrapolation capabilities and consistency is incorrect derived properties from good thermodynamic properties. Figure 33 shows the temperature-density behavior at constant pressure along with the saturation dome estimated by both the new equation of state for helium and the current standard (McCarty's equation of state). The plots are similar; except for the strong curvature on the liquid side around 2 K that the new equation reproduces following the data in Figure 18. Other than this significant difference, it would be hard to notice more complications.

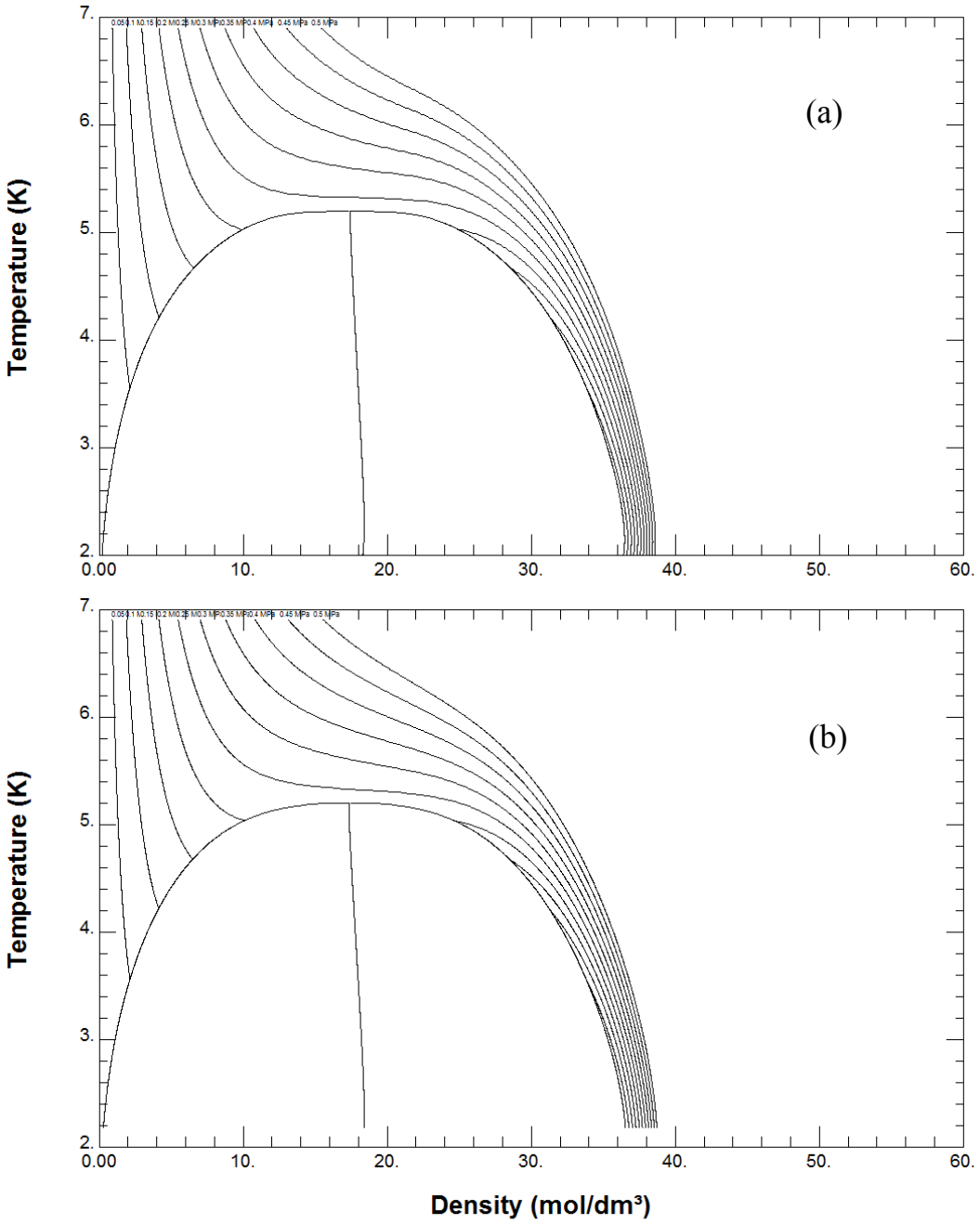

Figure 33. Temperature-density plot.(a) Helium equation of state presented in this document, and (b) McCarty's equation of state for helium. Lines are several isobars from 0.05 MPa to 5 MPa.

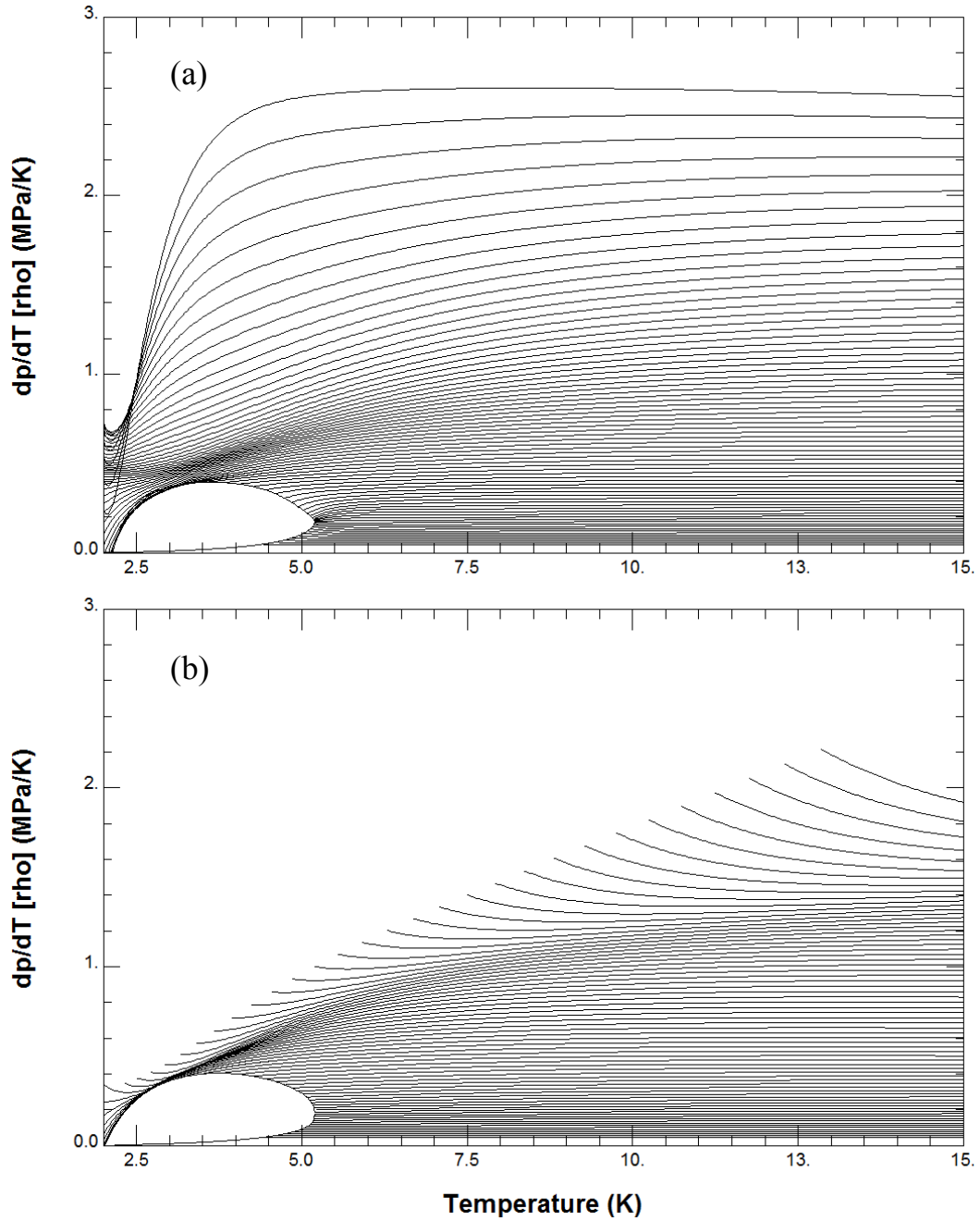

Figure 34. $\left(\partial p/\partial T\right)_{\rho}$-temperature plot.(a) New helium equation of state presented in this document, and (b) McCarty's equation of state for helium. Lines are several isochores from 5 mol dm^{-3} to 75 mol dm^{-3}.

Derivatives calculated from volumetric properties are similar to those presented in Figure 34, in which the derivatives $\left(\partial p/\partial T\right)_{\rho}$ for McCarty's equation are ill behaved for extrapolations to high densities and low temperatures. The equation of state presented here for helium reproduces these derived properties with reasonable behavior even at densities exceeding solid densities.

Figure 35 shows temperature as a function of density extending to conditions that are far beyond the limits of the fluid data. The purpose of this plot is to demonstrate that the equation continues to extrapolate well to high pressures, densities, and temperatures, and that no hidden irregularities exist beyond normal applications. Most often these regions are overlooked and most equations of state have poor behavior at extreme values. The difference between the new equation of state and McCarty's is obvious and again confirms the superior extrapolation capabilities of the new equation.

Probably the most visible difference between McCarty's equation of state and the current equation of state appears in Figure 36. Moldover [165] showed experimentally that the isochoric heat capacity (both saturated liquid and vapor) go to a sharp end at the critical point. McCarty's equation does not show this behavior for the vapor side, so that this is another improvement obtained with the new equation of state. Also, Figure 36 shows the singularity of the heat capacities around the lambda transition (~2 K), behavior that is reproduced by both equations.

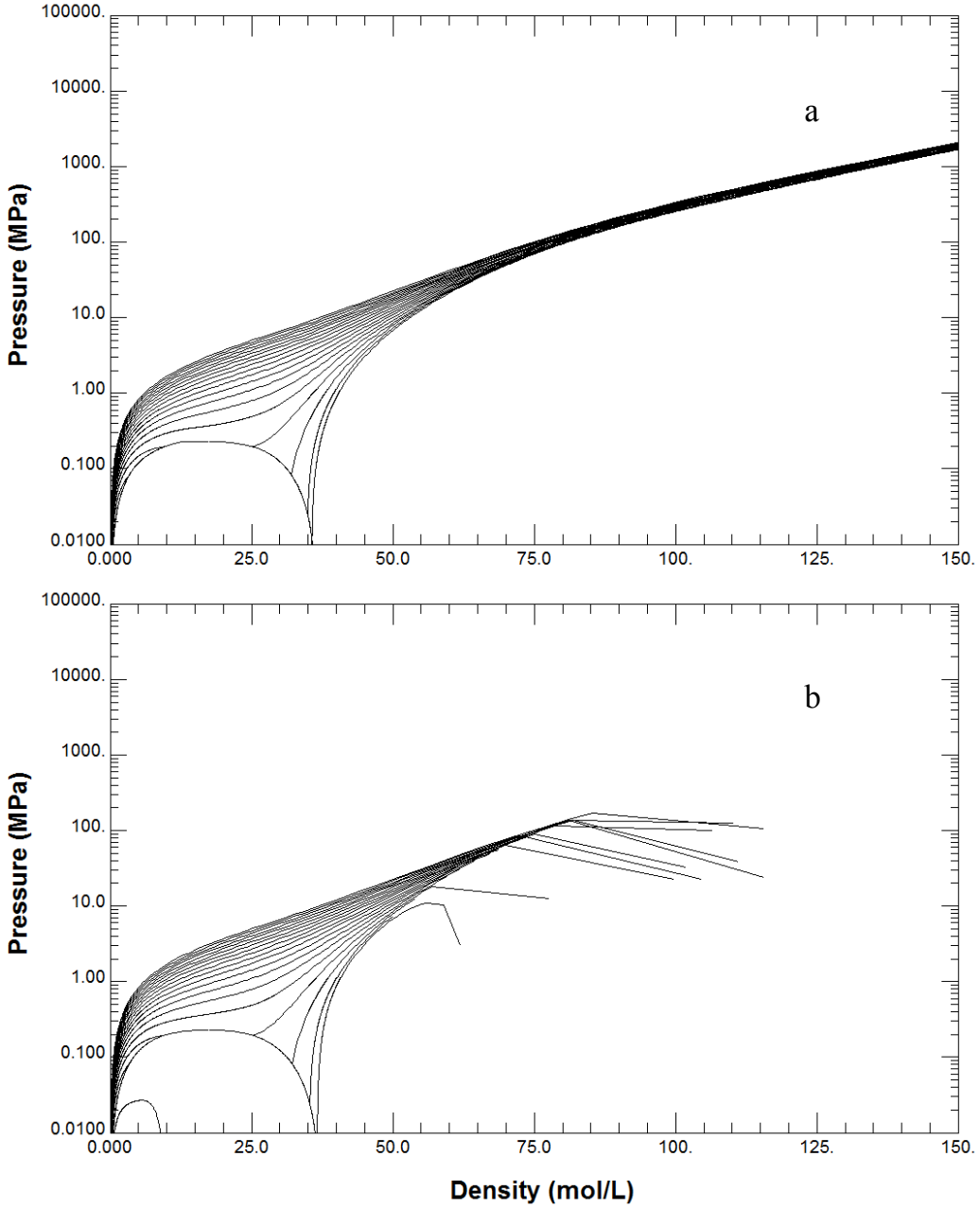

Figure 35. Pressure-density plot.(a) New helium equation of state presented in this document, and (b) McCarty's equation of state for helium. Lines are several isotherms from 2 K to 20 K.

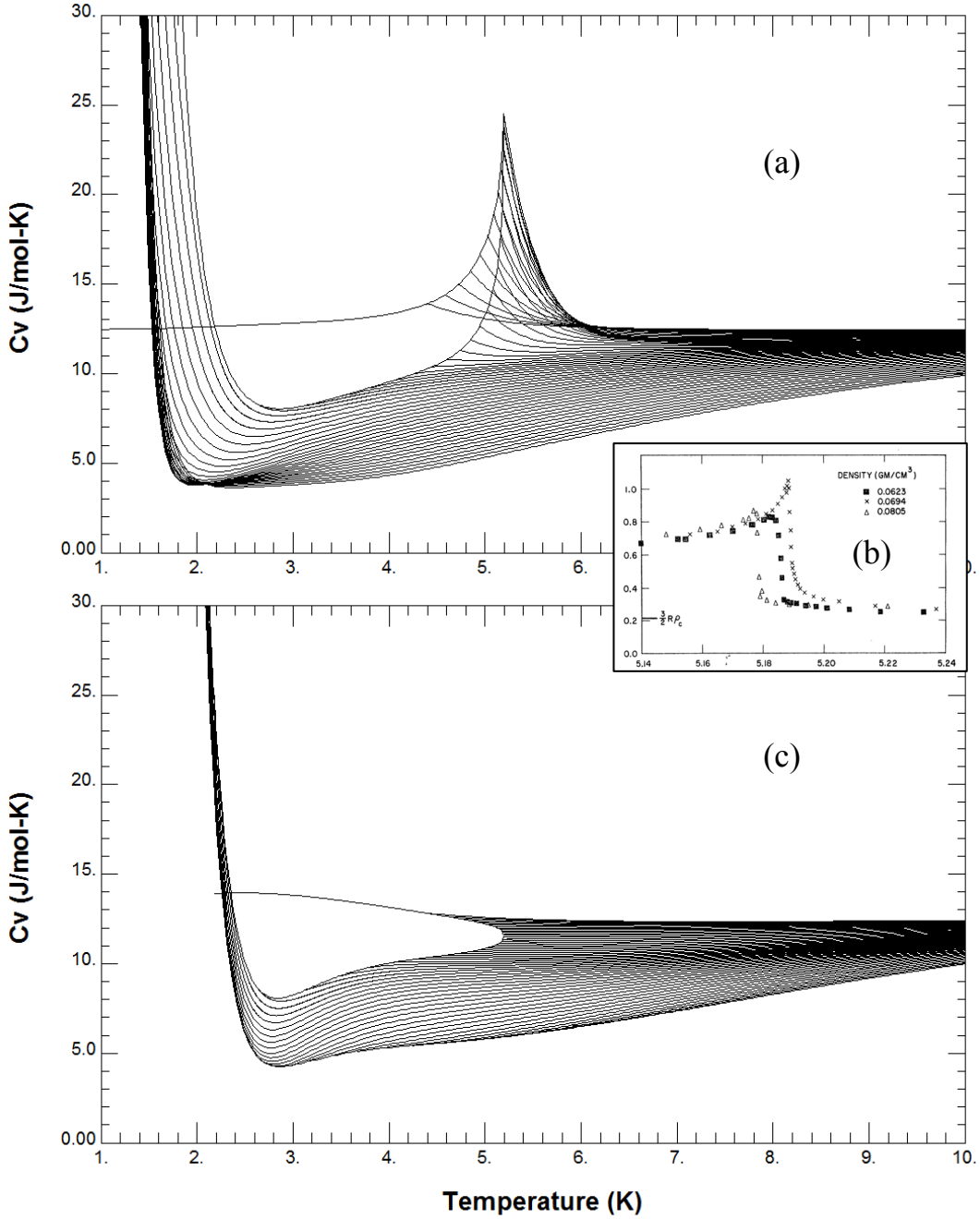

Figure 36. Isochoric heat capacity-temperature plot. (a) New helium equation of state presented in this document, (b) experimental behavior found around the critical temperature [165], and (c) McCarty's equation of state for helium. Lines are several isochores from 5 mol dm^{-3} to 60 mol dm^{-3}.

5.6 BASIC ASPECTS AROUND THE LAMBDA TRANSITION

This final section confirms the reasonable, qualitative predictions of the equation of state around the lambda line. So far, the equation has good results for volumetric properties and the isochoric heat capacity around the superfluid transition. Figure 37, Figure 38, Figure 39 and Figure 40 add more properties around the lambda line that compare to curves previously shown in Figure 13 and Figure 14 in Section 4. For all cases, the behavior of the thermodynamic properties was as expected above the actual lambda temperature. One limitation of the functional form used for the multiparameter equation of state lies in predicting superfluid properties. No combination and/or number of terms produced acceptable results in the superfluid area. However, the transition was represented well.

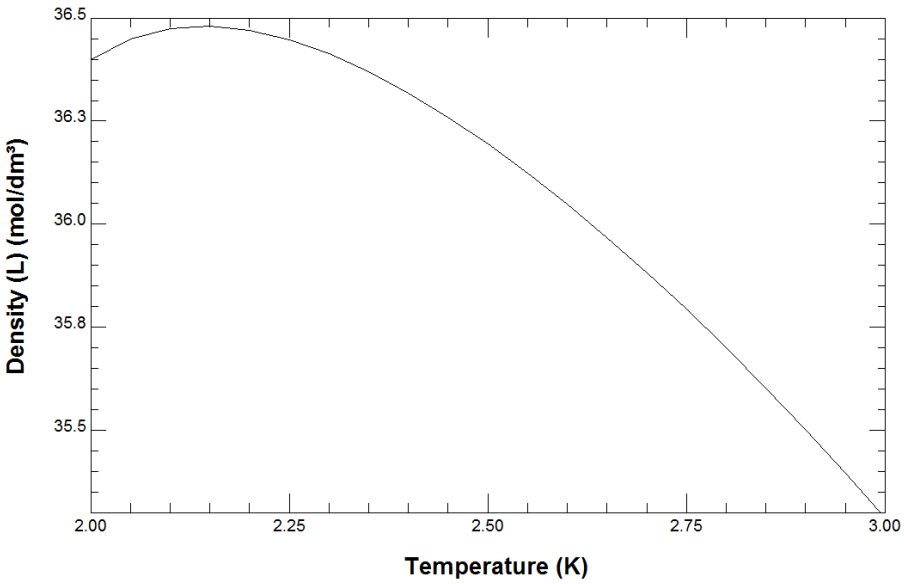

Figure 37. Density of liquid ^{4}He along the saturation curve in the vicinity of the lambda transition.

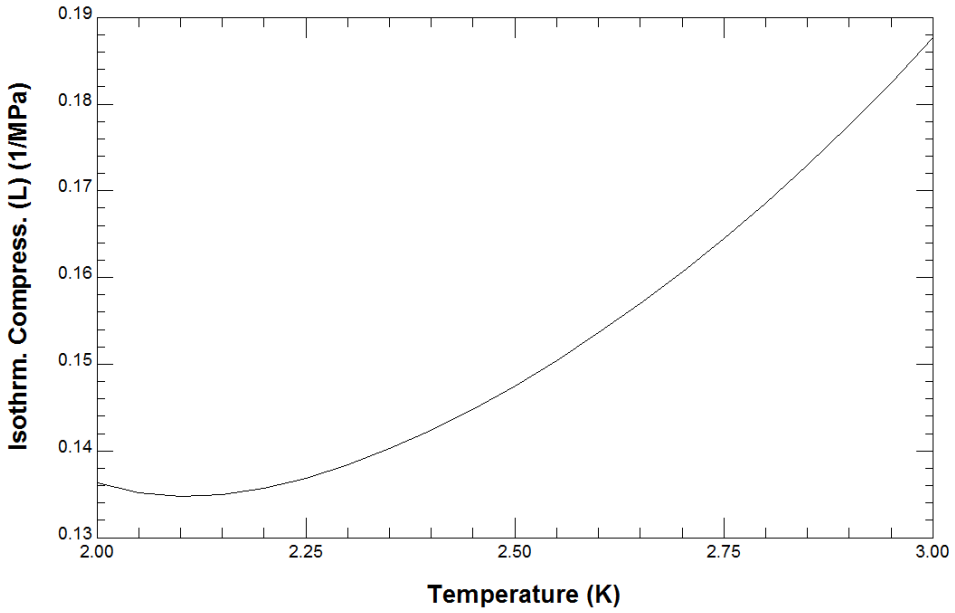

Figure 38. Isothermal compressibility of liquid ^{4}He along the saturation curve in the vicinity of the lambda transition.

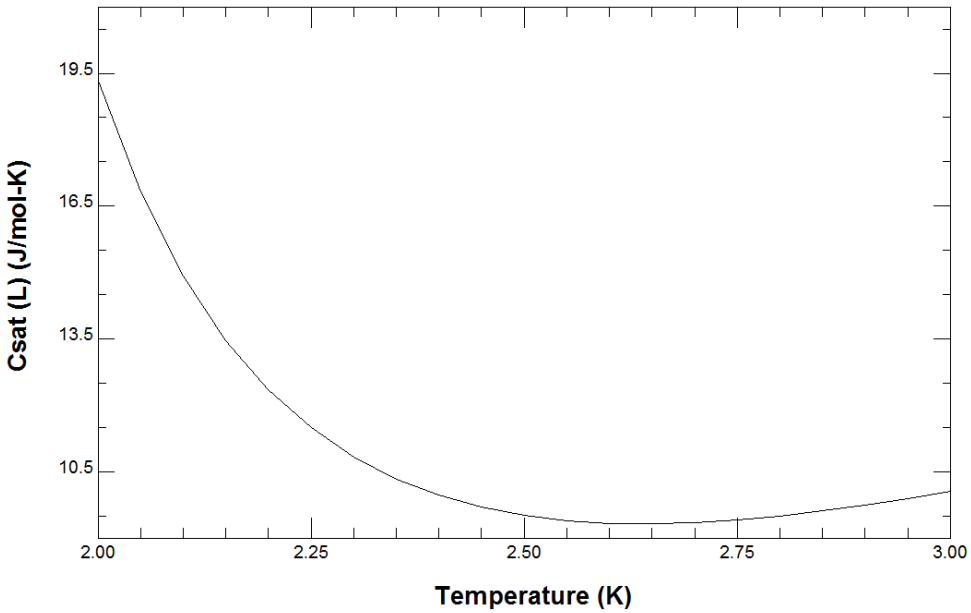

Figure 39. Saturation heat capacity of liquid ^{4}He in the vicinity of the lambda transition.

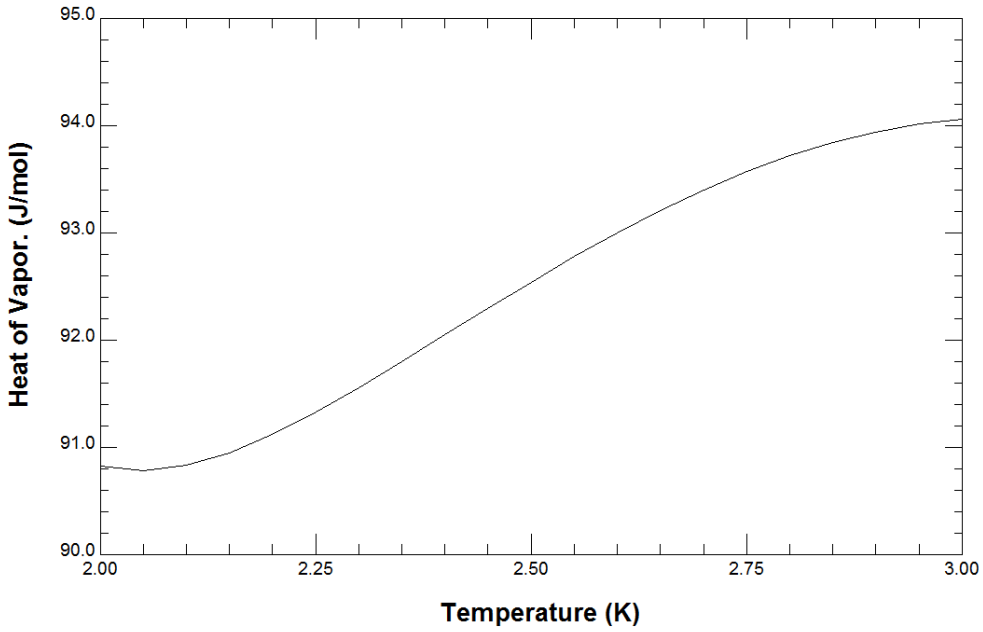

Figure 40. Heat of vaporization of liquid ^{4}He in the vicinity of the lambda transition.

6. CONCLUSIONS

The uncertainty statement (k=2) for both the new equation of state and McCarty and Arp [32] equation of state are:

- This work: Below 50 K, the uncertainties in density are 0.20% at pressures up to 20 MPa. From 50 K to 200 K the uncertainties decrease to 0.05 % at pressures up to 80 MPa. At higher temperatures the uncertainties in density are 0.02 % up to pressures of 80 MPa. At all temperatures and at pressures higher than listed here, the uncertainties may increase to 0.3% in density. The uncertainties in the speed of sound are 0.02%. The uncertainties in vapor pressure are less than 0.02%, and for the heat capacities are about 2%. Uncertainties in the critical region are higher for all properties except vapor pressure.
- McCarty and Arp: The uncertainties of the equation of state range from 1% at low temperatures (<20 K) to 0.1% at temperatures between 200 and 400 K, and from 3% in the speed of sound in the liquid phase to 0.1% in the speed of sound between 100 and 500 K. The uncertainty of heat capacities is about 5%.

Comparing both uncertainty statements, the major conclusion is that the new equation of state for helium is more accurate. Also, the new equation has improved extrapolation capabilities, and more accurate temperature (ITS-90) values. The difficulties associated with unreasonable thermodynamic behavior (*i.e.* critical isochoric heat capacity) are significantly reduced with the new equation. Nonetheless, two major

limitations appeared during development of the equation of state: fourth virial coefficient predictions and superfluid properties. These two problems are associated with the current functional form in multiparameter equations of state and can be resolved with new terms in future investigations.

This equation of state was released as one of the new features of Refprop [192] in its version 9.1 on April 9th of 2013. Therefore, the equation of state presented here represents the new thermodynamic standard for ^{4}He adopted by the National Institute of Standards and Technology.

REFERENCES

[1] V.V. Sychev, A.A. Vasserman, A.D. Kozlov, G.A. Spiridinov, V.A. Tsymarny, Thermodynamic properties of helium, First ed., Hemisphere Publishing Corporation, Moscow, 1987.

[2] R.P. Feynman, Physical Review 94 (2) (1954) 262.

[3] O. Penrose, L. Onsager, Physical Review 104 (3) (1956) 576.

[4] R. Ray, The impact of selling the federal helium reserve by the committee on the impact of selling the federal helium reserve, comission on physical sciences, mathematics and applications, commission on engineering and technical systems, National Research Council, Washington DC, 2000.

[5] H. Preston-Thomas, Metrologia 27 (1990) 7.

[6] U.S.G. Survey. Helium statistics-Historical statistics for mineral and material commodities in the United States. Resources and evaluation group, Amarillo field office, Amarillo TX, 2010.

[7] A. Griffin, D.W. Snoke, S. Stringari, eds. Bose-Einstein condensation. 1995, Cambridge University Press: Cambridge, UK. 600.

[8] M.H. Anderson, J.R. Ensher, M.R. Matthews, C.E. Wieman, Science 269 (1995) 3.

[9] M.A. Barrufet, P.T. Eubank, Fluid Phase Equilibria 35 (1-3) (1987) 107-116.

[10] J. Hurly, J. Schmidt, S. Boyes, M. Moldover, International Journal of Thermophysics 18 (3) (1997) 579-634.

[11] J.E. Kilpatrick, W.E. Keller, E.F. Hammel, N. Metropolis, Physical Review 94 (5) (1954) 1103.

[12] N.G. Whitelaw, Physica 1 (7-12) (1934) 749-751.

[13] K.R. Hall, F.B. Canfield, Physica 47 (1) (1970) 99-108.

[14] K.A. Chalyy, L.A. Bulavin, A.V. Chalyi, Journal of Molecular Liquids 127 (1-3) (2006) 151-152.

[15] J.M. Pfotenhauer, R.J. Donnelly, Heat transfer in liquid helium, in *Advances in Heat Transfer*, P.H. James and Thomas F. Irvine, Jr., Editors. 1985, Elsevier. p. 65-158.

[16] D.F. Brewer, J.G. Daunt, A.K. Sreedhar, Physical Review 115 (4) (1959) 836.

[17] A. van Itterbeek, W. de Laet, Physica 24 (1-5) (1958) 59-67.

[18] A. Van Itterbeek, G. Forrez, Physica 20 (7-12) (1954) 767-772.

[19] W.K. Walstra, Physica 13 (10) (1947) 643-652.

[20] R.L. Rusby, M. Durieux, Cryogenics 24 (7) (1984) 363-366.

[21] S.Q. Wang, G.B. Chen, Y.H. Huang, Cryogenics 48 (1-2)) 12-16.

[22] H. van Dijk, M. Durieux, Physica 22 (6-12) (1956) 760-760.

[23] J.R. Clement, J.K. Logan, J. Gaffney, Physical Review 100 (2) (1955) 743.

[24] R.A. Erickson, L.D. Roberts, Physical Review 93 (5) (1954) 957.

[25] T. Doiron, R.P. Behringer, H. Meyer, Journal of Low Temperature Physics 24 (1976) 18.

[26] W. Schulze, Fluid Phase Equilibria 87 (2) (1993) 199-211.

[27] Y.S. Wei, R.J. Sadus, Fluid Phase Equilibria 122 (1-2) (1996) 1-15.

[28] R. Span, Multiparameter equations of state. An accurate source of thermodynamic property data., First ed., Springer, Berlin, 2000.

[29] R. Span, E.W. Lemmon, R.T. Jacobsen, W. Wagner, A. Yokozeki, Journal of Physical and Chemical Reference Data 29 (6) (2000) 1361-1433.

[30] E.W. Lemmon, M.O. McLinden, W. Wagner, Journal of Chemical and Engineering Data 54 (12) (2009) 3141-3180.

[31] R. Span, W. Wagner, Journal of Physical and Chemical Reference Data 25 (6) (1996) 1509-1596.

[32] R.D. McCarty, V.D. Arp, Advances in Cryogenic Engineering 35 (1990) 1465-1475.

[33] R. Donnelly, Journal of physical and chemical reference data 27 (6) (1998) 1217.

[34] R. Span, W. Wagner, E.W. Lemmon, R.T. Jacobsen, Fluid Phase Equilibria 183-184 (2001) 1-20.

[35] G.E. Volovik, The universe in a helium droplet, First ed., Clarendon press, Moscow, 2003.

[36] J.D. Van Der Waals, J.S. Rowlinson, On the Continuity of the Gaseous and Liquid States ed., Dover Publications, 2004.

[37] P.H.V. Konynenburg, R.L. Scott, Philosophical Transactions of the Royal Society of London. Series A, Mathematical and Physical Sciences 298 (1442) (1980) 495-540.

[38] O. Redlich, J.N.S. Kwong, Chemical Reviews 44 (1) (1949) 233-244.

[39] P.L. Chueh, P. Jm, Industrial and Engineering Chemistry 59 (5) (1967) 14-&.

[40] P.L. Chueh, P. Jm, Industrial and Engineering Chemistry Fundamentals 6 (4) (1967) 492-&.

[41] P.L. Chueh, P. Jm, AIChE journal 13 (6) (1967) 1107-&.

[42] P.L. Chueh, P. Jm, AIChE journal 13 (6) (1967) 1099-&.

[43] P.L. Chueh, P. Jm, AIChE journal 13 (5) (1967) 896-&.

[44] L.E. Baker, K.D. Luks, Society of Petroleum Engineers journal 20 (1) (1980) 15-24.

[45] U. Deiters, G.M. Schneider, Berichte der Bunsengesellschaft für Physikalische Chemie 80 (12) (1976) 1316-1321.

[46] A. Anderko, Cubic and generalized van der Waals equations, in *Equations of state for fluids and mixtures*, J.V. Sengers, et al., Editors. 2000, Elsevier: Amsterdam.

[47] G. Soave, Soave, Chemical engineering science 27 (6) (1972) 1197-&.

[48] D. Peng, D.B. Robinson, Industrial and Engineering Chemistry Fundamentals 15 (1) (1976) 59-64.

[49] D. Peng, D.B. Robinson, AIChE Journal 23 (2) (1977) 137-144.

[50] N.C. Patel, A.S. Teja, Chemical Engineering Science 37 (3) (1982) 463-473.

[51] R. Stryjek, J.H. Vera, The Canadian Journal of Chemical Engineering 64 (2) (1986) 334-340.

[52] R. Stryjek, J.H. Vera, The Canadian Journal of Chemical Engineering 64 (2) (1986) 323-333.

[53] R. Stryjek, J.H. Vera, The Canadian Journal of Chemical Engineering 64 (5) (1986) 820-825.

[54] J.O. Valderrama, Industrial and Engineering Chemistry Research 42 (8) (2003) 1603-1618.

[55] A. Mulero, C. Galan, F. Cuadros, Physical Chemistry Chemical Physics 3 (22) (2001) 4991-4999.

[56] H. Reiss, H.L. Frisch, J.L. Lebowitz, Journal of Chemical Physics 31 (2) (1959) 369-380.

[57] E. Thiele, Journal of Chemical Physics 39 (2) (1963) 474-&.

[58] F.H. Ree, W.G. Hoover, Journal of Chemical Physics 40 (4) (1964) 939-&.

[59] E.A. Guggenheim, Molecular Physics 9 (2) (1965) 199-+.

[60] N.F. Carnahan, K.E. Starling, Journal of Chemical Physics 51 (2) (1969) 635-&.

[61] K.R. Hall, Journal of Chemical Physics 57 (6) (1972) 2252-&.

[62] T. Boublik, Berichte Der Bunsen-Gesellschaft-Physical Chemistry Chemical Physics 85 (11) (1981) 1038-1041.

[63] J.J. Erpenbeck, W.W. Wood, Journal of Statistical Physics 35 (3-4) (1984) 321-340.

[64] A. Malijevsky, J. Veverka, Physical Chemistry Chemical Physics 1 (18) (1999) 4267-4270.

[65] Y.S. Wei, R.J. Sadus, AIChE Journal 46 (1) (2000) 169-196.

[66] S.S. Chen, A. Kreglewski, Berichte Der Bunsen-Gesellschaft-Physical Chemistry Chemical Physics 81 (10) (1977) 1048-1052.

[67] B.J. Alder, D.A. Young, M.A. Marx, Journal of Chemical Physics 56 (6) (1972) 3013-&.

[68] T. Boublík, Journal of Molecular Liquids 134 (1–3) (2007) 151-155.

[69] M. Christoforakos, E.U. Franck, Berichte Der Bunsen-Gesellschaft-Physical Chemistry Chemical Physics 90 (9) (1986) 780-789.

[70] M. Heilig, E.U. Franck, Berichte Der Bunsen-Gesellschaft-Physical Chemistry Chemical Physics 93 (8) (1989) 898-905.

[71] U. Deiters, Chemical Engineering Science 37 (6) (1982) 855-861.

[72] R.t.L.K.O. Laboratorium, H.K. Onnes, W.H. Keesom, W.J. de Haas, Communications from the Kamerlingh Onnes Laboratory of the University of Leiden ed., Kamerlingh Onnes Laboratorium, Rijksuniversiteit., 1907.

[73] T.L. Hill, An Introduction to Statistical Thermodynamics ed., Dover Publ., 1960.

[74] J.M. Prausnitz, R.N. Lichtenthaler, E.G. de Azevedo, Molecular Thermodynamics of Fluid-Phase Equilibria ed., Pearson Education, 1998.

[75] A. Bellemans, C. Naarcolin, I. Prigogine, Journal of Chemical Physics 26 (3) (1957) 712-712.

[76] S. Beret, J.M. Prausnitz, AIChE Journal 21 (6) (1975) 1123-1132.

[77] G. Jackson, W.G. Chapman, K.E. Gubbins, International Journal of Thermophysics 9 (5) (1988) 769-780.

[78] J.A. Barker, Henderso.D, Journal of Chemical Physics 47 (11) (1967) 4714-&.

[79] I. Nezbeda, Fluid Phase Equilibria 182 (1-2) (2001) 3-15.

[80] Y. Rosenfeld, Physical Review Letters 63 (9) (1989) 980-983.

[81] L.L. Lee, Molecular thermodynamics of nonideal fluids ed., Butterworths, 1988.

[82] M. Benedict, G.B. Webb, L.C. Rubin, The Journal of Chemical Physics 8 (4) (1940) 334-345.

[83] M. Benedict, G.B. Webb, L.C. Rubin, Journal of Chemical Physics 10 (12) (1942) 747-758.

[84] K.E. Starling, Fluid thermodynamic properties for light petroleum systems ed., Gulf Pub. Co., 1973.

[85] V.V. Altunin, Gadetski.Og, Thermal Engineering 18 (3) (1971) 120-&.

[86] V.V. Altunin, Gadetski.Og, High Temperature 9 (3) (1971) 480-&.

[87] R.B. Stewart, R.T. Jacobsen, Cryogenics 13 (9) (1973) 526-534.

[88] W. Wagner, Cryogenics 12 (3) (1972) 214-221.

[89] R.T. Jacobsen, S.G. Penoncello, E.W. Lemmon, R. Span, Multiparameter equations of state, in *Equations of state for fluids and fluid mixtures*, J.V. Sengers, et al., Editors. 2000, Elsevier: Amsterdam.

[90] T.R. Strobridge, National Bureau of Standards Tech. Note 129 (1962.

[91] E. Bender, Cryogenics 13 (1) (1973) 11-18.

[92] J.H. Keenan, Steam tables: thermodynamic properties of water, including vapor, liquid, and solid phases (English units) ed., Wiley, 1969.

[93] R. Pollak, Brennstoff-Warme-Kraft 27 (5) (1975) 210-215.

[94] L. Haar, J.S. Gallagher, Journal of Physical and Chemical Reference Data 7 (3) (1978) 635-&.

[95] R. Schmidt, W. Wagner, Fluid Phase Equilibria 19 (3) (1985) 175-200.

[96] R.T. Jacobsen, R.B. Stewart, M. Jahangiri, International Journal of Thermophysics 7 (3) (1986) 503-511.

[97] M. Jahangiri, R.T. Jacobsen, R.B. Stewart, R.D. McCarty, International Journal of Thermophysics 7 (3) (1986) 491-501.

[98] P.J. Mohr, B.N. Taylor, Reviews of Modern Physics 72 (2) (2000) 351-495.

[99] U. Setzmann, W. Wagner, Journal of Physical and Chemical Reference Data 20 (6) (1991) 1061-1155.

[100] W. Wagner, A. Pruss, Journal of Physical and Chemical Reference Data 31 (2) (2002) 387-535.

[101] C. Tegeler, R. Span, W. Wagner, Journal of Physical and Chemical Reference Data 28 (3) (1999) 779-850.

[102] J. Smukala, R. Span, W. Wagner, Journal of Physical and Chemical Reference Data 29 (5) (2000) 1053-1121.

[103] E.W. Lemmon, R.T. Jacobsen, Journal of Physical and Chemical Reference Data 34 (1) (2005) 69-108.

[104] E.W. Lemmon, R.T. Jacobsen, S.G. Penoncello, D.G. Friend, Journal of Physical and Chemical Reference Data 29 (3) (2000) 331-385.

[105] M.O. McLinden, C. Lösch-Will, The Journal of Chemical Thermodynamics 39 (4) (2007) 507-530.

[106] M.R. Moldover, M.O. McLinden, Journal of Chemical Thermodynamics 42 (10) (2010) 1193-1203.

[107] S.I. Sandler, M. Castier, Pure and Applied Chemistry 79 (8) (2007) 1345-1359.

[108] G. Garberoglio, M.R. Moldover, A.H. Harvey, Journal of Research of the National Institute of Standards and Technology 116 (4) (2011) 729-742.

[109] J.B. Mehl, Comptes Rendus Physique 10 (9) (2009) 859-865.

[110] C. Gaiser, B. Fellmuth, Metrologia 46 (5) (2009) 525-533.

[111] J.J. Hurly, M.R. Moldover, Journal of Research of the National Institute of Standards and Technology 105 (5) (2000) 667-688.

[112] R. Berman, C.F. Mate, Philosophical Magazine 3 (29) (1958) 461-469.

[113] K.H. Berry, Molecular Physics 37 (1) (1979) 317-318.

[114] A.L. Blancett, K.R. Hall, F.B. Canfield, Physica 47 (1) (1970) 75-&.

[115] A.L. Blancett, K.R. Hall, F.B. Canfield, Physica 47 (1) (1970) 75-91.

[116] A.L. Blancett, K.R. Hall, F.B. Canfield, Physica 47 (1) (1970) 75-&.

[117] T.C. Briggs, Compressibility data for helium over the temperature range -5/sup 0/ to 80/sup 0/C and at pressures to 800 atmospheres, 1970.

[118] U.S.B.o. Mines, B.J. Dalton, T.C. Briggs, Compressibility Data for Helium at 0 Degrees C and Pressures to 800 Atmospheres ed., 1969.

[119] E. Buchmann, Zeitschrift Fur Physikalische Chemie-Abteilung a-Chemische Thermodynamik Kinetik Elektrochemie Eigenschaftslehre 163 (5/6) (1933) 461-468.

[120] F.B. Canfield, T.W. Leland, R. Kobayashi, Journal of Chemical and Engineering Data 10 (2) (1965) 92-96.

[121] F.B. Canfield, T.W. Leland, R. Kobayashi, Advanced Cryogenics Engineering Journal 8 (1963) Medium: X; Size: Pages: 146-57.

[122] G. Cataland, H. Plumb, Journal of Research of the National Bureau of Standards Section a-Physics and Chemistry A 69 (6) (1965) 531.

[123] J.D. Cramer, The compressibility of gaseous mixtures of helium-nitrogen and helium-deuterium at high pressures, Los Alamos Scientific Laboratory 1965.

[124] D.D. Dillard, M. Waxman, R.L. Robinson, Journal of Chemical and Engineering Data 23 (4) (1978) 269-274.

[125] J.S. Dugdale, J.P. Franck, Philosophical Transactions of the Royal Society of London. Series A, Mathematical and Physical Sciences 257 (1076) (1964) 1-29.

[126] F.J. Edeskuty, R.H. Sherman. Pressure-Volume-Temperature relations of liquid He-3 and He-4. in *International Conference of Low Temperature Physics*. 1958.

[127] M.H. Edwards, W.C. Woodbury, Canadian Journal of Physics 39 (12) (1961) 1833-&.

[128] M.H. Edwards, W.C. Woodbury, Physical Review 129 (5) (1963) 1911.

[129] Z.E.H.A. El Hadi, M. Durieux, H. van Dijk, Physica 41 (2) (1969) 289-304.

[130] Z.E.H.A. El Hadi, M. Durieux, Physica 41 (2) (1969) 305-319.

[131] C. Evers, H.W. Lösch, W. Wagner, International Journal of Thermophysics 23 (6) (2002) 1411-1439.

[132] C.W. Gibby, C.C. Tanner, I. Masson, Proceedings of the Royal Society of London. Series A, Containing Papers of a Mathematical and Physical Character 122 (789) (1929) 283-304.

[133] A.P.M. Glassford, J.L. Smith Jr, Cryogenics 6 (4) (1966) 193-206.

[134] E.R. Grilly, R.L. Mills, Annals of Physics 18 (2) (1962) 250-263.

[135] E.R. Grilly, R.L. Mills, Annals of Physics 8 (1) (1959) 1-23.

[136] D. Gugan, G.W. Michel, Molecular Physics 39 (3) (1980) 783-785.

[137] K.R. Hall, F.B. Canfield, Physica 47 (2) (1970) 219-226.

[138] R.W. Hill, O.V. Lounasmaa, Philosophical Transactions of the Royal Society of London. Series A, Mathematical and Physical Sciences 252 (1013) (1960) 357-395.

[139] L. Holborn, J. Otto, Zeitschrift Fur Physik 38 (4/5) (1926) 359-367.

[140] J.C. Holste, M.Q. Watson, M.T. Bellomy, P.T. Eubank, K.R. Hall, Aiche Journal 26 (6) (1980) 954-964.

[141] A.E. Hoover, F.B. Canfield, R. Kobayashi, T.W. Leland, Journal of Chemical and Engineering Data 9 (4) (1964) 568-573.

[142] W.H. Keesom, W.K. Walstra, Physica 7 (10) (1940) 985-991.

[143] W.H. Keesom, W.K. Walstra, Physica 13 (4-5) (1947) 225-230.

[144] G.S. Kell, G.E. McLaurin, E. Whalley, The Journal of Chemical Physics 68 (5) (1978) 2199-2205.

[145] W.E. Keller, Physical Review 97 (1) (1955) 1.

[146] E.C. Kerr, The Journal of Chemical Physics 26 (3) (1957) 511-514.

[147] W.D. Kessler, D.V. Osborne, Journal of Physics C: Solid State Physics 13 (11) (1980) 2097.

[148] H.A. Kierstead, Physical Review A 7 (1) (1973) 242.

[149] J. Kistemaker, W.H. Keesom, Physica 12 (4) (1946) 227-240.

[150] G.M. Kramer, J.G. Miller, The Journal of Physical Chemistry 61 (6) (1957) 785-788.

[151] P.S. Ku, B.F. Dodge, Journal of Chemical and Engineering Data 12 (2) (1967) 158-164.

[152] D.H. Liebenberg, R.L. Mills, J.C. Bronson, Thermodynamic properties of fluid 4He in the 75 to 300 K and 2- to 20-kbar range, 1980.

[153] L.R. Linshits, I.B. Rodkina, D.S. Tsiklis, Zhurnal Fizicheskoi Khimii 49 (8) (1975) 2141-2143.

[154] L.R. Linshits, I.B. Rodkina, N.G. Tyurikova, D.S. Tsiklis, Zhurnal Fizicheskoi Khimii 51 (11) (1977) 2948-2949.

[155] O.V. Lounasmaa, The specific heat of liquid helium, University of Turku, Finland, 1957.

[156] O.V. Lounasmaa, E. Kojo, Annales Academiæ Scientiarum Fennicæ Mathematica 36 (1959) 1-26.

[157] O.V. Lounasmaa, Cryogenics 1 (4) (1961) 212-221.

[158] O.V. Lounasmaa, L. Kaunisto. Direct measurements of (dP/dT)(V) of liquid helium near the lambda-curve. in *7th International conference on low temperature physics*. 1961. Toronto, Canada.

[159] B.V. Mallu, G. Natarajan, D.S. Viswanath, The Journal of Chemical Thermodynamics 19 (5) (1987) 549-554.

[160] H. Mansoorian, K.R. Hall, J.C. Holste, P.T. Eubank, The Journal of Chemical Thermodynamics 13 (11) (1981) 1001-1024.

[161] A. Michels, H. Wouters, Physica 8 (8) (1941) 923-932.

[162] J.E. Miller, L. Stroud, L.W. Brandt, Journal of Chemical and Engineering Data 5 (1) (1960) 6-9.

[163] M.R. Moldover, Physical Review 182 (1) (1969) 342.

[164] M.R. Moldover, Investigation of the specific heat of helium in the neighborhood of the critical point, Standford University, California, 1966.

[165] M.R. Moldover, Physical Review 182 (1) (1969) 342.

[166] G.P. Nijhoff, W.H. Keesom, Proceedings of the Koninklijke Akademie Van Wetenschappen Te Amsterdam 31 (1/5) (1928) 408-409.

[167] M.R. Patel, L.L. Joffrion, P.T. Eubank, Aiche Journal 34 (7) (1988) 1229-1232.

[168] W.C. Pfefferle, J.A. Goff, J.G. Miller, The Journal of Chemical Physics 23 (3) (1955) 509-513.

[169] M. Prasad, A.P. Kudchadker, Journal of Chemical and Engineering Data 23 (3) (1978) 190-191.

[170] J.A. Provine, Physica 52 (1) (1971.

[171] P.R. Roach, Physical Review 170 (1) (1968) 213.

[172] J.M.H.L. Sengers, J.R. Hastings, International Journal of Thermophysics 2 (3) (1981) 269-288.

[173] J.W. Stewart, Journal of Physics and Chemistry of Solids 1 (3) (1956) 146-158.

[174] L. Stroud, J.E. Miller, L.W. Brandt, Journal of Chemical and Engineering Data 5 (1) (1960) 51-52.

[175] K.W. Suh, T.S. Storvick, Aiche Journal 13 (2) (1967) 231-&.

[176] J.A. Sullivan, R.E. Sonntag, Cryogenics 7 (1-4)) 13-17.

[177] C.C. Tanner, I. Masson, Proceedings of the Royal Society of London. Series A, Containing Papers of a Mathematical and Physical Character 126 (801) (1930) 268-288.

[178] Tsederbe.Nv, V.N. Popov, V.R. Petrov, Thermal Engineering 19 (6) (1972) 125-130.

[179] D.S. Tsiklis, L.R. Linshits, I.B. Rodkina, Zhurnal Fizicheskoi Khimii 48 (6) (1974) 1541-1544.

[180] D.S. Tsiklis, L.R. Linshits, I.B. Rodkina, Zhurnal Fizicheskoi Khimii 48 (6) (1974) 1544-1546.

[181] W.F. Vogl, K.R. Hall, Physica 59 (3) (1972) 529-535.

[182] D. White, T. Rubin, P. Camky, H.L. Johnston, The Journal of Physical Chemistry 64 (11) (1960) 1607-1612.

[183] R. Wiebe, V.L. Gaddy, C. Heins, Journal of the American Chemical Society 53 (2) (1931) 1721-1725.

[184] J. Zelmanov, Journal of Physics-Ussr 8 (1-6) (1944) 129-134.

[185] W. Zhang, J.A. Schouten, H.M. Hinze, M. Jaeschke, Journal of Chemical and Engineering Data 37 (1) (1992) 114-119.

[186] E. Grüneisen, Handbuch der Physik ed, ed. V.J. Springer. Vol. 10. 1926.

[187] V. Arp, Y.H. Huang, R. Radebaugh, G.B. Chen, International Journal of Thermophysics 28 (2) (2007) 417-428.

[188] Y.H. Huang, G.B. Chen, V.D. Arp, Applied Physics Letters 88 (9) (2006) 091905-091905-3.

[189] G. Venkatarathnam, L.R. Oellrich, Fluid Phase Equilibria 301 (2) (2011) 225-233.

[190] G.V. Pasad, G. Venkatarathnam, Industrial and Engineering Chemistry Research 38 (9) (1999) 3530-3534.

[191] W.E. Keller, Helium-3 and helium-4, First ed., Plenum press, New York, 1969.

[192] E.W. Lemmon, M.L. Huber, M.O. McLinden, NIST Standard Reference Database 23: Reference Fluid Thermodynamic and Transport Properties-REFPROP, National Institute of Standards and Technology, Standard Reference Data Program, Gaithersburg, 2013.

[193] H.K. Onnes, "Further experiments with liquid helium.", in *Through Measurement to Knowledge*, K. Gavroglu and Y. Goudaroulis, Editors. 1990, Springer Netherlands. p. 201-220.